

**Florida A & M University - Florida State University  
College of Engineering**

**Department of Civil & Environmental Engineering**

**APPLICATION OF FIBER REINFORCED CONCRETE  
IN THE END ZONES OF  
PRECAST PRESTRESSED BRIDGE GIRDERS**

**By**

**Nur Yazdani, Ph.D., P.E.  
Professor**

**Lisa Spainhour, Ph.D.  
Associate Professor**

**Saif Haroon  
Research Assistant**

**FDOT Contract No. BC-386**

**Final Report Submitted to the  
Florida Department of Transportation**

December 2002

1. Report No.		2. Government Accession No.		3. Recipient's Catalog No.	
4. Title and Subtitle  Application of Fiber Reinforced Concrete in the End Zones of Precast Prestressed Bridge Girders				5. Report Due December 15, 2002	
				6. Performing Organization Code  1902-145-11	
				8. Performing Organization Report No.  1902-145-11	
7. Author's Nur Yazdani, Ph.D., P.E., Lisa Spainhour, Ph.D., and Saif Haroon				10. Work Unit No. (TRAIS)	
9. Performing Organization Name and Address FAMU-FSU College of Engineering Civil and Environmental Engineering Department 2525 Pottsdamer St. Tallahassee FL 32310				11. Contract or Grant No.  BC-386	
				13. Type of Report and Period Covered	
				14. Sponsoring Agency Code	
12. Sponsoring Agency Name and Address Florida Department of Transportation 605 Suwannee Street Tallahassee, FL 32399-0450				15. Supplementary Notes	
16. Abstract  The secondary spiral and skin reinforcement in the anchorage zone of prestressed post-tensioned girders cause congestion and poses difficulty in the placement of concrete. It is also labor intensive to produce and place the secondary anchorage reinforcement. The objectives of this study was to determine the feasibility of reducing the secondary reinforcement with fibers for post-tensioned anchor zones, because of the expected improvement in mechanical properties of fiber reinforced concrete (FRC) over non-fibrous concrete. The first phase of the test program involved the determination of split tensile strength, compressive strength and flexural toughness of FRC and non-fibrous concrete. Two steel fibers and one synthetic fiber with various amounts were utilized. Steel fibers enhanced the properties of concrete, whereas the role of synthetic fiber was not encouraging. In the second phase, AASHTO Special Anchorage Device Acceptance Test was performed. Variations of spiral and skin reinforcement, with two levels of concrete strengths, were utilized to investigate the performance of the two types and various amounts of steel fibers. The experimental results indicated that 1% steel fiber could be used to replace all the secondary reinforcement for minimum concrete strength of 5900 psi (40.7 MPa), and could reduce a maximum of 79% of the secondary reinforcement for a minimum concrete strength of 4710 psi (32.5 MPa). Lower volumes of steel fibers may also result in reduction of secondary reinforcements. A finite element model of AASHTO test block was also developed to validate the experimental results. Good agreement was found between theoretical and experimental strain values. Usage of steel fiber reinforced concrete in the anchorage zones will result in negligible change in the girder costs.					
17. Key Words  Post-tensioned girder, Local anchorage zone, Secondary reinforcement, Fiber reinforced Concrete. Segmental bridge, AASHTO girder			18. Distribution Statement  No restriction This report is available to the public through the National Technical Information Service, Springfield VA 22161		
19. Security Classif. (of this report)  Unclassified		20. Security Classif. (of this page)  Unclassified		21. No. of Pages  208	22. Price

# TABLE OF CONTENTS

	<b>Page</b>
<b>LIST OF TABLES</b> .....	vi
<b>LIST OF FIGURES</b> .....	viii
<b>ABSTRACT</b> .....	xiii
 <b>CHAPTER</b>	
<b>1. INTRODUCTION</b> .....	1
1.1. Prestressed Concrete and Anchorage Zone Reinforcement.....	1
1.2. Failure of the Anchorage Zone.....	7
1.3. Fiber Reinforced Concrete.....	9
1.4. Specific Problems with Bridges.....	10
1.5. Objectives of the Study.....	11
1.6. Scope of the Study.....	12
<b>2. BACKGROUND REVIEW</b> .....	13
2.1. Anchorage Zones in Prestressed Concrete.....	13
2.2. Local Zone and General Zone.....	14
2.2.1. Local Zone.....	16
2.2.2. Dimensions of the Local Anchorage Zone.....	17
2.2.3. Local Zone Reinforcement.....	19
2.2.4. General Zone.....	21
2.2.5. Dimensions of the General Zone.....	24
2.2.6. Interface Between Local and General Zones.....	24
2.3. Fiber Reinforced Concrete.....	24
2.3.1. Basic Concepts of Fiber Reinforced Concrete.....	25
2.3.2. History of Fibers.....	27
2.3.3. Types of Fibers.....	28
2.3.4. Advantages of Fiber Reinforced Concrete.....	28

2.4.	Steel Fiber Reinforced Concrete (SFRC).....	32
2.4.1.	Properties of Steel Fibers.....	32
2.5.	Polypropylene Fiber Reinforced Concrete (PFRC).....	44
2.5.1.	Properties of PFRC.....	45
2.6.	Application of Fiber Reinforced Concrete.....	49
2.6.1.	Application of SFRC.....	51
2.6.2.	Application of PFRC.....	54
<b>3.</b>	<b>PROPERTY TESTING OF FIBER REINFORCED CONCRETE.....</b>	<b>58</b>
3.1.	Introduction.....	58
3.2.	Property Test Program.....	59
3.3.	Procurement of Materials.....	59
3.3.1.	Concrete.....	59
3.3.2.	Selection of Fibers.....	60
3.4.	Mixing Procedure.....	62
3.5.	Compressive Strength Test.....	65
3.5.1.	Specimen Preparation.....	65
3.5.2.	Specimen Testing.....	67
3.6.	Split Tensile Strength Test.....	67
3.6.1.	Specimen Preparation.....	67
3.6.2.	Specimen Testing.....	67
3.7.	Flexural Toughness Test.....	68
3.7.1.	Specimen Preparation.....	68
3.7.2.	Specimen Testing.....	68
3.8.	Workability of FRC.....	69
3.9.	Placement and Finishing of FRC.....	72
<b>4.</b>	<b>RESULTS OF FRC PROPERTY TESTING.....</b>	<b>74</b>
4.1.	Introduction.....	74
4.2.	Results and Analysis.....	74
4.2.1.	Compressive Strength Test.....	74
4.2.2.	Tensile Strength Test.....	77
4.2.3.	Flexural Toughness Test (ASTM C-1018).....	81
<b>5.</b>	<b>AASHTO SPECIAL ANCHORAGE DEVICE ACCEPTANCE TEST..</b>	<b>95</b>
5.1.	Introduction.....	95
5.2.	AASHTO Special Anchorage Device Acceptance Test.....	95
5.2.1.	Selection of Anchorage Type.....	97
5.2.2.	Configuration of The Test Block.....	97
5.3.	Test Plan.....	104
5.3.1.	Selection of Fiber Configuration.....	104
5.3.2.	Selection of Specimen Reinforcement.....	105
5.3.3.	Compressive Strength Validation.....	108

5.4.	Construction Details.....	108
5.5.	Testing Details.....	110
<b>6.</b>	<b>AASHTO ACCEPTANCE TEST RESULTS.....</b>	<b>116</b>
6.1.	Introduction.....	116
6.2.	Test Hierarchy.....	116
6.3.	Results from Type 1 Specimens.....	120
6.3.1.	Results for Type 1 Specimens with 1% ZP305 Steel Fiber.....	120
6.3.2.	Results for Type 1 Specimens with 0.75% ZP305 Steel Fiber.....	126
6.3.3.	Results for Type 1 Specimens with 1% XOREX Steel Fiber.....	129
6.3.4.	Results for Type 1 control Specimens without Fiber.....	131
6.4.	Results from Type 2 Specimens.....	133
6.4.1.	Results for Type 2 Specimens with 1% ZP305 Steel Fiber.....	134
6.4.2.	Results for Type 2 Specimens with 0.75% ZP305 Steel Fiber.....	135
6.4.3.	Results for Type 2 Specimens with 1% XOREX Steel Fiber.....	137
6.5.	Observations from AASHTO Cyclic Load Test.....	138
<b>7.</b>	<b>FINITE ELEMENT MODELING.....</b>	<b>152</b>
7.1.	Introduction to Finite Element Methods.....	152
7.2.	Types of Elements.....	153
7.2.1.	Structural Solid Element for the Anchorage and the Duct.....	153
7.2.2.	Concrete Element.....	154
7.2.3.	Spar Element for the Skin Reinforcement.....	154
7.3.	Development of FEM.....	155
7.3.1.	Material Properties.....	155
7.3.2.	The Anchorage.....	155
7.3.3.	The Plastic Duct.....	158
7.3.4.	Concrete.....	158
7.3.5.	Fiber.....	158
7.3.6.	Skin Reinforcement.....	161
7.4.	Loading.....	161
7.5.	Specimens Modeled for FEM Analysis.....	161
7.6.	Limitations of FEM Analysis.....	164
<b>8.</b>	<b>THEORETICAL VS. EXPERIMENTAL COMPARISON.....</b>	<b>165</b>
8.1.	Comparison of Strains.....	165

8.2.	Nature of Stress Contour.....	170
<b>9.</b>	<b>COST COMPARISON.....</b>	<b>172</b>
9.1.	Introduction.....	172
9.2.	Factors Affecting the Cost of Girders.....	172
	9.2.1. Factors Increase the Cost.....	173
	9.2.2. Factors Decrease the Cost.....	174
<b>10.</b>	<b>CONCLUSIONS AND RECOMMENDATIONS.....</b>	<b>177</b>
10.1.	Conclusions.....	177
10.2.	Recommendations.....	183
	<b>REFERENCES.....</b>	<b>186</b>
<b>APPENDIX A.</b>	<b>CALCULATIONS.....</b>	<b>194</b>
A.1.	The Ultimate Tensile Capacity for a Tendon.....	194
	A.1.1. General Equation.....	194
	A.1.2. Ultimate Load for VSL EC Type Anchorage.....	195
A.2.	Skin Reinforcement.....	195

## LIST OF TABLES

No.	Title	Page
3.1	Ingredients of design concrete mix (Class IV).....	61
3.2	Mix proportions of design concrete mix (for 1 yd <sup>3</sup> ).....	61
3.3	Source, type and geometry of fibers used in the study.....	64
3.4	Amount of fibers used in the study (for 1 yd <sup>3</sup> mix).....	64
3.5	Concrete batch designations used in the study.....	66
3.6	Slump for non-fibrous concrete and various FRC.....	71
4.1	Compressive strength results.....	78
4.2	Tensile strength results.....	83
4.3	First crack strengths of FRC and control specimens.....	91
4.4	Comparisons of residual strength factors of various FRC.....	91
5.1	Spiral and skin combinations.....	107
6.1	Test results for Type 1 specimens with 1% ZP305 steel fiber.....	121
6.2	Test results for Type 1 specimens with 0.75% ZP305 steel fiber.....	127
6.3	Test results for Type 1 specimens with 1% XOREX steel fiber.....	130
6.4	Test results for Type 1 control specimens without any fiber.....	132
6.5	Test results for Type 2 specimens with 1% ZP305 steel fiber.....	132
6.6	Test results for Type 2 specimens with 0.75% ZP305 steel fiber.....	136
6.7	Test results for Type 2 specimens with 1% XOREX steel fiber.....	139

6.8	Acceptable anchorage zone reinforcement with 1% ZP305 steel fiber...	147
6.9	Acceptable anchorage zone reinforcement with 0.75% ZP305 steel fiber.....	148
6.10	Acceptable anchorage zone reinforcement with 1% XOREX steel fiber.....	149
7.1	Material Properties for ANSYS FEM.....	156
7.2	Specimens modeled using ANSYS.....	163
8.1	Strain comparisons from the cyclic loading test and FEM.....	169
9.1	Cost associated with spiral reinforcement.....	176
10.1	Minimum properties of acceptable SFRC.....	185
10.2	Recommended SFRC configurations.....	185

## LIST OF FIGURES

No.	Title	Page
1.1	Flow of forces in concentrically loaded anchorage zone (Breen <i>et al</i> 1994).....	3
1.2	Stress contours for concentrically loaded anchorage zone (Breen <i>et al</i> 1994).....	3
1.3	Special anchorage device.....	5
1.4	Anchorage zone reinforcement.....	6
2.1	Local and general anchorage zone.....	15
2.2	Definition of the local zone (Burdet 1990).....	15
2.3	AASHTO local zone definitions for special bearing plates (Breen <i>et al</i> 1994).....	18
2.4	Definition of the general zone (Burdet 1990).....	22
2.5	State of tensile stresses in the general zone (Burdet 1990).....	23
2.6	Fibers bridging across a concrete crack (Beaudoin 1990).....	26
2.7	Load versus deflection curves for unreinforced and fiber reinforced concrete (ACI 544.1R 1996).....	26
2.8	Various types of steel fibers.....	29
2.9	Glass fiber.....	29
2.10	Various types of synthetic fibers.....	30
2.11	Fracture surface of steel fiber reinforced concrete.....	30
2.12	Various geometries of steel fibers (ACI 544.1R 1996).....	33

2.13	Influence of steel fiber volume on compressive stress-strain diagram.....	33
2.14	Stress-strain curves for SFRC in tension.....	36
2.15	Load-deflection curve and toughness parameters (ASTM C-1018).....	41
2.16	Stress-strain curves for cement composites containing polypropylene fibers (Beaudoin 1990).....	46
2.17	Compressive strength ratio versus polypropylene fiber concentration (Dardare 1975).....	46
2.18	Compressive stress-strain curves for plain concrete and PFRC cubes (Hughes and Fattuhi 1977).....	48
2.19	Typical load-deflection curves for PFRC containing various fiber volume fractions (Dave and Ellis 1979).....	48
2.20	Drying shrinkage strain for PFRC and companion plain concrete specimens (Zollo <i>et al</i> 1986).....	50
2.21	Industrial floor with SFRC, Sparrow's Point, Maryland (SI Concrete Systems).....	52
2.22	Office building with SFRC, Brandon, Florida (SI Concrete Systems).....	52
2.23	Road overlays with SFRC, Houston, Texas (SI Concrete Systems).....	53
2.24	Slabs of an apartment complex with SFRC, Destin, Florida (SI Concrete Systems).....	53
2.25	Storage facility project with PFRC, Destin, Florida (SI Concrete Systems).....	55
2.26	Tilt-up slabs with PFRC, Redmond, Washington (SI Concrete Systems).....	55
2.27	Parking area with PFRC, Mobile, Alabama (SI Concrete Systems).....	57
3.1	Photographs of selected fibers.....	63
3.2	Compressive and tensile strength test set up.....	66
3.3	Flexural toughness test set up.....	70

3.4	MTS 407 controller (load observation).....	70
3.5	Displacement readout box.....	71
4.1	Compressive strength results for specimens with XOREX steel fiber.....	75
4.2	Compressive strength results for specimens with ZP305 steel fiber.....	75
4.3	Compressive strength results for specimens with Harbourite H-330 synthetic fiber.....	76
4.4	Compressive strengths of specimens with 0.5% steel fiber.....	79
4.5	Compressive strengths of specimens with 0.75% steel fiber.....	79
4.6	Compressive strengths of specimens with 1.0% steel fiber.....	80
4.7	Tensile strength results for specimens with XOREX steel fiber.....	80
4.8	Tensile strength results for specimens with ZP305 steel fiber.....	82
4.9	Tensile strength results for specimens with Harbourite H-330 synthetic fiber.....	82
4.10	Tensile strengths of specimens with 0.5% steel fiber.....	84
4.11	Tensile strengths of specimens with 0.75% steel fiber.....	84
4.12	Tensile strengths of specimens with 1.0% steel fiber.....	85
4.13	Failed specimens with 1.0% ZP305 steel fiber.....	85
4.14	Flexural load vs. deflection curves for specimens with XOREX steel fiber.....	86
4.15	Flexural load vs. deflection curves for specimens with ZP305 steel fiber.....	86
4.16	Flexural load vs. deflection curves for specimens with Harbourite H-330 synthetic fiber.....	87
4.17	Flexural toughness specimens after failure.....	87
4.18	Crack development in a beam containing ZP305 steel fibers.....	89
4.19	Influence of fiber type and volume fractions on first crack strengths.....	89

4.20	Influence of fiber types and volume fractions on toughness indices.....	92
4.21	Influence of fiber types and volume fractions on residual strength factors.....	94
5.1	VSL EC 5-7 type anchorage (VSL 2002).....	98
5.2	Configuration of AASHTO test block .....	102
5.3	Schematic diagram of the experimental set up and cyclic loading.....	103
5.4	Test matrix for each fiber configuration.....	106
5.5	Formwork for the AASHTO test block.....	109
5.6	Crack detection microscope.....	111
5.7	Location of crack gages on AASHTO test blocks with lower concrete strengths.....	113
5.8	Location of crack gages on AASHTO test blocks with higher concrete strengths.....	114
5.9	AASHTO cyclic loading test set up.....	115
6.1	Flow chart of the test hierarchy.....	117
6.2	Spiral and skin reinforcement in specimens.....	118
6.3	Failure loads and crack widths for Reinforcement 7, 6-turn spiral, no skin, 1% ZP305 steel fiber, Type 1 concrete.....	123
6.4	Failure loads and crack widths for Reinforcement 2, 3 skin, no spiral, 1% ZP305 steel fiber, Type 1 concrete.....	125
6.5	Typical location of crack formation in AASHTO specimens.....	140
6.6	Horizontal cracks at the upper corner of AASHTO specimen.....	140
6.7	Horizontal and vertical cracks in AASHTO specimen .....	142
6.8	Cracks at the upper face of AASHTO specimen.....	143
6.9	Spalling of concrete in control AASHTO specimen without fibers.....	144

6.10	Failure of a FRC AASHTO specimen.....	144
6.11	Bridging of fibers across cracks.....	145
6.12	Suppression or separation of anchorage at failure.....	146
7.1	VSL type EC 5-7 anchorage.....	157
7.2	Plastic post-tensioning duct.....	159
7.3	ANSYS Model of the AASHTO specimen.....	160
7.4	Anchor head in the AASHTO cyclic loading test.....	162
7.5	Loaded nodes on the AASHTO specimen FEM.....	163
8.1	Crack gages locations on AASHTO specimens.....	166
8.2	Cyclic loads and strains.....	167
8.3	Trend lines for loading and strains in Model 1, Reinforcement 1, Type 2 concrete.....	167
8.4	FEM nodal strain contour for Model 2, Reinforcement 2, Type 2 concrete.....	168
8.5	FEM nodal stress contours in Model 2 specimen, Type 2 concrete, Reinforcement 2.....	171

## ABSTRACT

The secondary spiral and skin reinforcement in the anchorage zone of prestressed post-tensioned girders cause congestion and poses difficulty in the placement of concrete. It is also labor intensive to produce and place the secondary anchorage reinforcement. The objectives of this study was to determine the feasibility of reducing the secondary reinforcement with fibers for post-tensioned anchor zones, because of the expected improvement in mechanical properties of fiber reinforced concrete (FRC) over non-fibrous concrete. The first phase of the test program involved the determination of split tensile strength, compressive strength and flexural toughness of FRC and non-fibrous concrete. Two steel fibers and one synthetic fiber with various amounts were utilized. Steel fibers enhanced the properties of concrete, whereas the role of synthetic fiber was not encouraging. In the second phase, AASHTO Special Anchorage Device Acceptance Test was performed. Variations of spiral and skin reinforcement, with two levels of concrete strengths, were utilized to investigate the performance of the two types and various amounts of steel fibers. The experimental results indicated that 1% steel fiber could be used to replace all the secondary reinforcement for minimum concrete strength of 5900 psi (40.7 MPa), and could reduce a maximum of 79% of the secondary reinforcement for a minimum concrete strength of 4710 psi (32.5 MPa). Lower volumes of steel fibers may also result in reduction of secondary reinforcements. A finite element model of AASHTO test block was also developed to validate the experimental results. Good agreement was found between theoretical and experimental strain values. Usage of steel fiber reinforced concrete in the anchorage zones will result in negligible change in the girder costs.

# CHAPTER 1

## INTRODUCTION

### 1.1. Prestressed Concrete and Anchorage Zone Reinforcement

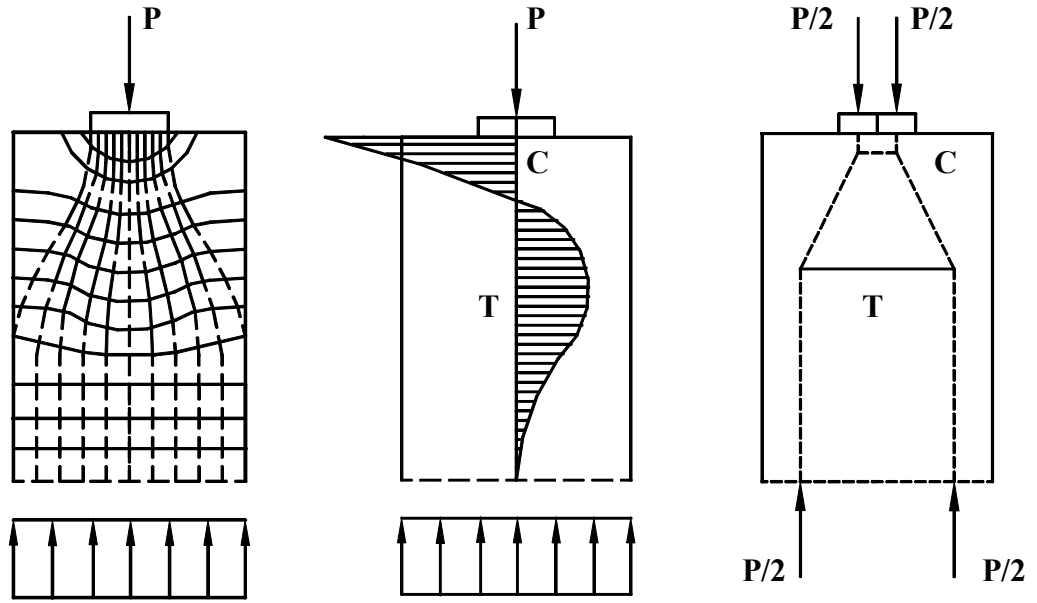
Prestressed concrete is a widely used material for bridge construction. Compared to its compressive strength, the tensile strength of reinforced concrete is limited. Consequently, prestressing becomes essential in many applications in order to fully utilize the compressive strength and, through proper design, to eliminate or control cracking and deflection. The high-technology advancements in the science of materials have made it possible to construct and assemble large-span prestressed concrete systems such as cable-stayed bridges, nuclear reactor vessels, and offshore oil drilling platforms – work hitherto impossible to undertake.

Prestressing of concrete requires the introduction of large, concentrated steel forces into the member. The dispersion of this tendon force induces tensile stresses over some distance ahead of and behind the anchorage. The region affected by the introduction of the tendon force is called the “*Anchorage Zone*”. The concentrated

prestressing force is transferred through anchorage hardware from the tendon onto the concrete and then spreads out to reach a more nearly linear stress distribution over the cross section of the member at some distance from the anchor. Figure 1.1 shows the flow of forces in concentrically loaded anchorage zone. As the compressive stresses spread out, they deviate from the direction parallel to the load. This induces lateral compressive stresses immediately ahead of the anchor and then lateral tensile stresses, which eventually diminish. The lateral tensile stresses are usually referred to as “bursting stresses”. Three critical regions can be identified (Breen *et al* 1994) as follows:

- The region immediately ahead of the load is subjected to large bearing and compressive stresses.
- The bursting zone extends over some distance ahead of the anchorage and is subjected to lateral tensile stresses.
- Local tensile stress concentrations exist along the loaded edge of the member. The tensile stresses along the loaded edge are commonly known as “spalling stresses”, despite the fact that they do not cause any spalling of the concrete.

Figure 1.2 shows the stress contours in the anchorage zone. The magnitude of the compressive stresses is the highest immediately ahead of the anchor, but decreases rapidly as the stresses spread out into the structure. For this reason, proprietary special anchorage devices are frequently used. They enhance the local compressive strength by some form of confinement and/or reduce the bearing pressure by distributing the anchorage force over a series of bearing plates or ribs. The presence of tensile stresses in the concrete, both in the local and in the general zone, results in the potential for cracking in the concrete. Cracking has often been observed when the post-tensioning force is first

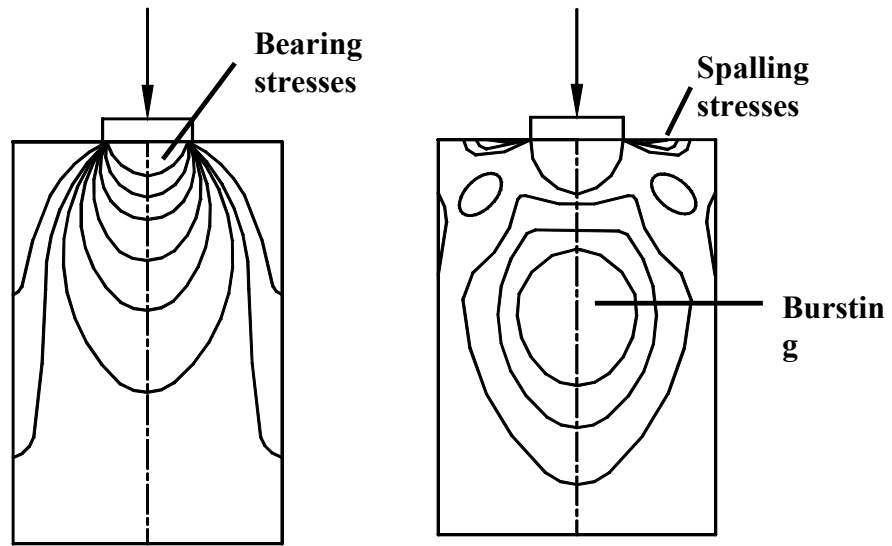


(a) Stress trajectories

(b) Lateral stresses

(c) Load path

**Figure 1.1: Flow of forces in concentrically loaded anchorage zone (Breen *et al* 1994)**



(a) Compression

(b) Tension

**Figure 1.2: Stress contours for concentrically loaded anchorage zone (Breen *et al* 1994)**

applied to the structure. If cracking occurs after the tensile capacity of the concrete is exceeded, it is necessary that a mechanism be available to resist the tensile forces acting in the structure. The use of passive reinforcement is a common and simple solution to resist tensile forces after cracking. If sufficient passive reinforcement is present in the anchorage zone and if it is located in the vicinity of the cracks, the progression and opening of the cracks will be stopped and the forces that were initially carried by the concrete in tension will be transferred to the steel. If, on the other hand, the reinforcement of the anchorage zone is insufficient or inadequately located, the cracks will propagate in the structure until failure of anchorage zone eventually occurs.

Excessive cracking is the most commonly observed problem with anchorage zones, particularly during the stressing of post-tensioning tendons (Breen *et al* 1994). Even if the structure is uncracked after the tendons have been stressed, cracking may still occur at a later stage, due to creep of the concrete or external causes such as differential settlements or temperature effects. The anchorage zone is, therefore, confined with secondary closed stirrups and/or spirals (Fig. 1.3) made of conventional steel rebars to prevent such cracks. Figure 1.4 shows the anchorage zone reinforcement in the bridge girder and the bridge deck for the safe introduction of post-tensioning forces into the concrete.

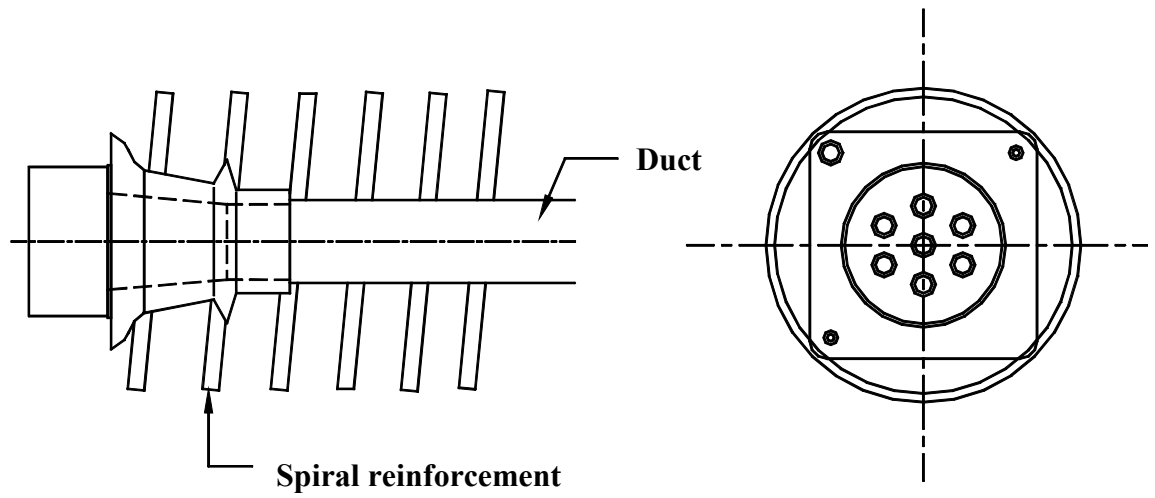
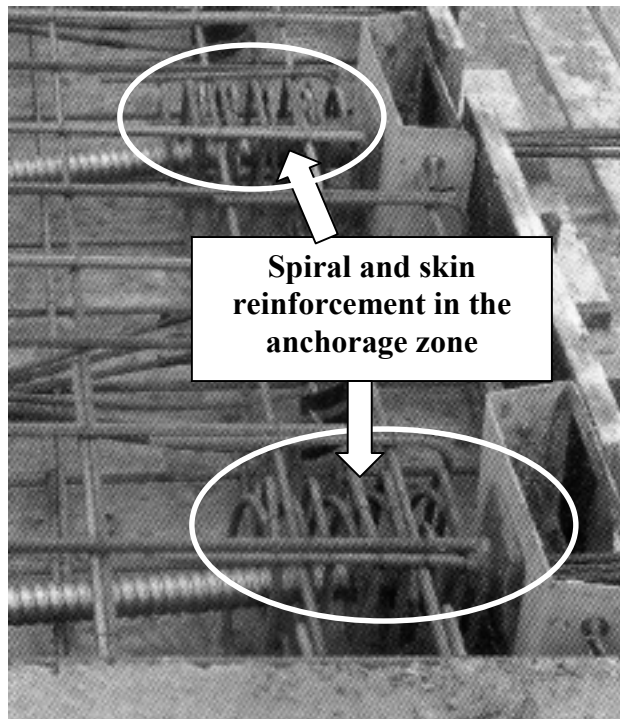


**Figure 1.3: Special anchorage device**



**(a) Bridge girder**



**(b) Bridge deck**

**Figure 1.4: Anchorage zone reinforcement**

## 1.2. Failure of the Anchorage Zone

Failure of the anchorage zone occurs when no stable state of equilibrium can develop to resist the tendon force. Three principal modes of failure may be observed in anchorage zones of precast prestressed concrete girders (Burdet 1990):

- The first mode of failure is a local failure in the immediate vicinity of the anchorage device, similar to the punching of an isolated foundation. The surface of rupture is often in the shape of a pyramid or cone. The failure is caused by insufficient compressive strength of concrete, or from lack of confining reinforcement.
- The second mode of failure may occur away from the anchorage device at a distance about one half the depth of the member. It is characterized by large cracks running parallel to the post-tensioning duct extending from the anchorage. This mode of failure is caused by the inability of the transverse reinforcement to resist the transverse tensile forces in the concrete due to the lateral spreading of the post-tensioning force. This failure can occur at the time of first cracking or during subsequent loading.
- The third mode of failure may take place at the interface between concrete surrounded by confining reinforcement in the immediate vicinity of the anchorage device and unconfined concrete. As it involves a failure of concrete in compression, this mode of failure is similar to the first mode of failure. The main difference is that it occurs at a greater distance from the anchorage device. This

mode of failure is characterized by cracks in the vicinity of the anchorage device and a bulging out of the concrete cover.

As observed in tests by Sanders (1990) and Stone (1983), all three failure mechanisms exhibit a rather brittle behavior, even when the failure involves yielding of reinforcing steel. Because of this lack of ductility, any failure involving anchorage zones is undesirable. Ideally, the anchorage zones should be designed to safely transfer the tendon forces developed at ultimate stages, allowing a more ductile mode of failure to occur in another part of the girder.

The number of reported failures in the anchorage zones is significantly less than the number of reported cases where cracking occurred (Breen *et al* 1994). Two main reasons can account for this trend. The first is the inherent toughness of anchorage zones. The load carrying mechanism exhibited by anchorage zones is complex. Tests have shown that even apparently unimportant parts of the structure, such as uncracked concrete in the general zone or reinforcing bars located at a large distance from the anchorage, can resist significant forces. Although these factors are not taken into account in design, they can significantly enhance the strength of the anchorage zone. The second factor that can explain the small number of reported failures is the fact that, because the construction stage is generally the most critical case for anchorage zones, failure is likely to occur during construction. If a failure occurs during this phase, it will probably be promptly repaired and essentially unreported.

### 1.3. Fiber Reinforced Concrete

Portland cement concrete is a relatively brittle, nonductile material. Unreinforced concrete cracks when subjected to tensile stresses. This problem has been solved by placing steel reinforcing bars within the concrete to carry the tensile stresses. Deterioration and failure of concrete are closely related to the formation of cracks and micro cracks due to load and environmental effects. Thermal and moisture movement in cement paste produces micro cracks prior to loading. These are largely concentrated at the interface of coarse aggregates. As a result of environmental effects and loading, micro cracks propagate and eventually group and concentrate to form cracks. Dispersed short fibers enhance the durability of concrete through suppression and stabilization of micro cracks. Fibers also resist the widening and propagation of cracks.

For over two decades, fiber reinforced concrete (FRC) has gradually grown to worldwide acceptance as a construction material that exhibits increased dynamic force resistance and reduced cracking, which is known as toughness. FRC has been effectively used in shotcrete, precast concrete, slabs, pavements, metal decks/concrete floors, seismic structures and concrete repairs.

FRC has been found to have significantly better crack resistance, ductility, modulus of rupture, shear strength, torsional strength, fatigue endurance, abrasion resistance and energy absorption capabilities, as compared to plain concrete. Several studies have documented the application of FRC in structures (Vondran 1991, Naaman 1998, Richard *et al* 1998). It has been found that the shear strengths in FRC beams are at least comparable to that of beams with conventional stirrups (Narayanan and Darwish

1987). Methods of analysis and design for FRC beams have been proposed (ACI 1997, Casanova and Rossi 1997).

Suitable fibers for reinforcing concrete have been produced from steel, nylon, plastic, glass, and natural materials in various shapes and sizes. Naturally occurring asbestos fibers and vegetable fibers, such as sisal and jute, are also used for reinforcement. The concrete matrices may be mortars, normally proportioned mixes, or mixes specifically formulated for a particular application.

#### **1.4. Specific Problems with Bridges**

In general, post-tensioned concrete bridges have optimally designed small cross sections to limit the dead weight of the structure. The dimensions of the webs can often be reduced because the shear force is partly resisted by post-tensioning forces. However, as the web becomes thinner, the space to place anchorage devices, confining reinforcement, shear reinforcement and general zone reinforcement becomes very congested, complicating the construction process and the casting of the concrete.

Highway bridges are located outdoors, in potentially corrosive exposed environment. Any crack can let corrosive mediums seep into the structure and attack the reinforcing steel. This is especially critical for girder ends. To reduce corrosion of the reinforcement and degradation of the concrete, it is generally desirable to limit cracking in concrete bridge structures.

## 1.5. Objectives of the Study

Most damages to anchorage zones in post-tensioned concrete structures occur during construction, when large tendon stressing forces are applied to usually immature concrete. As described earlier, a considerable amount of spiral and skin reinforcement is required at the end zones of a prestressed bridge girder. Reinforcement congestion in the anchorage zone is a frequent cause for poor concrete consolidation, resulting in failures caused by crushing of the concrete ahead of the anchor (Libby 1976). Congested anchorage zone details also complicate placing of the reinforcement. Various reinforcement components used in close proximity cause congestion in the anchorage zone, posing difficulty in the placement of concrete, anchorages and post-tensioning ducts. It is also labor intensive to produce and place the secondary anchorage reinforcement. FRC possesses better properties, such as tension, compression, shear, bond, flexural toughness and ductility than conventional concrete. Therefore, it may be possible to utilise FRC in the end zones of prestressed bridge girders to reduce the amount of secondary reinforcement. This study theoretically and experimentally investigated such application of FRC. The objectives of the study are:

- To establish various properties FRC of relevance to bridge design.
- To select adequate synthetic or steel fibers for application in anchorage zones.
- To experimentally determine the feasibility of reducing or eliminating the secondary reinforcement with synthetic or steel fibers for post-tensioned anchor zones.

- To perform theoretical validation of the feasibility of FRC application in anchorage zones.
- To make a cost comparison between fiber reinforced and conventionally constructed girders, based on both material and labor costs.

## **1.6. Scope of the Study**

The study examined the feasibility of using fiber reinforced concrete in the end zones of the girder. This research initiated with the evaluation of mechanical properties of FRC using both synthetic and steel fibers. Properties of concrete without fiber and FRC were then compared. This work helped in understanding the structural properties of FRC. The understanding of these various properties of FRC helped in selecting fibers for further evaluation. AASHTO acceptance test for anchorage zones was subsequently utilized.

This study considers the effect of fiber reinforced concrete only in the local anchorage zone. The effect of FRC in the general anchorage zone is beyond the scope of this study.

## **CHAPTER 2**

### **BACKGROUND REVIEW**

#### **2.1. Anchorage Zones in Prestressed Concrete**

Tendons in prestressed concrete are typically stressed to very high stresses. These tendons need to be anchored at their ends in order to transfer (compressive) force to the concrete. In pretensioned concrete, the anchorage consists of a bonded length of tendon, in direct contact with the concrete. In post-tensioned concrete, an anchorage plate is used, which bears onto the concrete over a relatively small area. It is not rare for an anchorage device with a cross-sectional area of one square foot ( $0.093 \text{ m}^2$ ) and weighing only 20 pounds (9.1 kg) to transfer a tendon force of 300,000 pounds (6740 N).

The tendon is connected to the plate either through wedges, button-heads or other methods. The plates employed for this are much smaller than the area of concrete in compression. Therefore, a redistribution of stress occurs behind the anchorage plate as the compression trajectories spread out to form uniform stress patterns some distance into the concrete according to Saint Venant's Principle (Breen *et al* 1994). It is the distance

over which this redistribution occurs that is of interest to the Engineer. This disturbed region is known as the *Anchorage Zone*.

## **2.2. Local Zone and General Zone**

The main concerns in the anchorage zone design are the high compressive stresses immediately ahead of the anchorage device and tensile stresses in the remainder of the anchorage zone. Breen *et al* (1987) proposed the division of anchorage zones in two regions, as shown in Fig. 2.1. The region of very high compressive stresses immediately ahead of the anchorage device is the *local zone*, and the region subjected to tensile stresses due to spreading of the concentrated tendon force into the structure is the *general zone*.

Anchorage zones for post-tensioning tendons are regions of dual responsibility, which is shared between the engineer of record and the supplier of the post-tensioning system. The post-tensioning system supplier is usually responsible for the design of the anchorage device and the local zone surrounding the device (Wollmann and Roberts-Wollmann 2000). Included in this responsibility is the proper performance of the bearing plate and the local zone confinement reinforcement. The local zone confinement reinforcement is system dependent and an integral part of the anchorage device. Therefore, this reinforcement must be furnished by the post-tensioning system supplier. The engineer of record, on the other hand, is responsible for the design of the general zone, which surrounds the local zone.

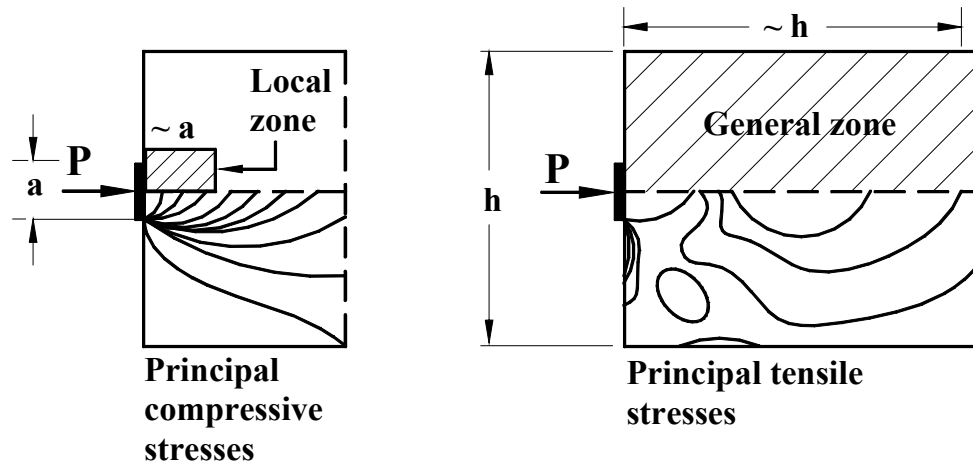


Figure 2.1: Local and general anchorage zone

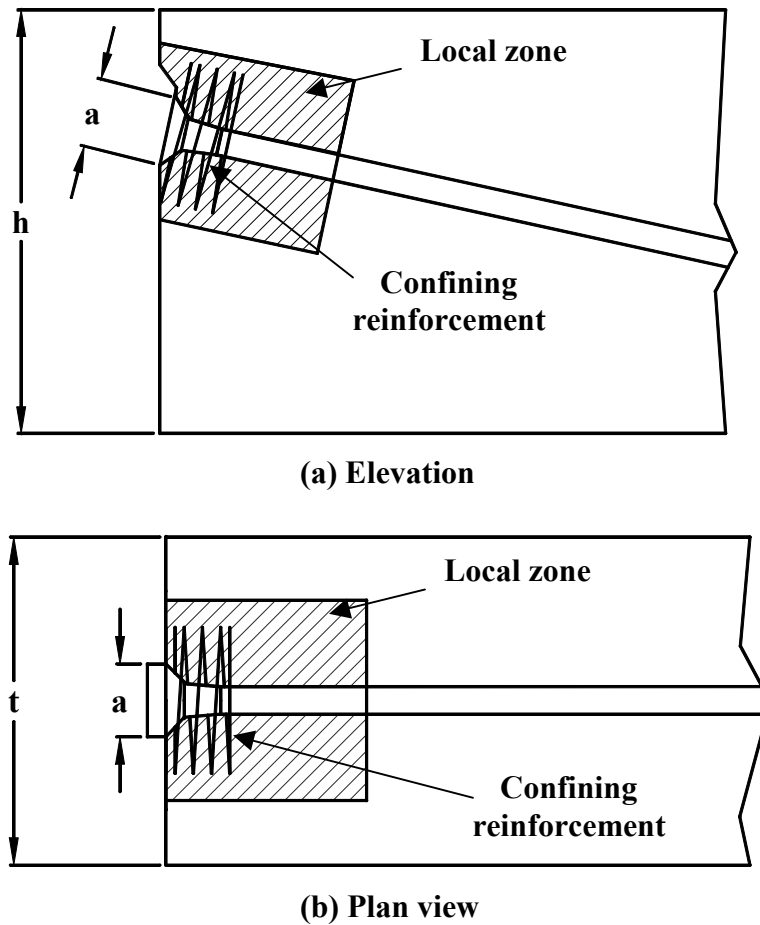


Figure 2.2: Definition of the local zone (Burdet 1990)

### **2.2.1. Local Zone**

The local zone may be defined as the volume of concrete surrounding and immediately ahead of the anchorage device through which the concentrated force applied to the anchorage device is transferred to the general zone. It encompasses the region in which concrete compressive stresses exceed acceptable values for design and detailing of this region in the presence of very high compressive stresses.

As the local zone is very close to the anchorage device, as shown in Fig. 2.2, its behavior is strongly influenced by the specific characteristics of the anchorage device. The geometry and the states of stress of the local zone are very complex, because of the duct hole, the confining reinforcement and the large tendon force. Large localized compressive stresses act at the interface between the anchorage device and the concrete of the local zone, and tensile hoop stresses are induced by the lateral spreading of the concentrated tendon force. Concrete may fail due to the compressive stress, with a surface of rupture generally in the form of a cone or a pyramid. The first mode of failure occurs in the local zone. The failure of the local zone may occur due to the lack of confinement, which can be provided either by confining reinforcement or by surrounding concrete, allowing large lateral stresses to develop. The principal parameters governing the behavior of the local zone are the nominal bearing stress ahead of the anchorage device and the amount of confining reinforcement. The local zone must resist the very high local pressures introduced by the anchorage device and transfer them to the general zone.

### 2.2.2. Dimensions of the Local Anchorage Zone

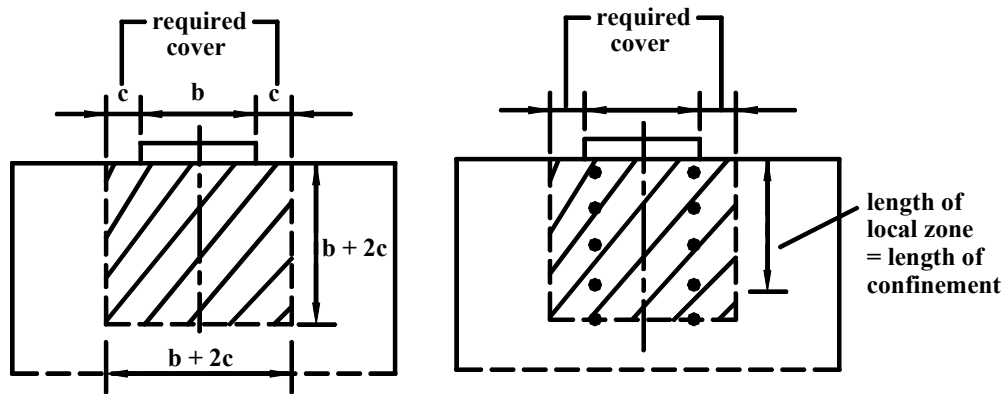
AASHTO (1996) gives detailed definitions of the local zone dimensions for isolated bearing plates. These definitions are tied to the specific anchorage device's dimensions and the supplier's specifications regarding minimum spacing and edge distance (Fig. 2.3). AASHTO (1996), Article 9.21.7, establishes the length of the local zone for special bearing plates as the greater of (Fig. 2.3.c):

1. Maximum width of the local zone
2. Length of the anchorage device confinement reinforcement
3. For anchorages with multiple bearing surfaces, the distance from the loaded concrete surface to the bottom of each bearing surface plus a length equal to the maximum dimension of that bearing surface.

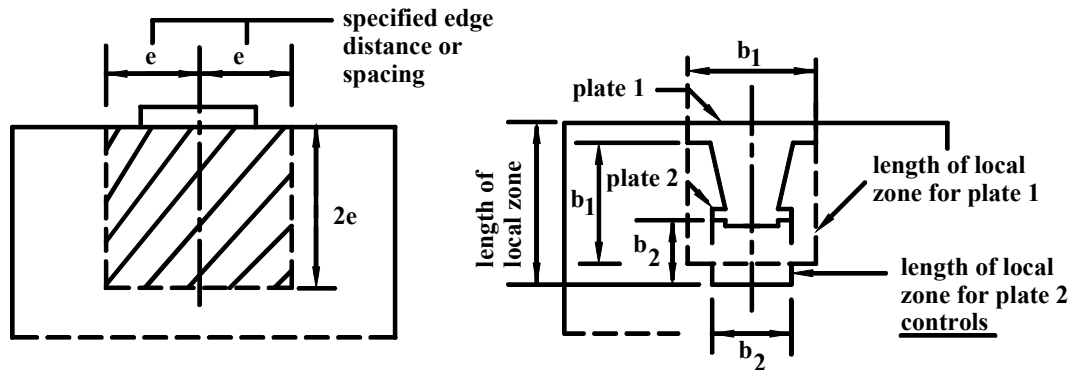
In no case shall the length of the local zone be greater than 1.5 times the width of the local zone. This requirement restricts the length of multiplane bearing plates and their integral confinement reinforcement.

The local zone dimensions described above depend on the dimensions and specifications provided by the post-tensioning supplier. However, the supplier is typically not known during the design phase. Equation 2.1 provides a simple way to obtain a preliminary estimate for the minimum local zone area from which minimum edge distance and center-to-center spacing may be derived (Wollmann and Roberts-Wollmann 2000). This requirement is independent of the geometry of the actual anchorage device. However, the tendon force must still be known.

$$A_{lz} = \frac{1.15A_{ps}f'_s}{f'_{ci}} \quad (2.1)$$



(a) Manufacturer's recommendations not available



(b) Manufacturer's recommendations available

(c) Length of local zone for multiple bearing plates

Figure 2.3: AASHTO local zone definitions for special bearing plates (Breen *et al* 1994)

where,  $A_{lz}$  = area of the local zone

$A_{ps}$  = nominal prestressing steel area

$f_s$  = nominal minimum tensile strength of prestressing steel

$f_{ci}$  = concrete cylinder strength at the time of jacking

### **2.2.3. Local Zone Reinforcement**

As mentioned earlier, proprietary special anchorage devices with complex geometries and or local confinement reinforcement are frequently used to increase the bearing strength of the concrete. Acceptance of such anchorage devices should be based on their performance in a standardized acceptance test. AASHTO describes “Special Anchorage Device Acceptance Test” (AASHTO 1998) for the acceptance of anchorage devices. The idea of this test is to prove that the anchorage zone is capable of transferring forces to the concrete without premature failure of the concrete or bursting reinforcement. It considers both the serviceability and ultimate behavior of the anchorage device as its performance criteria. According to AASHTO (1998), the test specimen allows the anchorage device to have confining reinforcement as well as the supplementary skin reinforcement in the test prism. However, identical confining reinforcement and equivalent supplementary reinforcement must be present in the actual structural application.

Roberts (1990) conducted a detailed study on behavior and design of local zones. The detailed tests showed that it was possible to accurately and conservatively express the ultimate load capacity of local zone by the following equation:

$$F_{ult} = 0.8f'_c \sqrt{\frac{A}{A_b}} (A_b) + 4.1f_{lat} A_{core} \left(1 - \frac{s}{D}\right)^2 \quad (2.2)$$

where,  $F_{ult}$  = ultimate load capacity of local zones

$f'_c$  = compressive strength of concrete

$A$  = net are of concrete supporting the bearing plate

$A_b$  = net area of the bearing plate

$f_{lat}$  = lateral pressure

$A_{core}$  = area of the compressive core

$s$  = pitch of the confining reinforcement

$D$  = diameter of the confining reinforcement

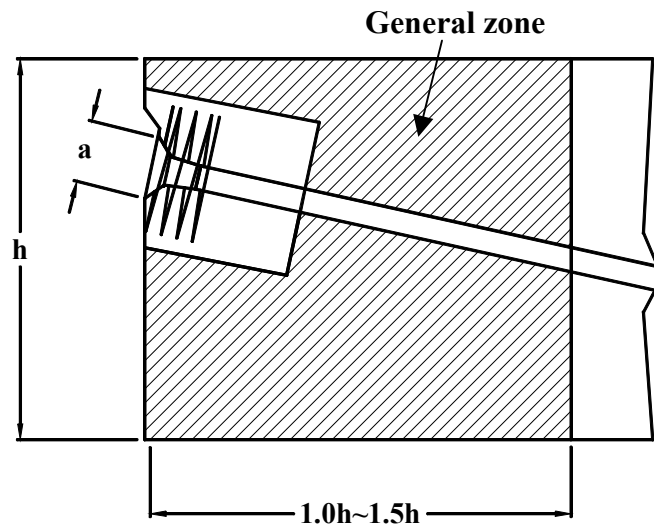
This equation is useful for preliminary evaluation of local zone capacity and for sizing confining reinforcement, but it does not address the problem of serviceability. A good estimation of ultimate capacity does not ensure satisfactory condition of the local zone at service loads. Therefore, “Special Anchorage Device Acceptance Test” is a must to ensure proper local zone behavior. The detailed procedure and acceptance criteria for this test are described in Chapter 5.

It is the responsibility of the anchorage device supplier to furnish hardware that can pass such an acceptance test. The anchorage device supplier should submit all information concerning details required to ensure satisfactory performance of the local zone to the engineer of record and to the contractor. This includes record of the anchorage device acceptance test and information on required confinement and auxiliary reinforcement, minimum edge distance and anchor spacing, and minimum concrete strength at time of stressing.

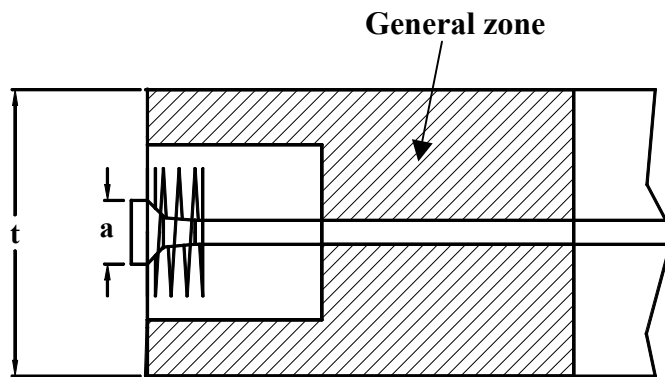
#### **2.2.4. General Zone**

The general zone is the region of the structure ahead of and behind the tendon anchorage device where the linear stress distribution of ordinary beam theory is distributed by the introduction of the concentrated tendon force. Figure 2.4 shows the general zone of a structure.

The second mode of failure may occur in the general zone, when a tensile crack may form along the tendon path at some distance ahead of the anchorage device. The state of tensile stresses in the general zone exhibits several characteristics, as shown in Fig. 2.5. The tensile stresses that act perpendicular to the tendon path in the concrete ahead of the anchorage plate are called bursting stresses. The tensile stresses that act parallel to the surface of the anchorage plate are called spalling stresses. Bursting stresses are caused by the lateral spreading of the tendon force from the concentrated location of the anchorage device to the entire cross section. Spalling stresses are mainly caused by the condition of compatibility of displacements. When these tensile stresses exceed the modulus of rupture of concrete, bursting or spalling cracks occur in the anchorage zone. After extension of the cracks along the tendon path, the reinforcing steel crossing the crack is highly stressed, and eventually yields. The cracks extend until no additional strength is available or the local deformation capacity of the anchorage zone is exhausted. At this point the failure of the anchorage zone occurs. To resist these cracks, vertical reinforcement must be provided.



(a) Elevation



(b) Plan view

Figure 2.4: Definition of the general zone (Burdet 1990)

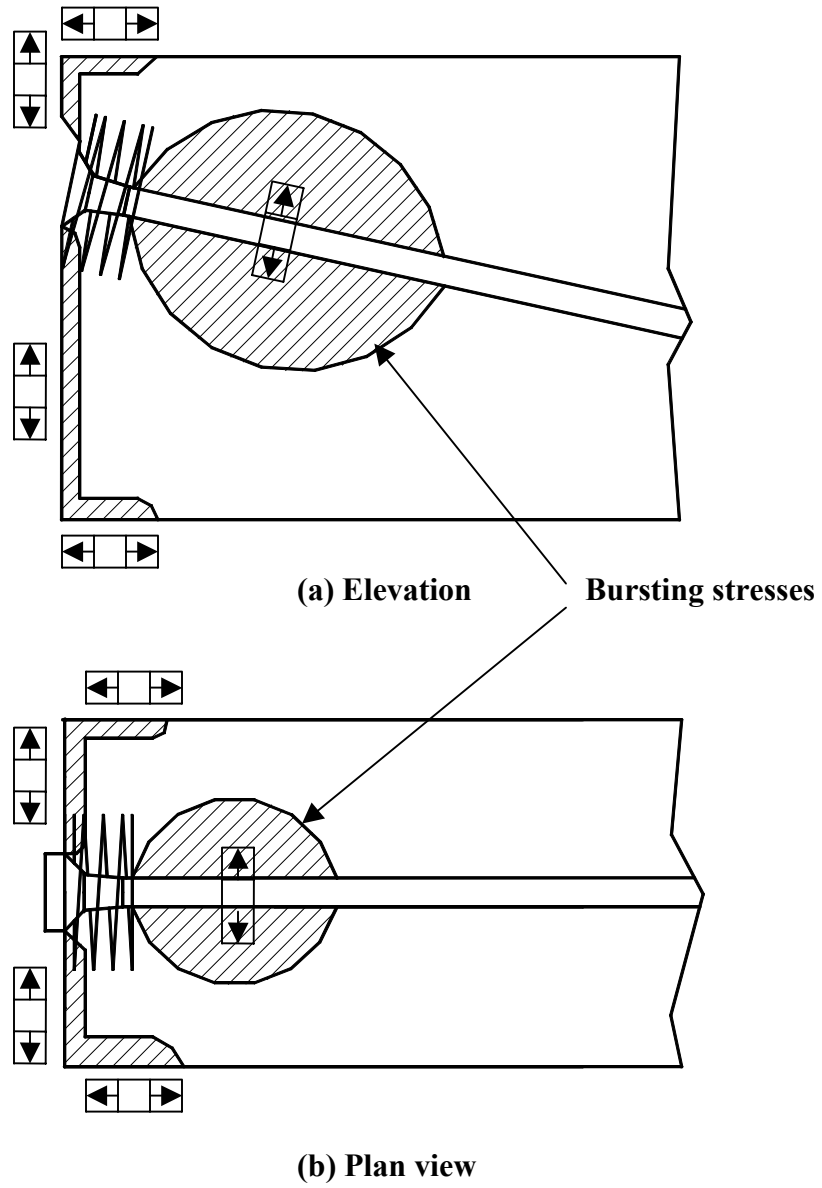


**Figure 2.5: State of tensile stresses in the general zone (Burdet 1990)**

### **2.2.5. Dimensions of the General Zone**

For beam type members, the general dimensions of the General Zone (Wollmann and Roberts-Wollmann 2000) may be taken as:

1. Length equal to the largest cross-sectional dimension of the member.
2. Depth and width equal to those of the member.

### **2.2.6. Interface Between Local and General Zones**

At the interface between the local zone and the general zone, the tendon force is transmitted from the confined concrete of the local zone to the concrete of the general zone. Depending on the size of the anchorage device and on the confining reinforcement provided in the local zone, the level of stresses at the interface between the local zone and the general zone can be very high. The third mode of failure may occur at the interface between the concrete of the local zone and the concrete of the general zone. The failure is caused by an excessive level of compressive stress transmitted from the concrete of the general zone, which is generally confined.

## **2.3. Fiber Reinforced Concrete**

Fiber reinforced concrete (FRC) is primarily made of hydraulic cements, fine and coarse aggregate, and discontinuous discrete reinforcing fibers. Fibers suitable for reinforcing concrete have been produced from steel, plastic, glass, and natural materials in various shapes and sizes. Naturally occurring asbestos fibers and vegetable fibers, such as sisal and jute, are also used for reinforcement. The concrete matrices may be mortars,

normally proportioned mixes, or mixes specifically formulated for a particular application.

A fiber contributes to the load carrying capacity of a body, which consists of a fiber embedded in a surrounding matrix. The load is transferred through the matrix to the fiber by shear deformation at the fiber-matrix interface (Beaudoin 1990). The load transfer arises, generally, as a result of the different physical properties of the fiber and the matrix, e.g. the different modulus of elasticity values of the fiber and the matrix.

### **2.3.1. Basic Concepts of Fiber Reinforced Concrete**

Concrete is very brittle under tensile stresses and impact loads. The cause of concrete cracks are due to the inherent tensile weakness of the material. Unreinforced concrete has a low tensile strength and a low strain capacity at fracture. These shortcomings are traditionally overcome by adding reinforcing bars or prestressing steel. It may be very labor intensive and time consuming to place all necessary regular reinforcement.

Brittle materials are considered to have no significant post-peak ductility. Fibers bridge across the concrete matrix (Fig. 2.6) helping to control shrinkage cracking during the plastic stage and matrix micro cracks that occur as the concrete is loaded. This helps to add post-cracking ductility to concrete. Fibrous composites have been and are being developed to provide improved mechanical properties to otherwise brittle materials. When subjected to tension, these unreinforced brittle matrices initially deform elastically. Micro cracking, localized micro cracking, and fracture follow the elastic response. Introduction of fibers into the concrete results in post-elastic property changes

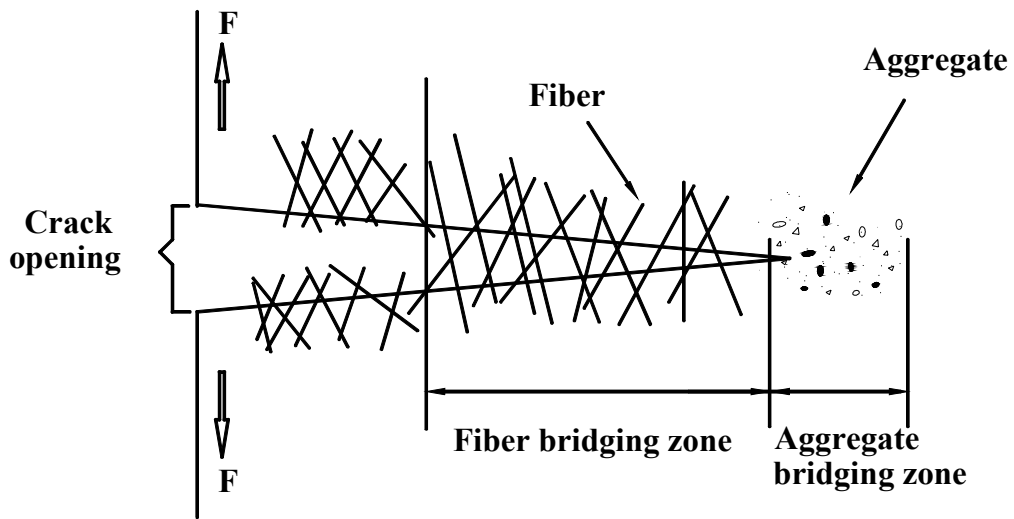


**Figure 2.6: Fibers bridging across a concrete crack (Beaudoin 1990)**

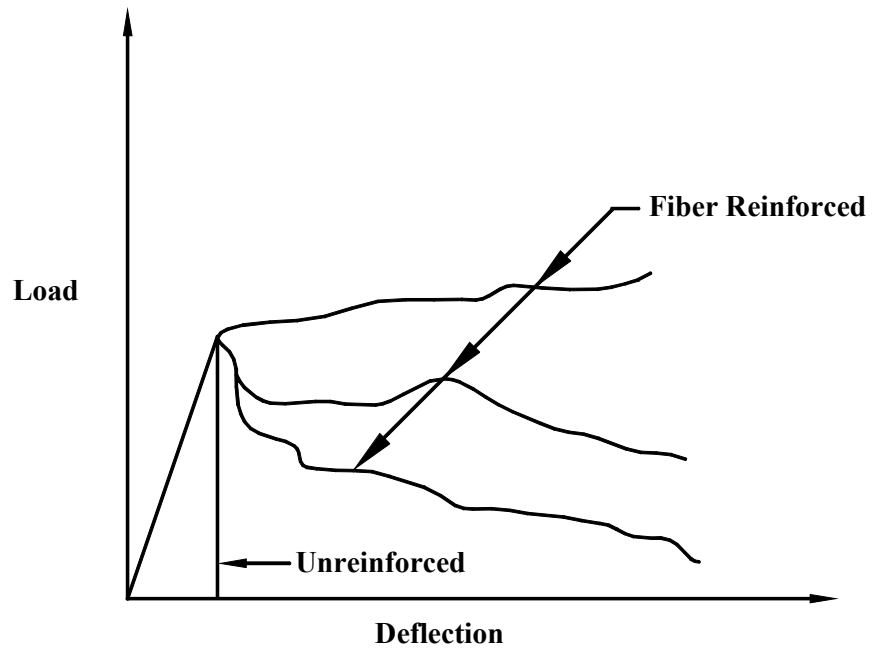


**Figure 2.7: Load versus deflection curves for unreinforced and fiber reinforced concrete (ACI 544.1R 1996)**

that range from subtle to substantial, depending upon a number of factors, including matrix strength, fiber type, fiber modulus, fiber aspect ratio, fiber strength, fiber surface bonding characteristics, fiber content, fiber orientation, and aggregate size effects. Figure 2.7 shows typical load-deflection curves for unreinforced and fiber reinforced concrete.

If properly engineered, one of the greatest benefits to be gained by using fiber reinforcement is improved long-term serviceability of the structure. One aspect of serviceability that can be enhanced by the use of fibers is control of cracking. Fibers can prevent the occurrence of large crack widths that are either unsightly or permit water contaminants to enter, causing corrosion of reinforcing steel or potential deterioration of concrete (Shah 1991). In addition to crack control and serviceability benefits, use of fibers at high volume percentages can substantially increase the matrix tensile strength (Shah 1991).

### **2.3.2. History of Fibers**

It has been found that the use of natural fibers was popular among the ancient people in various civilizations. They used straw, bamboo fibers in lime and soil mortar, which is still seen in some parts of the world. In the modern time, the possibility of steel fiber usage was first raised by Porter in 1910 (Naaman 1985). During the early 1960s in the United States, the first major investigation was made to evaluate the potential of steel fibers as a reinforcement for concrete (Romualdi and Batson 1963). The usage of glass fibers was documented in USSR in the late 1950s (Biryukovich and Yu 1965). Synthetic fibers were investigated as a component of constructional materials in 1965 (Goldfein 1965). Initially, 1.5 – 2% straight fibers by volume were used and were found

to be less workable. Later, deformed steel fibers with increased fine aggregate and water reducing admixtures were used for increasing workability.

### **2.3.3. Types of Fibers**

Numerous fiber types are currently available for commercial and experimental use. The basic fiber categories are steel, glass, synthetic, and natural fibers. Figures 2.8, 2.9 and 2.10 show photographs of steel, glass and synthetic fibers, respectively.

Generally, steel fiber reinforced concrete should be used in a supplementary role to inhibit cracking, to improve resistance to impact or dynamic loading, or to resist material disintegration (ACI 544.3R 1993). Synthetic fiber reinforced concrete should be applied to non-structural and non-primary load bearing applications (ACI 544.1R 1996). On the other hand, glass fiber reinforced concrete should be used in non-structural architectural cladding and other concrete products (ACI 544.1R 1996) and combined with mortar instead of concrete (Materschläger and Bergmeister 1998). The process to apply the glass fiber reinforced concrete (spray-up process) is not a conventional concrete operation. At present, the spray process accounts for the majority of all manufactured glass fiber reinforced concrete products in the United States (ACI 544.1R 1996). So, in the present study, only steel and synthetic (polypropylene) FRC were used and are discussed in this literature review.

### **2.3.4. Advantages of Fiber Reinforced Concrete**

The replacement of conventional rebar with fiber reinforcement has many structural advantages:

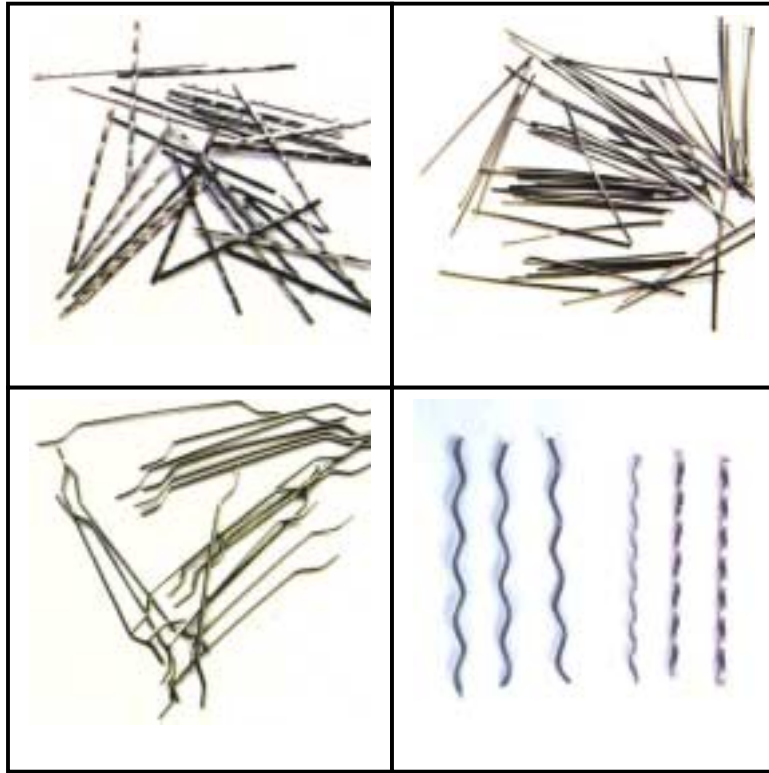


**Figure 2.8: Various types of steel fibers**

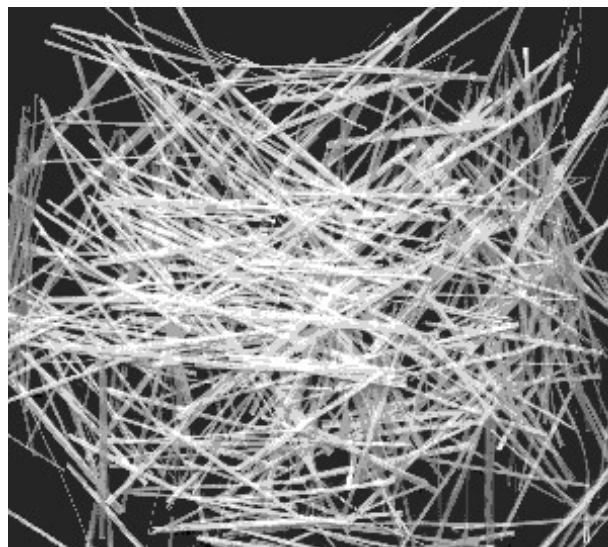


**Figure 2.9: Glass fiber**

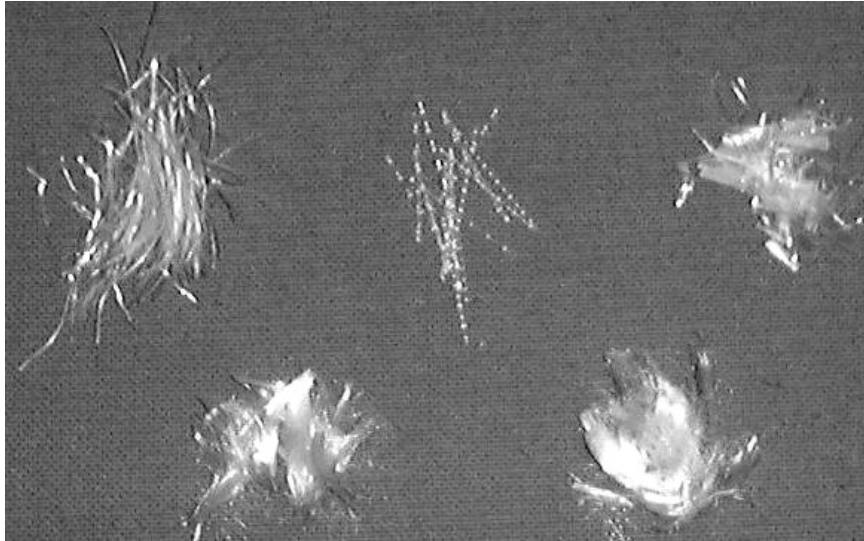


**Figure 2.10: Various types of synthetic fibers**



**Figure 2.11: Fracture surface of steel fiber reinforced concrete**

- Fibers enhance the flexural strength, shear strength, ductility, toughness and energy absorption capacity of concrete.
- With fibers, the internal stresses are much more evenly distributed throughout the cross section of the structure and along the length of the in-place concrete (Grzybowski 1989). Fibers provide multi-directional concrete reinforcement. Figure 2.11 shows the distribution of steel fibers in a FRC fractured member.
- Fibers prevent micro cracks, and thus protect the porous concrete from further aggressive environmental attack. Large visible cracks may occur with conventionally reinforced concrete. Even if a fiber reinforced structure cracks, the cracks are micro in size, or small enough to make them invisible and acceptable in width (Grzybowski 1989).
- Fibers reduce the increase in permeability due to cracking in concrete (Rapoport *et al* 2001).
- The starting time of cracking in concrete is delayed with the addition of fiber (Grzybowski and Shah 1990).
- Fibers are most effective in contributing to the post-cracking resistance of cementitious composites by bridging the cracks and providing restraint to their opening (Beaudoin 1990).
- The chance of corrosion is more in case of concrete reinforced with steel bars than that reinforced with steel fibers. Since fibers are short, discontinuous, and rarely touch each other, there is no continuous path for currents from electromotive potential between different areas of concrete (ACI 544.1R 1996).

- Replacing non-structural conventional steel rebar or wire mesh with SFRC eliminates the time consuming work of placing rebars (ACI 544.1R 1996). It also eliminates the need to bend and tie rebar or mesh. So it saves labor costs and time of a project.
- Most steel fiber reinforced concrete uses ordinary mixing, placing and finishing methods and equipment. So no special equipment to install reinforcement is needed (ACI 544.1R 1996).

## **2.4. Steel Fiber Reinforced Concrete (SFRC)**

SFRC is the concrete made of hydraulic cements containing fine or fine and coarse aggregate and discontinuous discrete steel fibers. Steel fibers intended for reinforcing concrete are defined as short, discrete lengths of steel having an aspect ratio (ratio of length to diameter) from about 20 to 100, with any of several cross-sections, and that are sufficiently small to be randomly dispersed in an unhardened concrete mixture using usual mixing procedures (ACI 544.1R 1996). Figure 2.12 shows various geometries of steel fibers used in concrete.

### **2.4.1. Properties of Steel Fibers**

The mechanical properties of steel fiber concrete are influenced by the type of fiber, length-to-diameter ratio (aspect ratio), the amount of fiber, the strength of the matrix, the size, shape, and method of preparation of the specimen, and the size of aggregate.

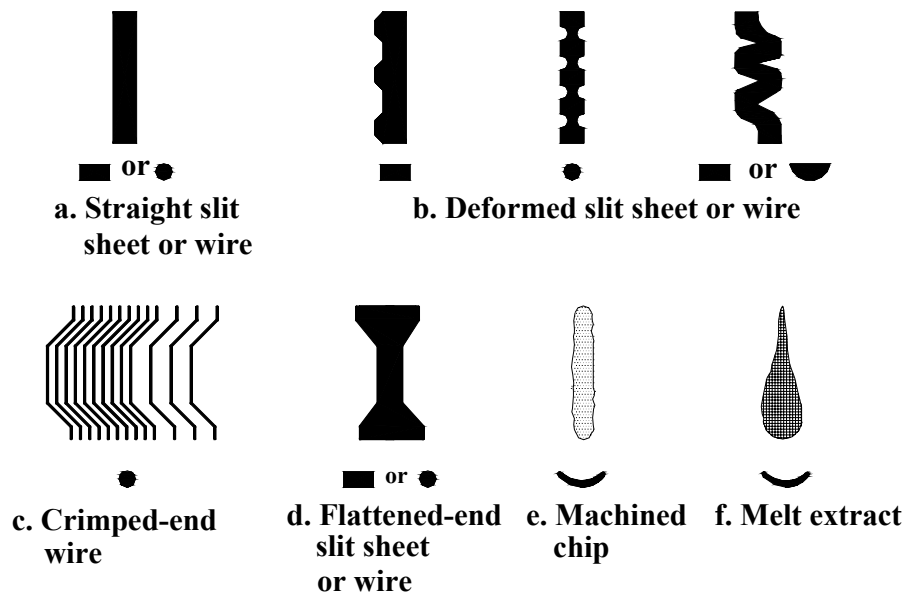


Figure 2.12: Various geometries of steel fibers (ACI 544.1R 1996)

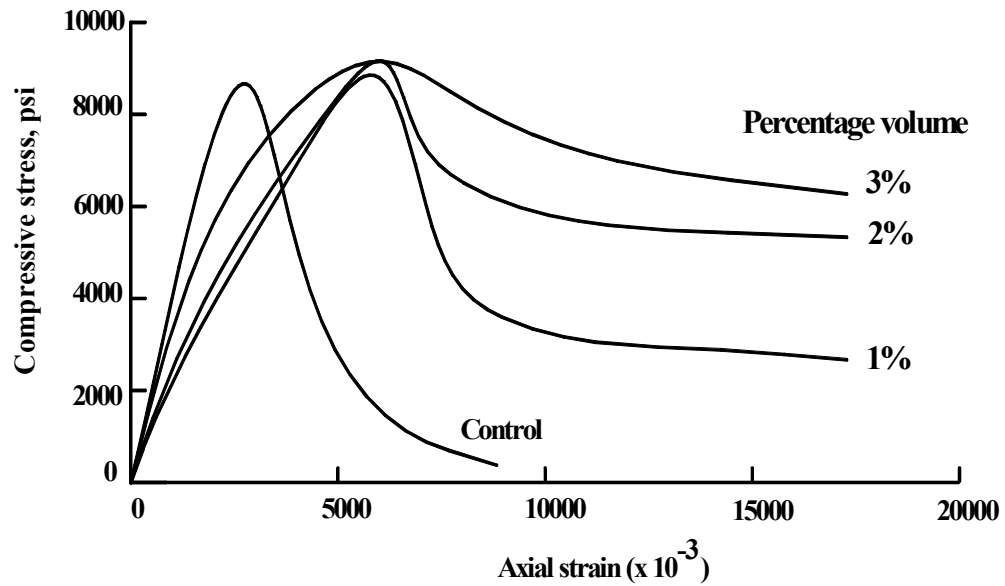


Figure 2.13: Influence of steel fiber volume on compressive stress-strain diagram

Fiber influences the mechanical properties of concrete in all failure modes (Gopalaratnam and Shah 1987), especially those that induce fatigue and tensile stress, e.g., direct tension, bending, impact, and shear. The strengthening mechanism of fibers involves transfer of stress from the matrix if the fiber surface is deformed. Thus, stress is shared by the fiber and matrix in tension until the matrix cracks, and then the total stress is progressively transferred to the fibers.

### **Compression**

In compression, the ultimate strength is only slightly affected by the presence of fibers. In case of steel fibers, an addition of up to 1.5% by volume increases the compressive strength from 0 to 15% (Johnston 1974, Dixon and Mayfield 1971). Figure 2.13 shows typical stress strain curves for SFRC in compression with various fiber ratios (Shah *et al* 1978). In these curves, a substantial increase in the strain at the peak stress may be noted, and the slope of the descending portion is less steep than that of control specimens without fibers, which is indicative of substantially higher toughness.

### **Direct Tension**

Behavior of concrete under increasing tensile stresses is dominated by the gradual growth and interconnection of internal flaws, such as micro cracks (Romualdi and Mandel 1964, McKee 1969). The ultimate tensile strength is reached when the internal flaw system grows to an unstable situation in which it can propagate catastrophically under tensile stresses. Restraining the internal flaws locally and preventing them from extending into the adjacent material can be achieved by using FRC. Hence, it is expected that the tensile strength of SFRC will be increased substantially. In direct tension, the

improvement in strength is significant, with increases in the order of 30 to 40% reported for the addition of 1.5% by volume of fibers (Williamson 1974).

Figure 2.14 shows typical stress strain curves for steel fiber reinforced mortar in tension (Shah *et al* 1978). The ascending part of the curve up to the first cracking is similar to that of unreinforced mortar. The descending part depends on the fiber reinforcing parameters, specially fiber shape, fiber amount and aspect ratio.

### **Shear**

Various researchers have shown that the inclusion of steel fibers in reinforced concrete beams results in a substantial increase in their shear strengths (Barr 1987, Narayanan and Darwish 1987, Oh *et al* 1999). For 1% volume of fibers, an increase of up to 170% in ultimate shear strengths was reported (Narayanan and Darwish 1987). Steel fibers have several potential advantages when used to replace vertical stirrups in beams (Williamson 1978). These advantages are: (1) the random distribution of fibers throughout the volume of concrete at much closer spacing than is practical for the smallest reinforcing bars which can lead to distributed cracking with reduced crack size; (2) the first crack tensile strength and the ultimate tensile strength of concrete may be increased by the fibers; and (3) the shear-friction strength is increased by resistance to pullout and by fibers bridging cracks.

Narayanan and Darwish (1987) reported the following conclusions from their experimental observations:

- The spacing of cracks in fiber concrete beams was reduced to a fifth of that in the companion beams with or without stirrups.

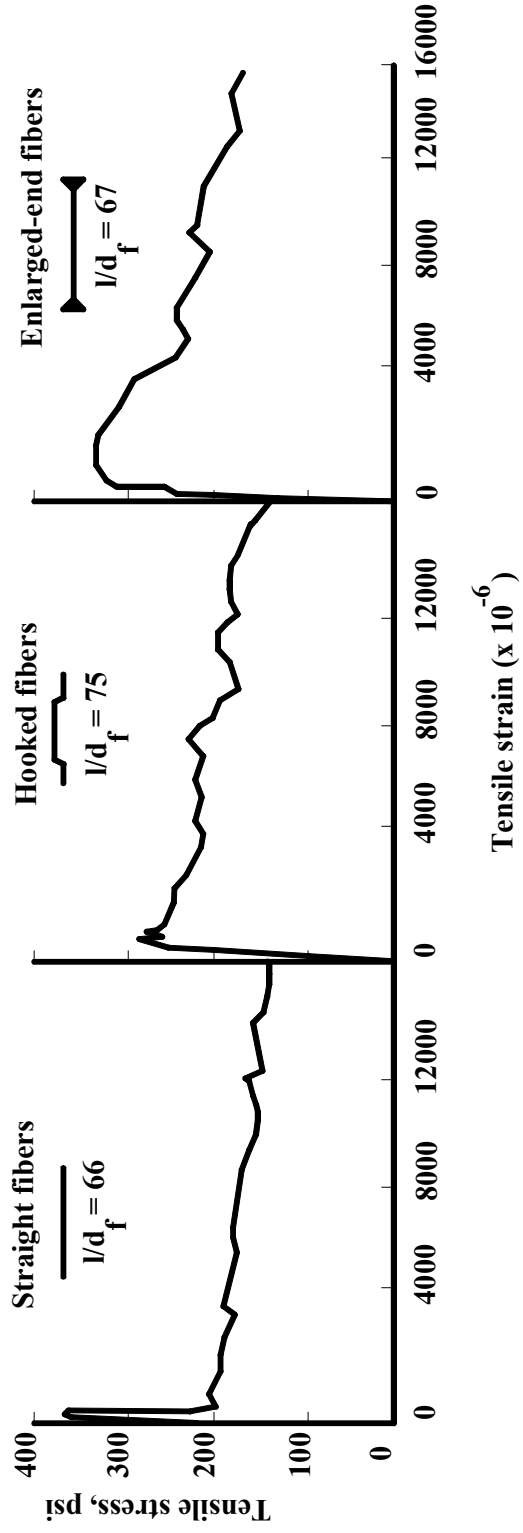


Figure 2.14: Stress-strain curves for SFRC in tension

- The mode of failure changed from shear to moment type when the volume fraction of fibers was increased beyond an optimum value (1%).
- More uniform redistribution of stresses was observed in the fiber concrete beams compared with conventional beams.

### **Flexural Strength and Toughness**

The influence of steel fibers on flexural strength of concrete is much greater than for direct tension and compression (Hannant 1978). Two flexural strength values are commonly used: first-crack flexural strength and ultimate flexural strength (or modulus of rupture). The point on the flexural loaded deflection or tensile load-extension curve at which the form of the curve first becomes non-linear is called the First Crack. The stress corresponding to the load at “First Crack” for a FRC composite in bending or torsion is called First Crack Flexural Strength. Modulus of rupture is the greatest bending stress attained in a flexural strength test of a FRC specimen. From the research conducted by Oh *et al* (1999), it was found that flexural strength of SFRC is greatly enhanced due to the addition of steel fibers. The increase of flexural strength was about 55% when fiber content was 2%. A very important observation was that SFRC showed great ductility and energy absorption capacity. The presence of coarse aggregate coupled with normal mixing and placing considerations limits the maximum fiber volume in concrete to 1.5 to 2.0%. Use of higher volume fractions, center point loading, small specimens or long fibers with significant fiber alignment in the longitudinal direction will produce improved flexural strengths up to 150% (Johnston 1974, Snyder and Lankard 1972, Waterhouse and Luke 1972, Johnston 1989). At lower fiber volume concentrations, a significant increase in flexural strength may not be realized using beam specimens.

Ultimate flexural strength generally increases in relation to the product of steel fiber volume concentration and aspect ratio. Concentrations less than 0.5% by volume of low aspect ratio fibers (less than 50) have negligible effect on static strength properties. Prismatic fibers, or hooked or enlarged end (better anchorage) fibers, have produced flexural strength increases over unreinforced matrices of as much as 100 percent (Johnston 1980). Post-cracking load-deformation characteristics depend greatly on the choice of steel fiber type and the volume percentage of the specific fiber type used. Crimped fibers, surface-deformed fibers, and fibers with end anchorage produce strengths above those for smooth fibers of the same volume concentration, or allow similar strengths to be achieved with lower fiber concentrations.

Swamy and Al-Ta'an (1981) concluded the following from their investigation on SFRC:

- The fibers are effective in resisting deformation at all stages of loading, from the first crack to failure.
- Fibers inhibit crack growth and crack widening at all stages of loading.
- The number of cracks at the working load stage is about half of those fully developed before failure.
- Increase in the fiber content results in consistent increase in ductility and energy-absorption capacity.
- The influence of fibers in reducing deformation and increasing flexural stiffness is evident even at the failure stage.

The enhanced performance of SFRC over its unreinforced counterpart comes from its improved capacity to absorb energy during fracture. While a plain unreinforced

matrix fails in a brittle manner at the occurrence of cracking stresses (Fig. 2.7), the ductile SFRC continues to carry stresses beyond matrix cracking, which helps to maintain structural integrity and cohesiveness in the material. Further, if properly designed, steel fibers undergo pullout process, and the fractional work needed for pullout leads to a significantly improved energy-absorption capability. Thus, SFRC exhibits better performance not only under static and quasi-statically applied loads but also under fatigue, impact, and impulsive loadings (Banthia *et al* 1987). This energy-absorption attribute of SFRC is often termed “toughness”. According to ACI 544.1R (1996), flexural toughness may be defined as the area under the load-deflection curve in flexure, which is the total energy absorbed prior to complete separation of the specimen. So the determination of flexural toughness characteristics reflects the performance of the SFRC in a structure.

The performance of SFRC may be compared by first crack strengths, toughness indices and residual strength factors (ASTM C-1018 1997). The first crack strength reflects the behavior of SFRC up to the first crack, and toughness indices and residual strength factors reflect the post-crack behavior of SFRC under static flexural loading.

According to ASTM C-1018 (1997) specification, the first crack strength is defined as:

$$R = \frac{Pl}{bd^2} \quad (2.3)$$

where,  $R$  = first crack strength

$P$  = first crack load

$l$  = span length

$b$  = average width of the specimen at fracture

$d$  = average depth of the specimen at the fracture

Toughness is expressed as a ratio of the amount of energy required to deflect the beam to a specified deflection, expressed as multiples of the first crack deflection (ASTM C-1018 1997). Figure 2.15 shows the load-deflection curves and toughness parameters as per ASTM C-1018 (1997). Toughness indices  $I_5$ ,  $I_{10}$  and  $I_{20}$  are defined as:

$$I_5 = \frac{A_{3\delta}}{A_\delta} \quad (2.4)$$

$$I_{10} = \frac{A_{5.5\delta}}{A_\delta} \quad (2.5)$$

$$I_{20} = \frac{A_{10.5\delta}}{A_\delta} \quad (2.6)$$

where,  $\delta$  = the deflection at first crack

$A_\delta$  = Area under the load deflection curve up to  $\delta$

$A_{3\delta}$  = Area under the load deflection curve up to  $3\delta$

$A_{5.5\delta}$  = Area under the load deflection curve up to  $5.5\delta$

$A_{10.5\delta}$  = Area under the load deflection curve up to  $10.5\delta$

The determination of appropriate toughness index as a measure of the performance of SFRC for a specific application depends on the level of serviceability required in terms of cracking and deflection.

The residual strength factors represent the average level of strength retained after first crack as a percentage of the first crack strength for different deflection intervals (ASTM C-1018 1997). Lower values of residual strength factors indicate inferior performance of SFRC. The residual strength factors  $R_{5,10}$  and  $R_{10,20}$  are defined as:

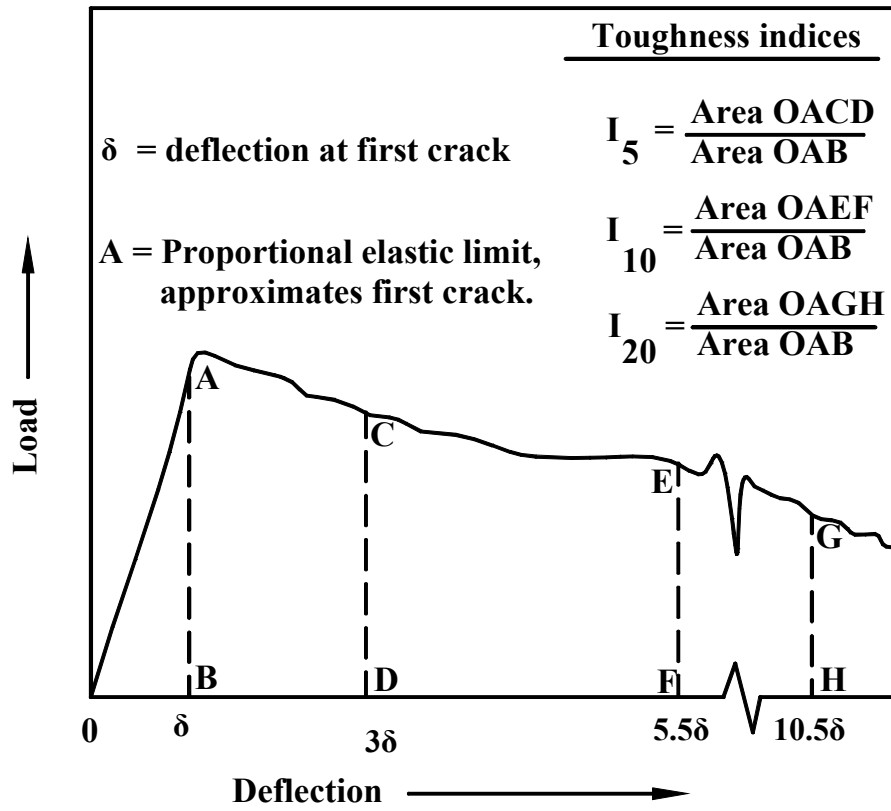


**Figure 2.15: Load-deflection curve and toughness parameters (ASTM C-1018)**

$$R_{5,10} = 20(I_{10} - I_5) \quad (2.7)$$

$$R_{10,20} = 10(I_{20} - I_{10}) \quad (2.8)$$

Two other test procedures as per ASTM specifications to measure the performance of SFRC are also available. These are ASTM C-1399 (1998) and ASTM C-1550 (2002). ASTM C-1399 (1998) measures the average residual strength of a SFRC test beam. ACI Committee 544 has recently recommended the new ASTM specifications C-1550 for the flexural toughness evaluation and acceptance of SFRC (ASTM C-1550 2002). This test is recommended because of its bi-axial bending conditions typically experienced by in-situ actual structures.

### **Fatigue**

Experimental studies show that, for a given type of fiber, there is a significant increase in flexural fatigue strength with increasing percentage of steel fibers (Brandshaug *et al* 1978, Batson 1972, Ramakrishnan and Josifek 1987). Depending on the fiber type and concentration, a properly designed SFRC mixture will have a fatigue strength of about 65 to 90% of the static flexural strength at about 2 million cycles when nonreversed loading is used (Ramakrishnan and Josifek 1987, Ramakrishnan *et al* 1987), with slightly less fatigue when fully reversed loading is used (Ramakrishnan and Josifek 1987). The addition of fibers to conventionally reinforced beams increases the fatigue life and decreases the crack width under fatigue loading (Kormeling *et al* 1980). It has also been shown that the fatigue strength of conventionally reinforced beams are enhanced with SFRC. The resulting deflection changes accompanying fatigue loading also decrease (Schrader 1971).

## **Shrinkage and Creep**

Concrete shrinks when it is subjected to a drying environment. If concrete is restrained from shrinkage, then tensile stresses develop and concrete may crack. One of the methods to reduce the adverse effect of shrinkage cracking is reinforcing the concrete with short and randomly distributed steel fibers. Steel fibers have three roles in such situations: (1) they allow multiple cracking to occur, (2) they allow tensile stresses to be transferred across cracks, i.e., the composite maintains residual tensile strength even if tensile shrinkage cracks occur, and (3) stress transfer can occur for a long time, permitting healing or sealing of the cracks (Hoff 1987). Tests have shown that steel fibers have little effect on free shrinkage of concrete (Hannant 1978).

## **Corrosion of Fibers**

Experience to date has shown that if a concrete has a 28-day compressive strength over 3000 psi (21MPa), is well compacted, and complies with ACI 318 (2002) recommendations for water-cement ratio, then corrosion of fibers will be limited to the surface skin of the concrete. Once the surface fibers corrode, there does not seem to be a propagation of the corrosion beyond 0.10 in (2.5 mm) below the surface. This limited surface corrosion seems to exist even when the concrete is highly saturated with chloride ions (Schupack 1986). Since the fibers are short, discontinuous, and rarely touch each other, there is no continuous conductive path for stray or induced currents or currents from electromotive potential between different areas of the concrete.

Laboratory and field-testing of cracked SFRC in an environment containing chlorides has indicated that cracks in concrete can lead to corrosion of the fibers passing across crack (Hoff 1987). However, crack width of less than 0.004 in (0.1 mm) do not

allow corrosion of steel fibers passing across the crack (Morse and Williamson 1977). If cracks wider than 0.004 in (0.1 mm) are limited in depth, the consequence of this localized corrosion may not always be structurally significant. However, if flexural or tensile cracking of SFRC can lead to a catastrophic structural condition, full consideration should be given to the possibility of corrosion at cracks.

## **2.5. Polypropylene Fiber Reinforced Concrete (PFRC)**

The incorporation of monofilament or collated fibrillated discrete discontinuous fibers into a cement brittle matrix serves to increase the fracture toughness of the reinforced concrete by the result of the crack arresting process and increase of the flexural and tensile strengths. In 1965, Shell Chemical Co. started investigations on Polypropylene to be used in concrete (Zonsveld 1975). Polypropylene fibers are stronger as a result of more developed plastic materials, which offered a potentially low priced polymer. The use of intrusion and stretching of melted polypropylene pellets produces thin films with molecular orientation, and consequently the mechanical strength is developed parallel to the direction of stretching. Modification of this film produces the modern collated fibrillated polypropylene fibers. The network structure of fibrillated polypropylene fibers before mixing consists of oriented fibrils linked together. After mixing, the fibrils will filamentize into multi-filament strands due to the mixing action exerted by the aggregates (Rice *et al* 1988), which produces reinforcement in all directions.

### **2.5.1. Properties of PFRC**

Polypropylene is hydrophobic, meaning it does not absorb water. Polypropylene fibers are not expected to bond chemically in a concrete mix, but bonding has been shown to occur by mechanical interaction (Rice *et al* 1988).

#### **Stress-Strain Curves**

Figure 2.16 shows the stress-strain curves for concrete reinforced with continuous polypropylene fiber, discontinuous polypropylene fibers and unreinforced matrix material (Beaudoin 1990). Curve 1 for continuously aligned fibers has three regions: an initial steep region that terminates when the cracking strain of the matrix is reached, a multiple cracking zone, where the stress remains relatively constant, a region, less steep, where the stress is transferred to the reinforcement, and ultimate failure. Curve 2 for discontinuous random fibers has three regions: an initial steep region and a second region, where the stress drops sharply as it is transferred to reinforcement bridging cracks; and another region, where the stress levels off and the fibers generally pull-out rather than break.

#### **Compressive Strength**

Compressive strength of concrete decreases by about 5-10% when collated fibrillated polypropylene mesh is incorporated into the mix (Zollo 1984). Use of fiber at different quantities generally does not result in any significant increase in compressive strength (ACI 544.1R 1996). The results of Dardare (1975), however, indicate that incorporation of polypropylene fiber in concrete can increase compressive strength (Fig. 2.17). The increase is dependent on the volume fraction and the length of the fiber. Stress-strain curves for non-fibrous concrete and concrete containing fibrillated

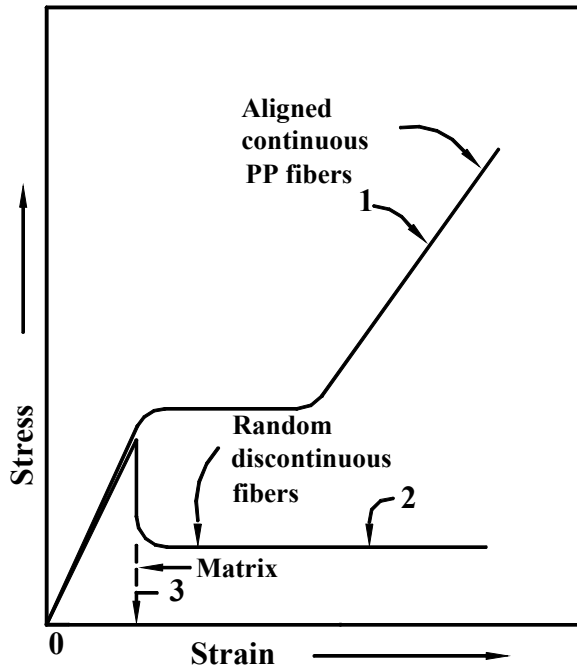


Figure 2.16: Stress-strain curves for cement composites containing polypropylene fibers (Beaudoin 1990)

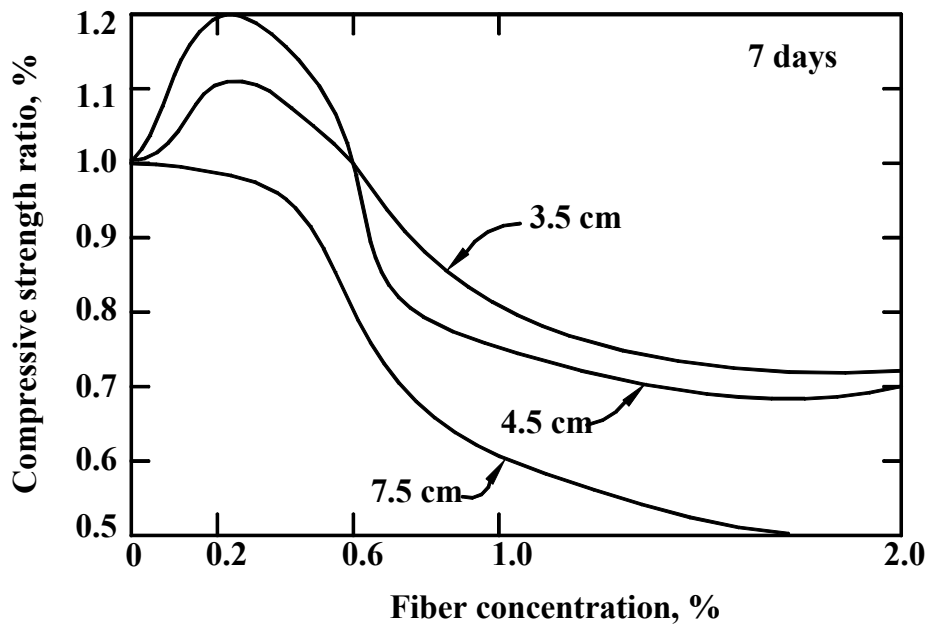


Figure 2.17: Compressive strength ratio versus polypropylene fiber concentration (Dardare 1975)

polypropylene fibers are presented in Fig. 2.18 (Hughes and Fattuhi 1977). There is a decrease of about 20% in the peak stress obtained for the FRC.

However, the addition of polypropylene fibers has a significant effect on the mode and mechanism of failure of concrete cylinders in a compression test; the FRC fails in a more ductile mode. This is particularly true for higher strength fiber concretes, while plain control concrete cylinders typically shatter due to an inability to absorb the energy release imposed by the test machine at failure. FRC cylinders continue to sustain load and endure large deformations without shattering (Nagabhushanam *et al* 1989, Ramakrishnan *et al* 1989). A FRC with high quantity of polypropylene fibers produces a concrete with poorer workability, more bleeding and segregation, relatively higher entrapped air (13.9%) and a lower unit weight (Ramakrishnan *et al* 1989). This results in a decrease in the compressive strength.

### **Flexural and Tensile Strength**

Typical load-deflection curves for PFRC are presented in Fig. 2.19 (Dave and Ellis 1979). The curves are useful for observed mechanical behavior of polypropylene fiber reinforced cement composites. The decrease in stress at first cracking is dependent on the volume concentration of fibers. In general, most researchers contend that incorporation of discontinuous polypropylene fibers in cement matrices does not improve flexural or tensile strength. It was reported (Zollo 1984) that at a fibrillated polypropylene fiber content of 0.1% by volume, there was a slight increase in the flexural strength (0.7 to 2.6%), and at 0.2 to 0.3% by volume, there was a slight decrease.

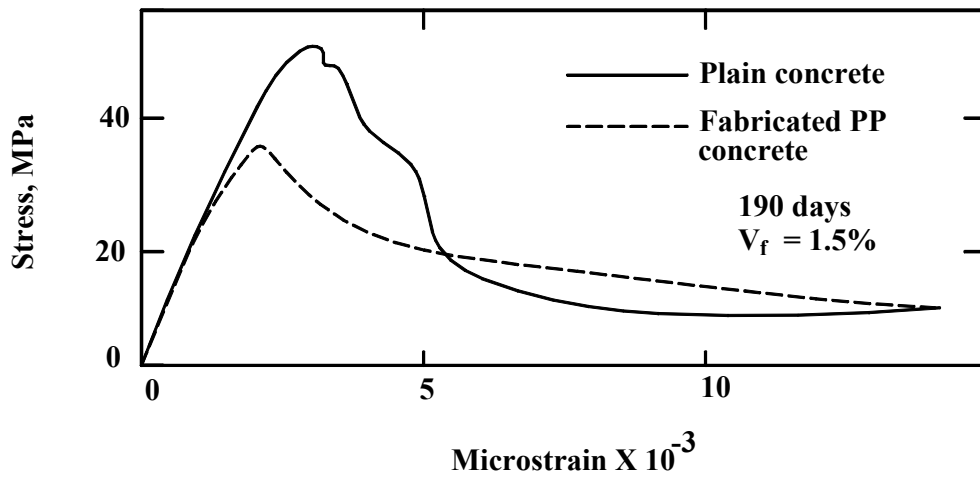


**Figure 2.18: Compressive stress-strain curves for plain concrete and PFRC cubes (Hughes and Fattuhi 1977)**

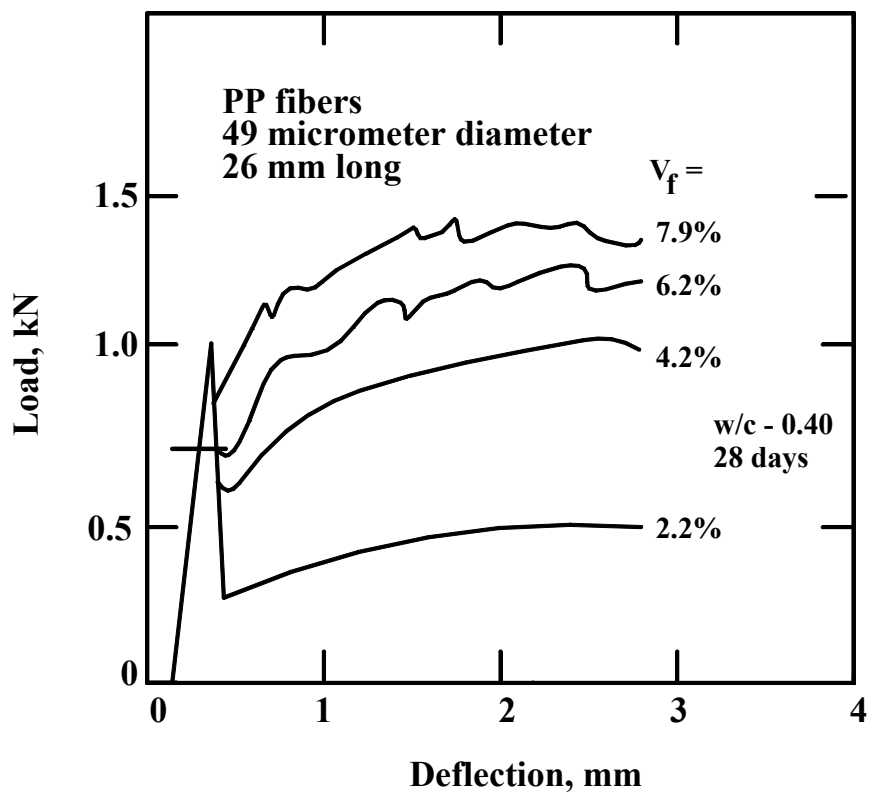


**Figure 2.19: Typical load-deflection curves for PFRC containing various fiber volume fractions (Dave and Ellis 1979)**

### **Fatigue Behavior**

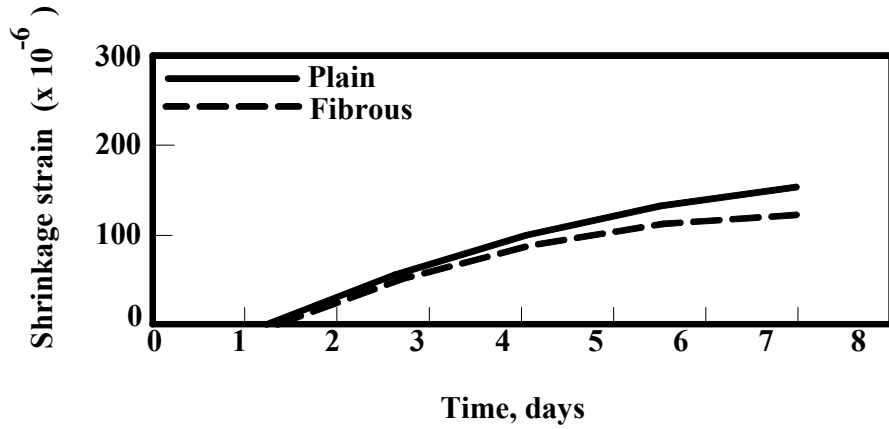
The addition of polypropylene fibers to concrete increases the fatigue life of concrete. Ramakrishnan et al (1987) concluded that the addition of low percentage by volume of fibers improved the fatigue strength. The research used flexural fatigue using rectangular beams, which were tested for an endurance limit of two million cycles. The addition of polypropylene fibers (0.1, 0.2 and 0.3% by volume) increased the endurance limit (15 to 18%), which would be beneficial when applied to pavement slabs, which in turn would substantially increase the life of highways.

### **Shrinkage and Cracking**

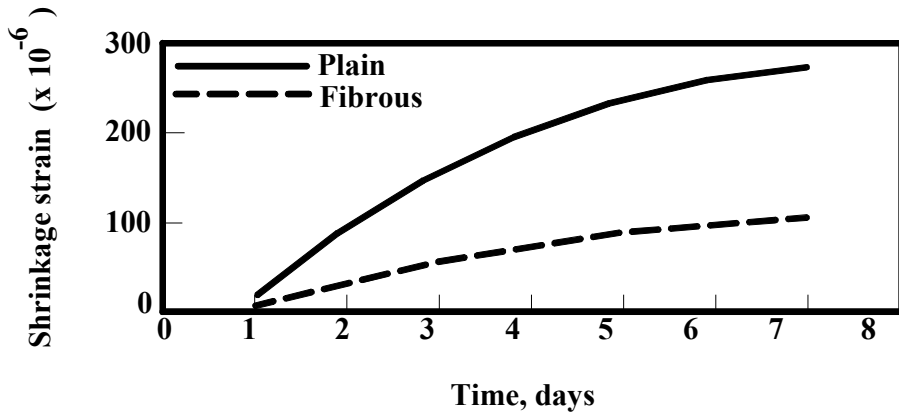
Grzybowski and Shah (1990) conducted tests using ring type specimens to simulate restrained shrinkage cracking. They concluded that polypropylene fibers had a great ability to control drying shrinkage cracking. With the addition of fiber, the average crack width decreased significantly, as compared to plain concrete. Zollo *et al* (1986) reported the reduction of 18, 59 and 10% in drying shrinkage for fiber volumes of 0.1, 0.2 and 0.3%, respectively. Figure 2.20 shows the shrinkage strain versus time curves plotted for specimens containing fibers and control specimens.

## **2.6 Application of Fiber Reinforced Concrete**

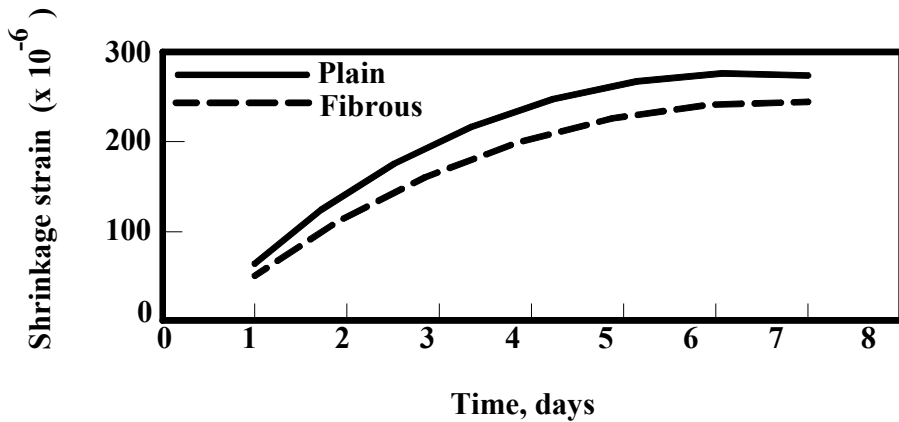
Choice of using of FRC depends upon ingenuity of the designer and the builder who want to take advantage of the improved static and dynamic strengths.



(a) 0.1% by volume



(b) 0.2% by volume



(c) 0.3% by volume

Figure 2.20: Drying shrinkage strain for PFRC and companion plain concrete specimens (Zollo *et al* 1986)

### 2.6.1 Application of SFRC

The uniform distribution of steel fiber throughout concrete provides isotropic strength property, which are not exhibited in conventional reinforced concrete. SFRC is used in various structural applications, such as: refractories, airport runways, pavements, tunnels supports and lining, piping, poles, piles, bridge decking, industrial floors, hydraulic structures, precast thin elements, etc. SFRC is also used in overlays of existing pavement (bonded or unbonded to slab beneath). Other applications of SFRC are in marine structures such as jetty armour, breakwaters, floating pontoon and caissons. Some specific applications of SFRC are listed below:

- Figure 2.21 shows a 850,000 ft<sup>2</sup> (79,000 m<sup>2</sup>), 9" (230 mm) thick SFRC floor slab designed to handle 71,000 lbs (32,200 kg) rolls of steel as well as equipment used to process the rolls. The structure is Bethlehem Steel's cold rolling mill, located in Sparrow's Point, Maryland. Novocon steel fibers were added to the concrete mix at 55 lbs/yd<sup>3</sup> (32.6 kg/m<sup>3</sup>) dosage. This eliminated the need for rebar and added the benefits of crack control and increased ductility.
- In Brandon, Florida, Household International Office Building (Fig. 2.22), a three-story structure, was constructed using 1,400 yd<sup>3</sup> (1,070 m<sup>3</sup>) of SFRC. The steel fibers were mixed at the concrete plant using a specially designed loading rack with a hopper. A 3500 psi (24 MPa) mix with 1/2" (12.7 mm) maximum aggregate size was used.
- In Houston, Texas, two three-lane feeder roads (Fig. 2.23) to Beltway Eight, one of Houston's busiest perimeter highways, were restored using Novocon steel



**Figure 2.21: Industrial floor with SFRC, Sparrow's Point, Maryland (SI Concrete Systems)**



**Figure 2.22: Office building with SFRC, Brandon, Florida (SI Concrete Systems)**



**Figure 2.23: Road overlays with SFRC, Houston, Texas (SI Concrete Systems)**



**Figure 2.24: Slabs of an apartment complex with SFRC, Destin, Florida (SI Concrete Systems)**

fiber for concrete reinforcement. A two-inch (51 mm) thick “thin bonded overlay” replaced the damaged top layer of the roadway. Steel fiber was added to the concrete at an addition rate of 75 lbs/yd<sup>3</sup> (44.5 kg/m<sup>3</sup>).

### **2.6.2 Application of PFRC**

Polypropylene fibers are mostly applied to non-structural and non-primary load bearing applications. Current applications include residential, commercial, and industrial slabs on grade, slabs for composite metal deck construction, floor overlays, shotcrete for slope stabilization, pool construction, and precast units. Some applications of PFRC are listed below:

- In Destin, Florida, Fibermesh fibers were used as concrete secondary reinforcement in the slabs in this upscale apartment complex (Fig. 2.24). The fibers were used at an addition rate of 1.5 lbs/yd<sup>3</sup> (0.9 kg/m<sup>3</sup>). All the slabs on ground were post-tensioned. The majority of the concrete was placed in severe summer conditions and the PFRC was used to help control the drying and shrinkage cracking.
- In Destin, Florida, Fibermesh fibers were used as secondary reinforcement on a storage facility project (Fig. 2.25). The 6” (152.4 mm) concrete was placed with a 138-ft (42-meter) pump truck in five different pours, and joints were saw-cut in 15 ft (4.6 m) by 20 ft (6.1 m) patterns. The use of fibers allowed for quicker placement and cost savings than traditional reinforcement.
- In Redmond, Washington, the Willows Commerce Park used more than 16,000 cubic yards (12,225 m<sup>3</sup>) of concrete in a five building tilt-up project (Fig. 2.26).



**Figure 2.25: Storage facility project with PFRC, Destin, Florida (SI Concrete Systems)**



**Figure 2.26: Tilt-up slabs with PFRC, Redmond, Washington (SI Concrete Systems)**

Fibermesh fibers were used to reinforce the concrete in the tilt-up slabs. The fiber was added at a rate of 1.5 lbs/yd<sup>3</sup> (0.9 kg/m<sup>3</sup>).

- In Mobile, Alabama, Fibermesh fibers were used at a rate of 1.5 lbs/yd<sup>3</sup> (0.9 kg/m<sup>3</sup>) to enhance the quality of this 200,000 square foot (18,580 m<sup>2</sup>) parking area (Fig. 2.27). PFRC was used in all of the paving and slabs for the metal frame buildings.



**Figure 2.27: Parking area with PFRC, Mobile, Alabama (SI Concrete Systems)**

## **CHAPTER 3**

### **PROPERTY TESTING OF FRC**

#### **3.1. Introduction**

Non-fibrous concrete is weak in tension and lacks necessary toughness and ductility. However, once it is reinforced, its mechanical characteristics are altered. Adding a small quantity of fibers into an ordinary concrete mix does not require special tools or working procedures, nor does it significantly affect concrete workability and productivity. The merits of incorporating fibers into conventional concrete are well known. Increased tensile and flexural strength, ductility, toughness and enhanced internal resistance to dynamic forces may be expected from the composite even with nominal addition of fibers into a standard concrete mix. Steel fibers resist the development of further cracking and, by implication, possess better residual strength that is not found in damaged conventional concrete. Sometimes it increases the compressive strength of the concrete. This property enhancement of FRC depends on the unreinforced concrete, volume percentage of fiber, fiber type (steel, glass, synthetic etc.), size and shape of fiber, etc. Nowadays, the availability of fibers with a variety of surface textures and deliberate

introduction of anchorage features have tended to enhance performance features of steel/synthetic fiber reinforced concrete.

Mechanical properties of FRC with various types and amounts of fibers were determined in this study. The results were used to verify expected FRC properties and also to aid in the selection of fiber type and amount for the anchor zone testing.

### **3.2. Property Test Program**

The property test program involved the determination of compressive strength, tensile strength and flexural toughness characteristics of FRC. All tests were performed as per ASTM standards. ASTM designations of these test standards are ASTM C-39 (1996), ASTM C-496 (1996) and ASTM C-1018 (1997), respectively. In this study, ASTM C-1018 specification was used, as this specification is the most commonly used test method to evaluate the performance of SFRC.

### **3.3. Procurement of Materials**

#### **3.3.1. Concrete**

Florida Department of Transportation (FDOT) and the precast industries were contacted for information on the concrete mix selection. According to FDOT, a Class IV or V concrete is used for prestressed bridge girders (FDOT 2000). For Class IV and Class V concrete, the minimum 28-day strengths are 4000 psi (38 MPa) and 6000 psi (57 MPa), respectively. Several concrete mix designs were collected from various concrete

suppliers. For this study, a Class IV concrete with a minimum 28-day compressive strength of 5500 psi (52 MPa) was selected.

The water-cement ratio for the design mix was 0.37 and the target slump was 5 in. (127 mm) to 8 in. (203 mm). Ordinary type-I portland cement was used, and the fineness modulus of fine aggregates was 2.4. The coarse aggregate was crushed limestone (No. 57). Table 3.1 shows the various ingredients and Table 3.2 lists the basic mix proportions for the concrete used.

### **3.3.2. Selection of Fibers**

From the discussion in Chapter 2, it is clear that the overall performance of SFRC is better than the PFRC. According to the ACI 544 (1996), steel fiber should be used in conjunction with properly designed continuous reinforcement for flexural structural components. But there are some applications where steel fibers were used without reinforcing bars to carry loads. A parking garage at Heathrow Airport with slabs 3 ft-6 in (1.07 m) square by 2.5 in (10 cm) thick, was constructed using steel fibers only (Precast-Concrete 1971). Full-scale tests showed that steel fibers were effective in supplementing or replacing stirrups in beams (Jindal 1984, Williamson 1978, Sharma 1986), although supplementing or replacing stirrups with steel fibers is not an accepted practice at present. On the other hand, no such application of synthetic fiber was obtained. Synthetic fibers are applied mostly to control plastic shrinkage cracking (ACI 544.1R 1996). So, SFRC is expected to perform better than the PFRC in the structural application for post-tensioned anchorage zones.

**Table 3.1: Ingredients of design concrete mix (Class IV)**

<b>Ingredient</b>	<b>Source</b>	<b>Type</b>
Cement	Southdown Inc.	Type I
Coarse aggregate	Tarmac Florida	Crushed Limestone (PENNCCEM)
Fine aggregate	Florida Rock Industries	Silica Sand
Fly ash	Boral Material Tech. Inc	Class F (Crystal River)
Air entraining admixture	Master Builders Inc.	MBVR Standard
Stabilizer	Master Builders Inc.	DELVO (Type D)
Water reducing admixture	Master Builders Inc.	RHEOBUILD 1000 (Type F)

**Table 3.2: Mix proportions of design concrete mix (for 1 yd<sup>3</sup>)**

<b>Ingredients of concrete</b>		<b>Amount of materials</b>
Cement, lb (kg)		584 (202.37)
Coarse aggregate, lb (kg)		1708 (591.88)
Fine aggregate, lb (kg)		1028 (356.24)
Admixtures	MBVR Standard, oz (ml)	14.6 (432.16)
	DELVO, oz (ml)	36 (1065.6)
	RHEOBUILD 1000, oz (ml)	87 (2575.2)
Water, lb (kg)		270 (93.56)
Fly ash, lb (kg)		146 (50.6)

Various steel and synthetic fibers are available in the commercial market. Synthetic Industries and Bekaert Corporation were contacted for information on available types of steel and synthetic fibers. Two different types of steel fibers were selected from their products, as they are the most commonly used fibers according to the manufacturing companies. The selected steel fibers are:

- Xorex steel fiber (Synthetic Industries)
- ZP305 steel fiber (Bekaert Corporation)

As seen from Fig. 3.1, the two chosen steel fibers have differing physical appearance.

The following synthetic fiber was also chosen for comparison purposes:

- Harbourite H-330 fiber (Synthetic Industries)

Figure 3.1 shows photographs of the selected fibers. Properties of the selected fibers obtained from the manufacturing companies are presented in Table 3.3. After review of the literature on fiber reinforced concrete and consultation with various fiber-manufacturing companies, the following volume percentages of fibers to be used in the experiments were selected: 0.5, 0.75 and 1.0%. The corresponding amounts of fiber (for 1 yd<sup>3</sup> mix) for these three volume percentages are listed in Table 3.4.

### **3.4. Mixing Procedure**

Concrete was mixed in a 6 ft<sup>3</sup> (0.1698 m<sup>3</sup>) capacity mixer at the FAMU-FSU College of Engineering. Mixing of concrete was performed according to the ASTM C-192 (1995) specification and ACI 544.1R (1986) guidelines. First, coarse and fine aggregates were soaked and blended in 2/3 of the required water for 1 minute. The air



**(a) XOREX steel fiber**



**(b) ZP305 steel fiber**



**(c) Harbourite H-330 fiber**

**Figure 3.1: Photographs of selected fibers**

**Table 3.3: Source, type and geometry of fibers used in the study**

<b>Fiber</b>	<b>Manufacturing company</b>	<b>Fiber length, in (mm)</b>	<b>Average diameter, in (mm)</b>	<b>Aspect ratio</b>	<b>Appearance</b>
<b>Xorex (steel)</b>	Synthetic Industries	1.5 (38)	0.04 (1)	38	Continuously deformed circular segment
<b>ZP305 (steel)</b>	Bekaert Corporation	1.2 (30)	0.022 (0.55)	55	Cold drawn wire fiber, with hooked ends, and glued in bundles
<b>H-330 (synthetic)</b>	Synthetic Industries	1.5 (38)	---	---	Fibrillated

**Table 3.4: Amount of fibers used in the study (for 1 yd<sup>3</sup> mix)**

<b>Fiber type</b>	<b>Volume percentage of fibers</b>	<b>Amount of fibers, lb (kg)</b>
Steel Fiber	0.5	66 (30)
Steel Fiber	0.75	99 (45)
Steel Fiber	1.0	132 (60)
Polypropylene Fiber	0.5	7.5 (3.4)
Polypropylene Fiber	0.75	11.25 (5.1)
Polypropylene Fiber	1.0	15 (6.8)

entraining admixture and plasticizer were added next. Fibers were added at the mixing speed. Lastly, cement, fly ash and the rest of the water were added and mixed for 3 minutes. This was followed by a 3-minutes rest period. Water reducing admixture was added at this stage, after which the ingredients were mixed for 2 minutes. Inspection of both fresh and hardened concrete showed uniform distribution of all three types of fibers.

### **3.5. Compressive Strength Test**

#### **3.5.1. Specimen Preparation**

For the compressive strength test, 30 (3 cylinders per batch) 6" x 12" (150 mm x 300 mm) cylinders were prepared using 10 batches of concrete. Except for fiber type and dosage, all other ingredients of concrete for all batches were identical to that in Table 3.2. Table 3.5 lists the batch designations with the amount and types of fibers. One batch was prepared as control specimen using no fiber. The other nine batches of concrete were prepared using Xorex steel fiber, ZP305 steel fiber and Harbourite fiber (H-330) with different amounts of fiber (0.5, 0.75 and 1.0% by volume). The cylinders were made using plastic molds and were compacted using a table vibrator. Surface finishing was performed using steel float and trowel. To retain the moisture during the first 24 hours until demolding, all the cylinders were covered with plastic lids.

The moist curing of the test specimens was carried out according to ASTM C-192 (1995). Following the 24 hours setting period, the plastic lids were removed and the specimens were taken out from their molds, and placed in a curing tank. The temperature

**Table 3.5: Concrete batch designations used in the study**

<b>Batch no.</b>	<b>Batch designation</b>	<b>Fiber type</b>	<b>Percentage of fiber</b>
1	NF	No fiber (control specimen)	0
2	X050	XOREX	0.5
3	X075	XOREX	0.75
4	X100	XOREX	1.0
5	Z050	ZP305	0.5
6	Z075	ZP305	0.75
7	Z100	ZP305	1.0
8	H050	H-330	0.5
9	H075	H-330	0.75
10	H100	H-330	1.0



**(a) Compressive strength**



**(b) Tensile strength**

### **Figure 3.2: Compressive (ASTM C-39) and tensile strength (ASTM C-496) test set up**

was maintained at  $73\pm 3$  °F ( $23\pm 2$  °C), as per ASTM C-192 (1995) specification. After 28 days of curing, the specimens were removed from the tank and prepared for the test.

#### **3.5.2. Specimen Testing**

ASTM C-39 (1996) specification was followed for the compressive strength test. The test was performed using a 55 kip (245 kN) Forney Universal Testing Machine at the FAMU-FSU College of Engineering. Figure 3.2 (a) shows the set up of the compressive strength test. The machine has a steel platen base and a steel loading platen. The compressive force was applied to the cylinder through the bottom platen. The failure load was obtained from the digital recorded reading of the machine.

## **3.6. Split Tensile Strength Test**

#### **3.6.1. Specimen Preparation**

For the split tensile strength test, 30 (3 cylinders per batch) 6" x 12" (150-mm x 300-mm) cylinders were prepared using the same 10 batches of concrete as those prepared for the compressive strength test. Specimens were prepared and cured in the same manner as described in Section 3.5.1.

#### **3.6.2. Specimen Testing**

ASTM C-496 (1996) specification was followed for the split tensile strength test. This test was performed using the Forney Universal Testing Machine at the FAMU-FSU

College of Engineering following procedure similar to that in Section 3.5.2. Figure 3.2 (b) shows the test set up for the split tensile strength test.

## **3.7. Flexural Toughness Test**

### **3.7.1. Specimen Preparation**

ASTM C-1018 (1997) specification was followed for the flexural toughness test. The test beam size was 6" x 6" x 20" (150 mm x 150 mm x 500 mm). Twenty Beams (2 beams per batch) were made using the previously mentioned 10 batches of concrete. Steel beam molds were used to prepare these beams. Molds were first coated with oil for easy demolding prior to the mixing process. The concrete was vibrated using a table vibrator. After casting, the specimens were covered with polythene sheets and left in the molds for 24 hours. Following the setting period, the specimens were taken out from their molds and placed in the curing tank, under the specified temperature and humidity, as per ASTM C-192 (1995). Thereafter, all the beam molds were cleaned, washed, assembled back and coated with oil for future use.

### **3.7.2. Specimen Testing**

The flexural toughness test was performed using a 50 kip (222.5 kN) servo-controlled electro-hydraulic, closed loop Material Testing System (MTS) at the FAMU-FSU College of Engineering. This system is composed of a loading frame, hydraulic system and control module. A steel bench is the base of the loading frame, which consists of two steel columns with a cross beam bolted to them. This cross beam supported the

load cell and the two 60" (235 mm) I-shaped steel beams supporting the specimen. The test set up is shown in Fig. 3.3. The 407-controller module was used for the test. The beams were tested using a third-point loading over a simply supported span of 18 in (450 mm). The center deflection was measured by LDT (Linear Displacement Transducer), with a reading accuracy of 0.001 in. (0.025 mm). The movement of the actuator was set to 0.0125 in/min (0.03175 mm/min). The deflections and load readings were recorded at a regular interval of 5 sec. The deflection readings were obtained from the computer through an E-415 read out box by using the Serial Acquisition System (SAS) software. The load readings were obtained manually from the MTS machine (MTS 407 Controller). The first drop in load was assumed to result in the first crack. The test components are shown in Figs. 3.4 and 3.5.

### **3.8. Workability of FRC**

The workability of freshly mixed concrete is a measure of its ability to be mixed, placed and finished. The slump test is a common, convenient and inexpensive test, but it may not be a good indicator of workability of FRC (ACI 544.2R 1989). However, once it has been established that a particular FRC mixture has satisfactory handling and placing characteristics at a given slump, the slump test may be used to monitor the FRC consistency. Various studies have established that a mixture with relatively low slump may have good consolidation properties under vibration (Balaguru and Ramakrishnan 1987). In general, the slump for SFRC, as per ASTM C-143 (1990), should be within the range of 1 to 4 in (25 to 100 mm) (ACI 544.3R 1993). But ACI 544 does not specify any



**Figure 3.3: Flexural toughness test set up**



**Figure 3.4: MTS 407 controller (load observation)**



**Figure 3.5: Displacement readout box**

**Table 3.6: Slump for non-fibrous concrete and various FRC**

<b>Fiber type</b>	<b>Fiber volume (%)</b>	<b>Slump, in (mm)</b>
No fiber	0	7 (178)
XOREX steel fiber	0.5	3 (75)
	0.75	2.5 (63.5)
	1.0	1.5 (38)
ZP305 steel fiber	0.5	2.5 (63.5)
	0.75	1.5 (38)
	1.0	1 (25)
Harbourite H-330 synthetic fiber	0.5	2.5 (63.5)
	0.75	2 (50)
	1.0	1.5 (38)

range for the slump of PFRC. The slump of FRC may also be determined by the inverted slump cone procedure (ASTM C-995 2001). According to ACI 544 (1997), any one of these two procedures should be used to determine the slump of FRC.

In this study, ASTM C-143 was used to measure the slump of FRC. Table 3.6 shows the slump values obtained from plain concrete and various FRC configurations. Non-fibrous concrete showed a slump of 7 in (178 mm), which is within the FDOT mix specification range of 5 to 8 in (127 to 203 mm). The slump values for all SFRC configurations were found to be within the ACI 544.3R (1993) range. PFRC slump values were in the range of 1.5 to 2.5 in (37.5 to 62.5 mm).

### **3.9. Placement and Finishing of FRC**

Conventional equipments were used for the placement of FRC in this study. The FRC appeared relatively stiff and unworkable, compared to plain concrete. Though slump values of PFRC were close to those of SFRC, PFRC was not as difficult to handle as SFRC. As the laboratory tests performed in this study dealt with a small amount of concrete for each batch, no special technique was required for the placement of FRC. Care was taken to place FRC so that significant segregation of fibers did not occur, and fibers were more or less uniformly dispersed.

SFRC may be finished with conventional equipment, but minor refinements in techniques and workmanship are needed (ACI 544.3R 1993). In this study, FRC was vibrated for a longer time than that needed for non-fibrous concrete. As mentioned earlier, a table vibrator was used for the consolidation of FRC. Vibration was continued

during the trowelling of the top surface so that fibers did not protrude from the finished surface.

## **CHAPTER 4**

### **RESULTS OF FRC PROPERTY TESTING**

#### **4.1. Introduction**

Test results obtained from the compressive strength, tensile strength and flexural toughness tests of FRC are presented in this chapter. Test results for control specimens with no fiber are compared with results from FRC specimens with various configurations of fiber to show if the specimens with fibers perform equally or better than the controls. Comparisons among specimens with fibers were also performed.

#### **4.2. Results and Analysis**

##### **4.2.1. Compressive Strength Test**

Average 28-day compressive strengths for cylinders with three types of fibers using three different volume percentages (0.5, 0.75 and 1.0%) are presented in Figs. 4.1, 4.2 and 4.3. It is observed from these figures that the use of steel fibers (XOREX and ZP305) increases the compressive strength. Greater volumes of steel fibers result in

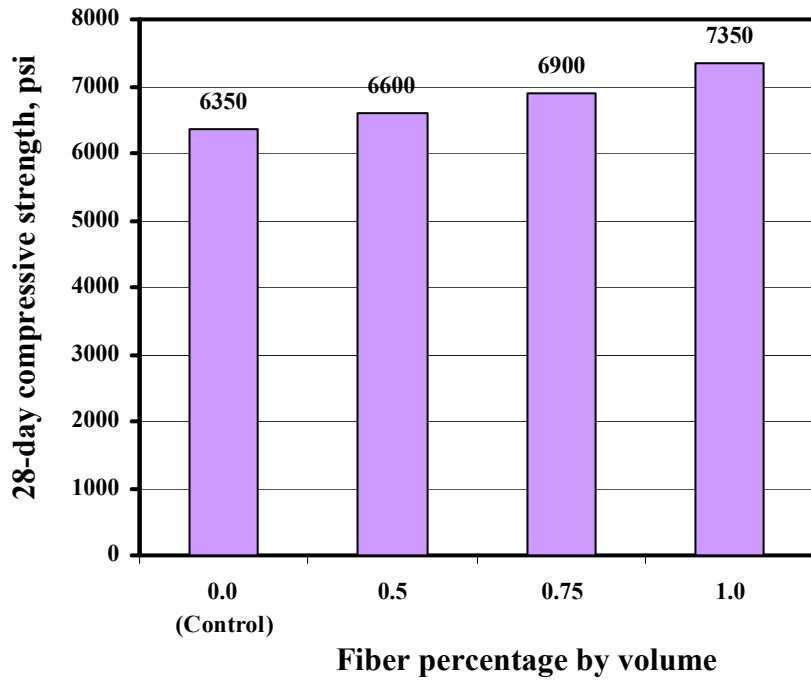


**Figure 4.1: Compressive strength results for specimens with XOREX steel fiber**

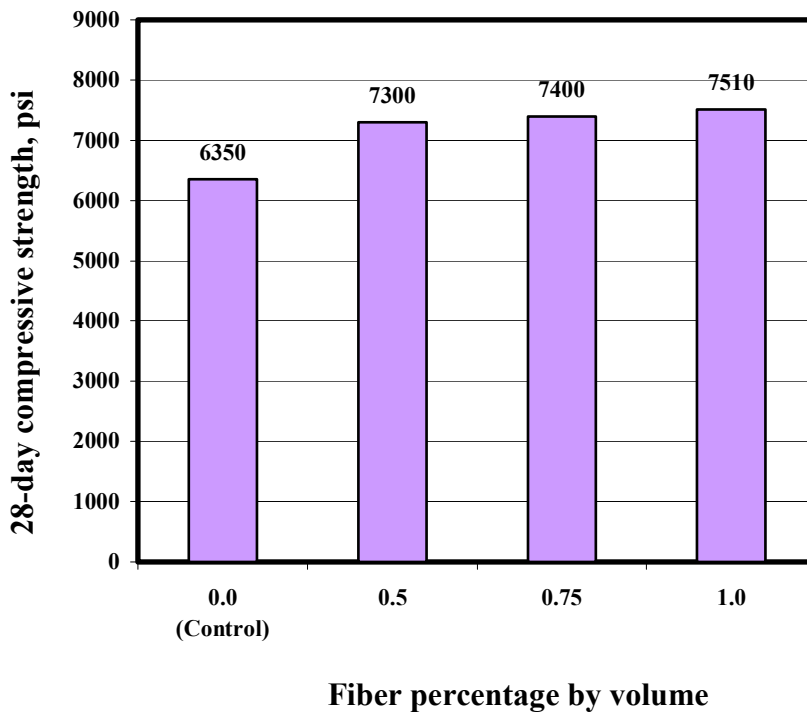


**Figure 4.2: Compressive strength results for specimens with ZP305 steel fiber**

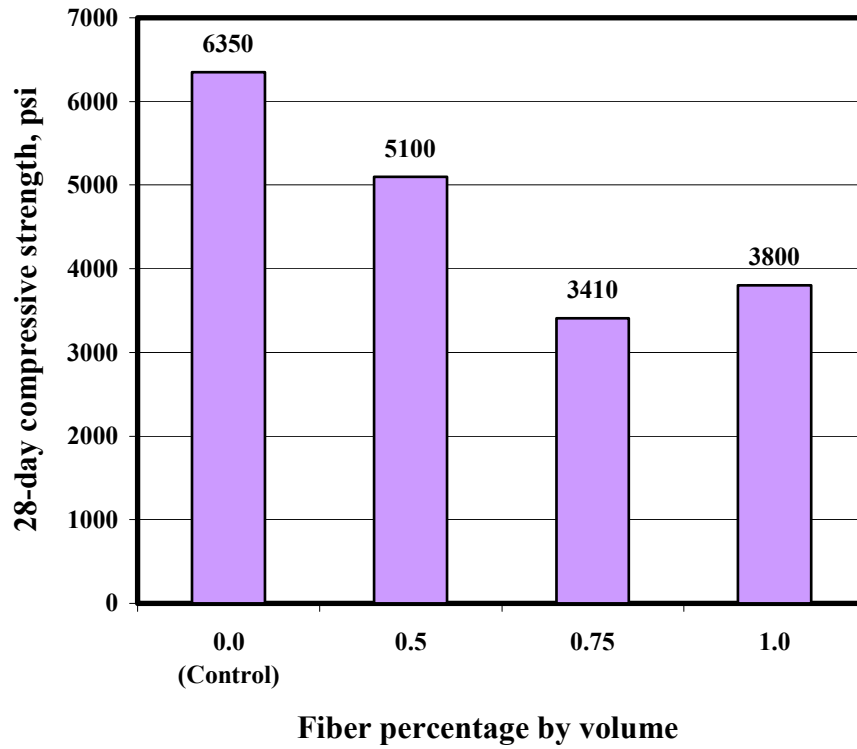


**Figure 4.3: Compressive strength results for specimens with Harbourite H-330 synthetic fiber**

increasing compressive strength. A maximum of 15.75% and 18.27% increase in the compressive strengths of FRC were obtained through the use of XOREX and ZP305 steel fibers, respectively. For synthetic fiber (Harbourite H-330), a somewhat erratic result was obtained, as seen in Fig. 4.3. The compressive strength was found to decrease in general, with the addition of H-330 fiber. The reason for this could be the lack of bonding between the concrete ingredients and the synthetic fiber. As mentioned in Chapter 2 (Section 2.5.1), the addition of polypropylene fiber sometimes decreases the compressive strength depending on the volume fraction and the length of the fiber. The percentile increase or decrease in compressive strengths of FRC specimens compared to control specimens is presented in Table 4.1.

Figures 4.4, 4.5 and 4.6 are the bar chart representations of the compressive strengths of the XOREX and ZP305 SFRC specimens using the same amount of fibers, as compared to the control specimens. As decreased compressive strengths were observed in case of Harbourite H-330 synthetic fiber, it was not considered here. From these charts it is observed that in all three cases ZP305 SFRC specimens showed better results than XOREX SFRC specimens.

#### **4.2.2. Tensile Strength Test**

Figures 4.7, 4.8 and 4.9 present the average 28-day strengths from cylinders with three different volume percentages (0.5, 0.75 and 1.0%) of XOREX, ZP305 and H-330 fibers. It is observed from these figures that the effect of fibers on the tensile strength of concrete is identical to that on the compressive strength. XOREX and ZP305 steel fibers increase the tensile strengths. Greater volumes of steel fibers result in increasing tensile

**Table 4.1: Compressive strength results**

Type of fiber	Fiber volume (%)	Compressive strength results	
		Test value, psi (MPa)	Difference with control (%)
<b>Control specimen with no fiber</b>	0.00	6350 (43.75)	----
<b>XOREX</b>	0.50	6600 (45.47)	+3.94
	0.75	6900 (47.54)	+8.66
	1.00	7350 (50.64)	+15.75
<b>ZP305</b>	0.50	7300 (50.30)	+14.96
	0.75	7400 (50.99)	+16.54
	1.00	7510 (51.74)	+18.27
<b>Harbourite H-330</b>	0.50	5100 (35.14)	-19.69
	0.75	3410 (23.5)	-46.3
	1.00	3800 (26.18)	-40.16

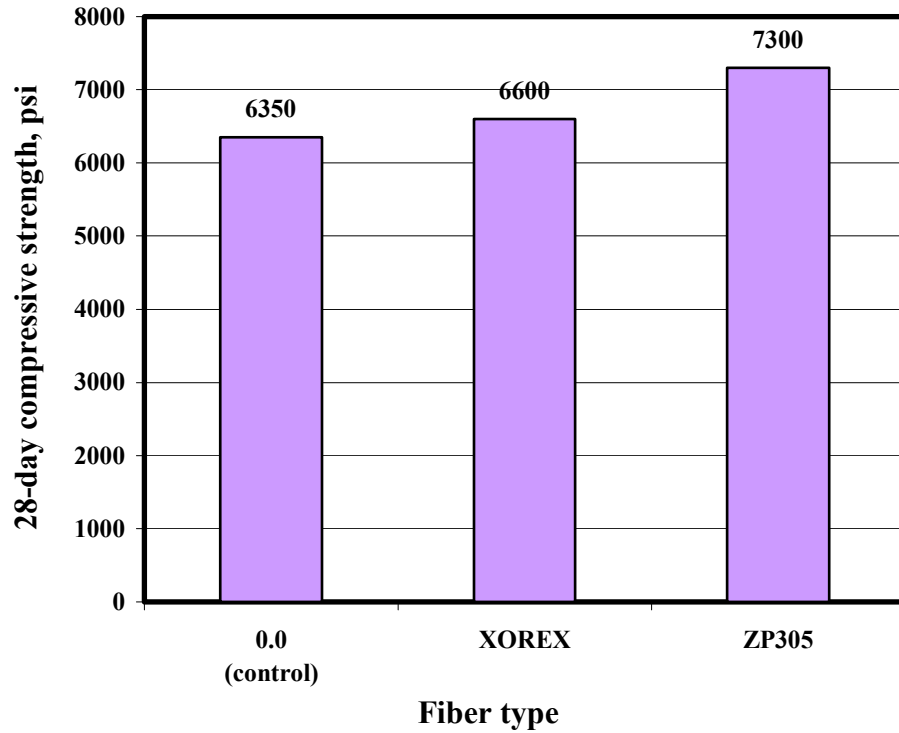


**Figure 4.4: Compressive strengths of specimens with 0.5% steel fiber**

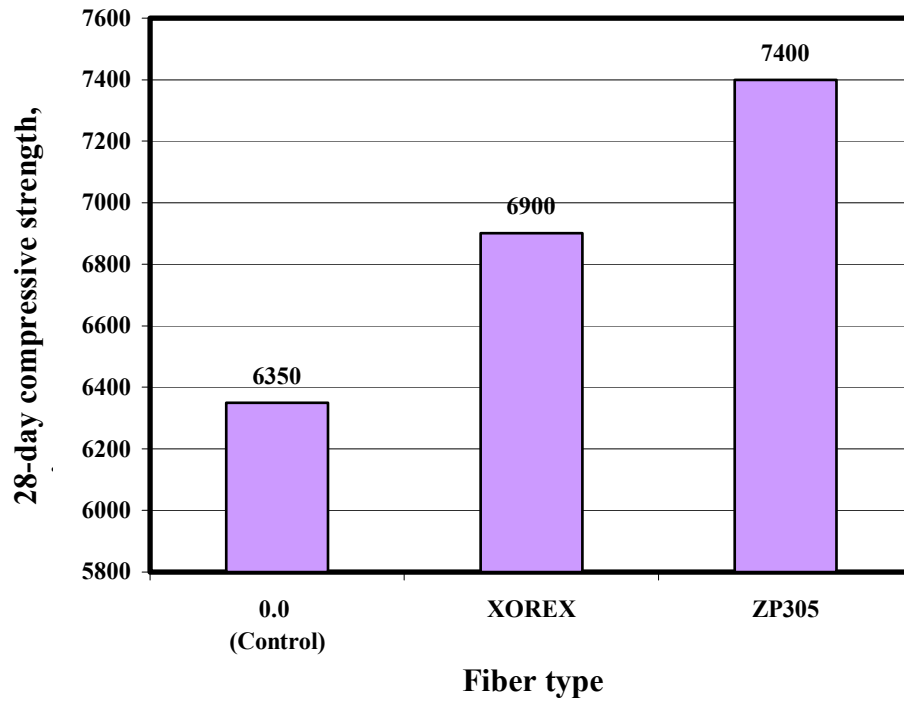


**Figure 4.5: Compressive strengths of specimens with 0.75% steel fiber**

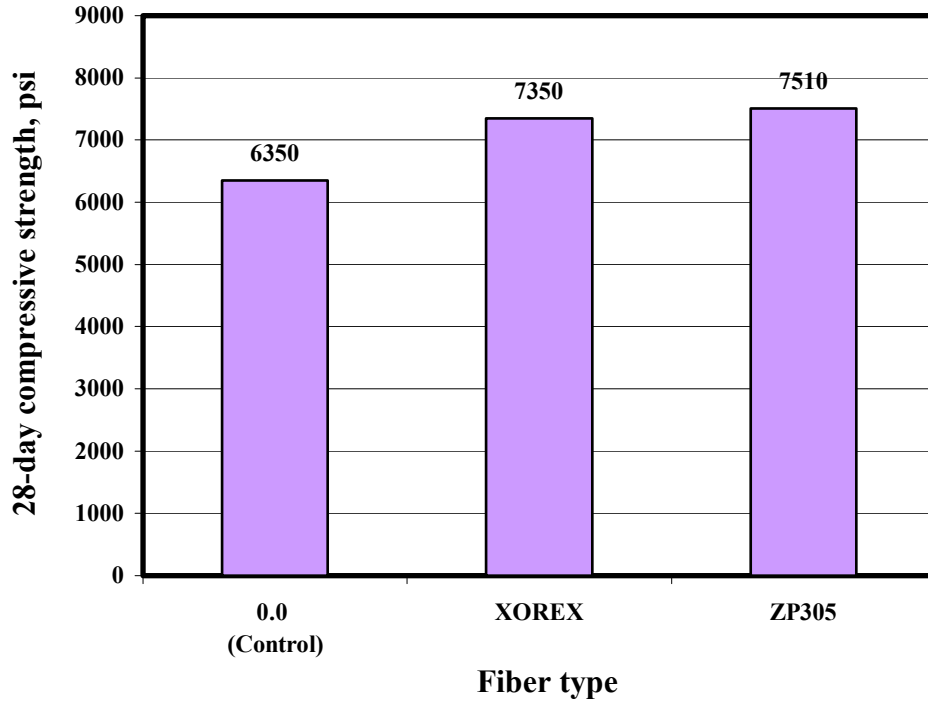


**Figure 4.6: Compressive strengths of specimens with 1.0% steel fiber**

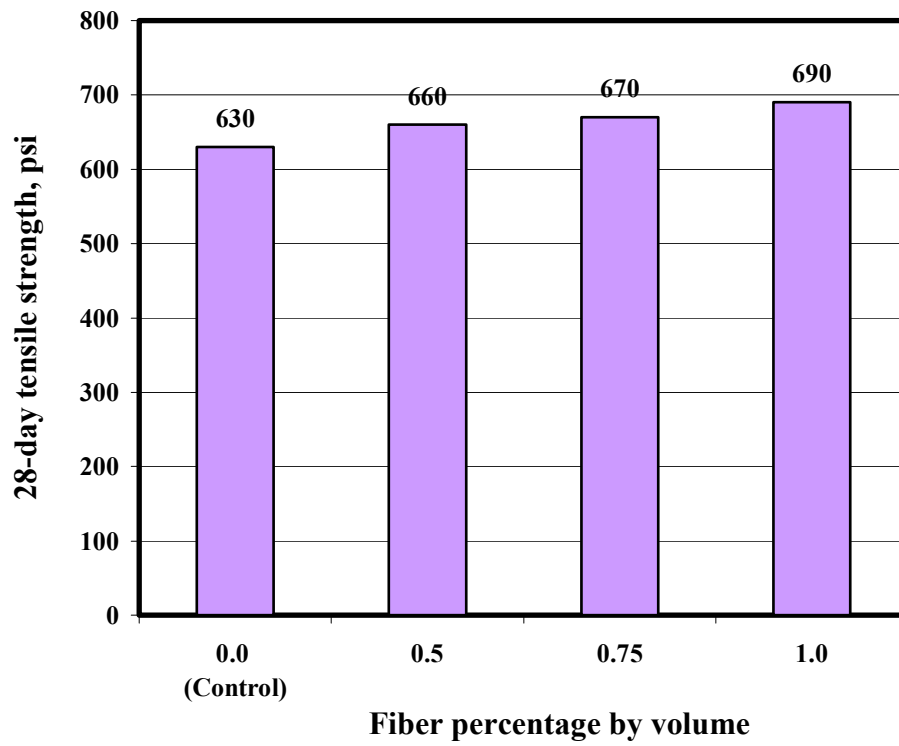


**Figure 4.7: Tensile strength results for specimens with XOREX steel fiber**

strengths, as seen in Fig. 4.7 and 4.8. Figure 4.9 indicates that the incorporation of H-330 fibers in concrete reduced the tensile strength.

Table 4.2 presents the percentile change in the tensile strength of FRC specimens compared to the control specimen. It is observed from the table that the use of 1.0% XOREX and ZP305 steel fibers result in a maximum of 9.52% and 37.3% increase in the tensile strength, respectively.

Figures 4.10, 4.11 and 4.12 present the comparison of tensile strengths of SFRC with the same amount of fibers and the control specimen. H-330 synthetic fiber was not considered here, as the addition of this fiber resulted in a reduced amount of tensile strength. From these charts it is observed that ZP305 SFRC specimens achieved better results than XOREX SFRC specimens for the three volume percentages of fibers.

In case of both the compressive and tensile strength tests, the fibers prevented the concrete from having severe failure mode, such as observed in the control specimens. Although the FRC specimens cracked, the load was transferred directly to the fibers, enabling the fibers to demonstrate their tensile and crack arresting capacities. Figure 4.13 presents sample failed sections from the compressive strength and tensile strength tests, showing the crack and the pattern of steel fibers in the specimens. Cracks were deliberately widened by loading the specimens beyond failure, in order to expose fiber patterns.

#### **4.2.3. Flexural Toughness Test (ASTM C-1018)**

Typical load-deflection curves for concrete beam specimens reinforced with XOREX, ZP305 and H-330 fibers are shown in Figs. 4.14, 4.15 and 4.16, respectively. It

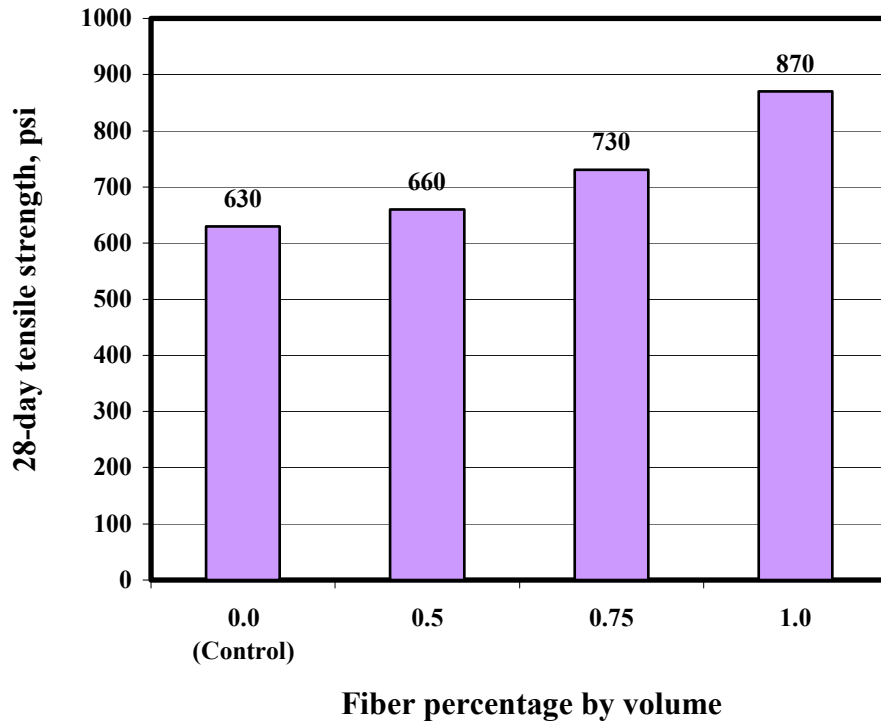


**Figure 4.8: Tensile strength results for specimens with ZP305 steel fiber**

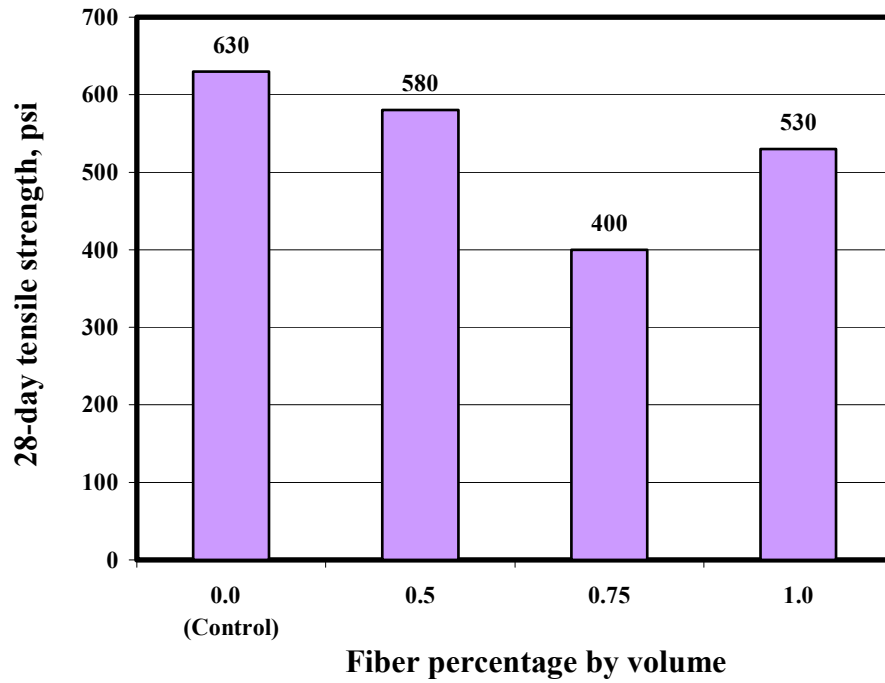


**Figure 4.9: Tensile strength results for specimens with Harbourite H-330 synthetic fiber**

**Table 4.2: Tensile strength results**

Type of fiber	Fiber volume (%)	Tensile strength results	
		Test value, psi (MPa)	Difference with control (%)
<b>Control specimen with no fiber</b>	0.00	630 (4.34)	----
<b>XOREX</b>	0.50	660 (4.55)	+4.76
	0.75	670 (4.63)	+6.68
	1.00	690 (4.75)	+9.52
<b>ZP305</b>	0.50	660 (4.58)	+5.56
	0.75	730 (5.03)	+15.87
	1.00	870 (5.96)	+37.3
<b>Harbourite H-330</b>	0.50	580 (4.03)	-7.14
	0.75	400 (2.76)	-36.5
	1.00	530 (3.62)	-16.67

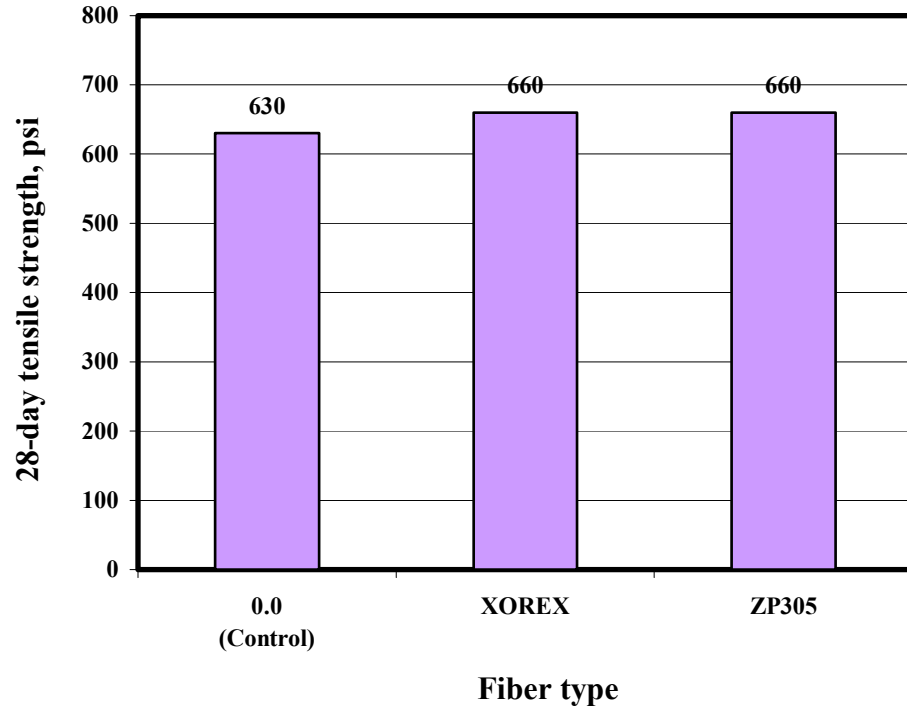


**Figure 4.10: Tensile strengths of specimens with 0.5% steel fiber**

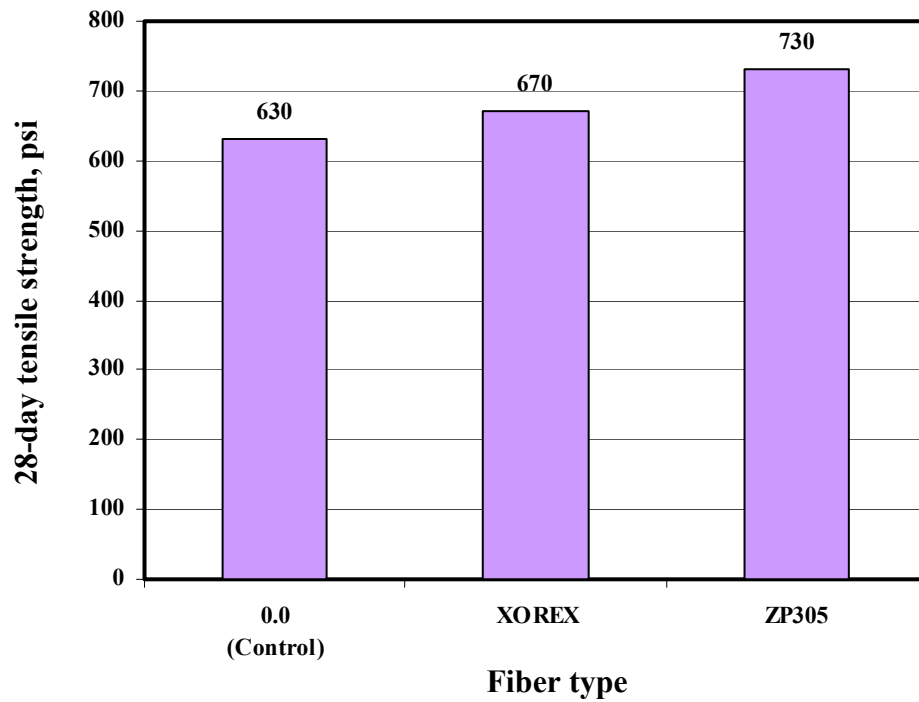


**Figure 4.11: Tensile strengths of specimens with 0.75% steel fiber**

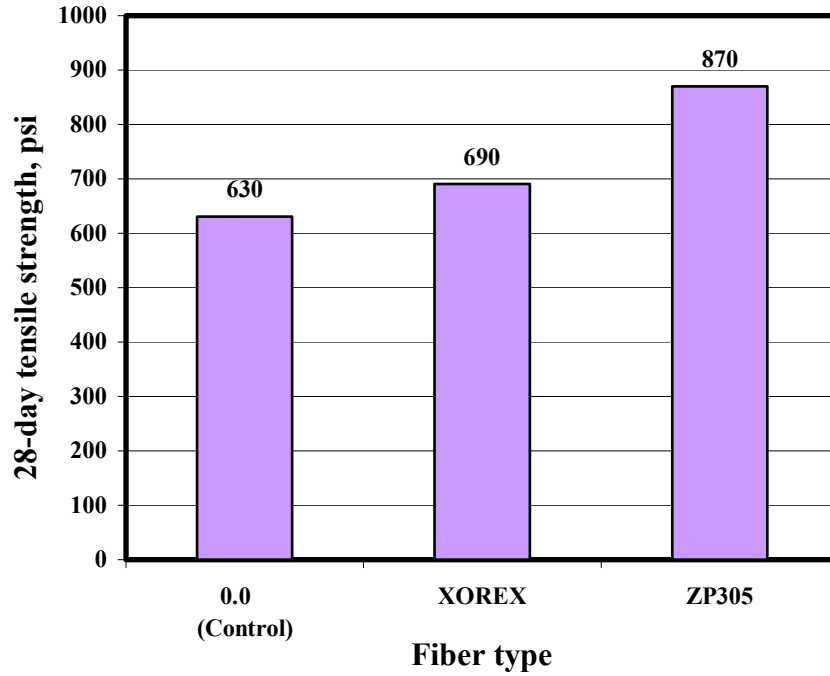


**Figure 4.12: Tensile strengths of specimens with 1.0% steel fiber**



**(a) Compressive strength      (b) Tensile strength**

**Figure 4.13: Failed specimens with 1.0% ZP305 steel fiber**

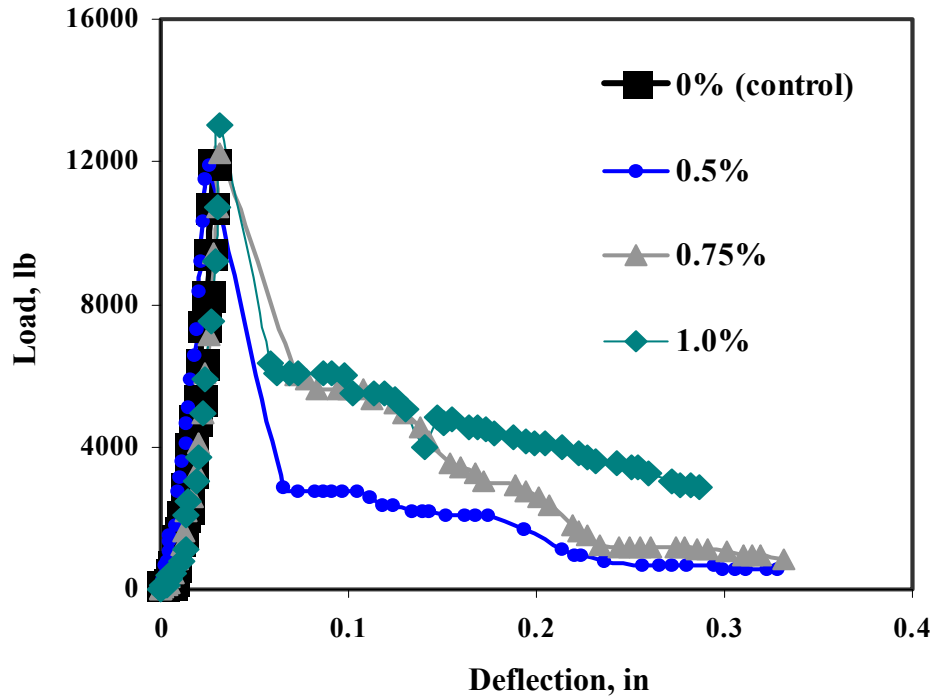


Figure 4.14: Flexural load vs. deflection curves for specimens with XOREX steel fiber

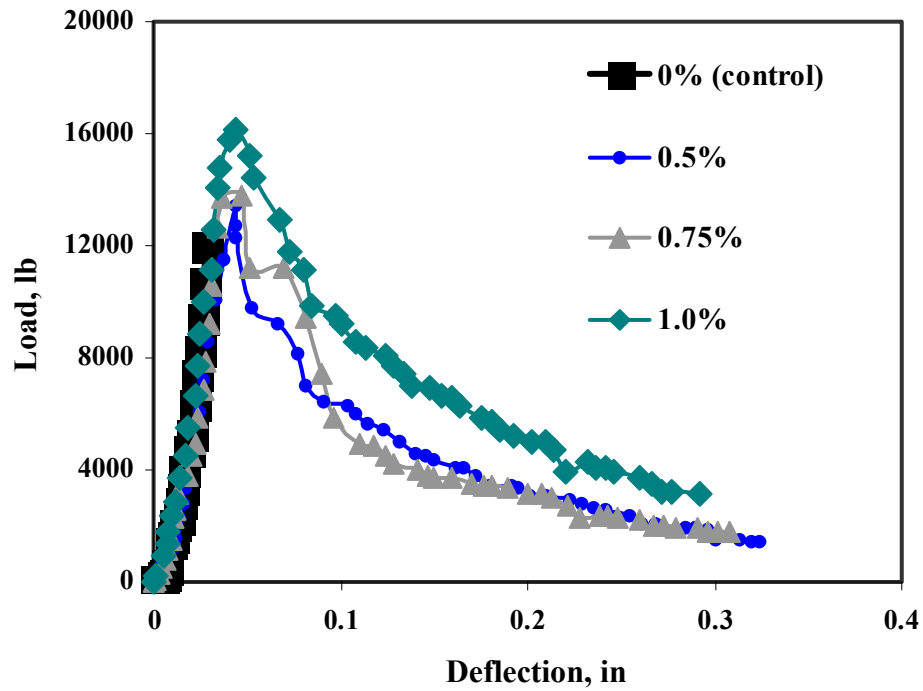
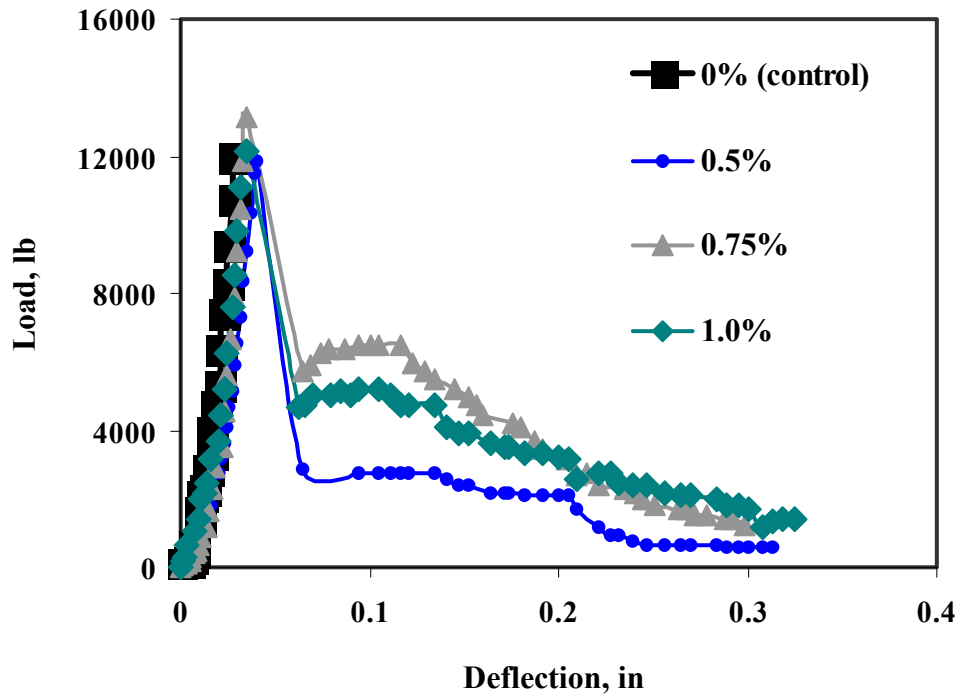


Figure 4.15: Flexural load vs. deflection curves for specimens with ZP305 steel fiber



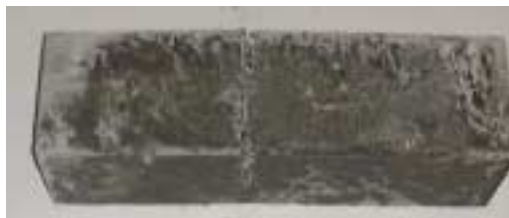
**Figure 4.16: Flexural load vs. deflection curves for specimens with Harbourite H-330 synthetic fiber**



**(a) Non-fibrous concrete**



**(b) 1% XOREX steel fiber**



**(c) 1% ZP305 steel fiber**



**(d) 1% H-330 PP fiber**

**Figure 4.17: Flexural toughness specimens after failure**

may be observed that beams without fibers failed suddenly when the first flexural crack formed. Plain concrete fails in a brittle mode immediately upon cracking without any further load carrying capabilities. Beams with fibers did not fail suddenly when cracking observed. It is also seen from these figures that the pre-peak response for both plain concrete and FRC is nearly identical and the influence of fibers is observed after the occurrence of the peak load. Greater volumes of fibers result in increasing first crack load for all three types of fibers. For XOREX and H-330 fibers, a sudden drop in the load was observed after the first crack, whereas a more gradual drop in the load occurred in case of ZP305 fiber. Instead of a little overlapping of the post-peak portions of these curves, it may be observed that greater volumes of fibers lead to a more stable failure of the specimen.

Figure 4.17 shows various flexural toughness test samples after failure. Figure 4.18 shows a close up view of the crack developed in the concrete beam from Fig. 4.17 (c) containing 1% ZP305 steel fibers. The following observations may be made from these figures:

- A concrete beam containing fibers suffers damage by gradual development of the crack with increasing deflection, but retains some degree of structural integrity and post-peak resistance, even with considerable deflection.
- A similar plain concrete beam without fibers fails suddenly at a small deflection by separation into two pieces.

It is clear from the load-deflection curves of FRC that the performance of a fiber in concrete may be characterized by two regions of the load-deflection curve:



**Figure 4.18: Crack development in a beam containing ZP305 steel fibers**

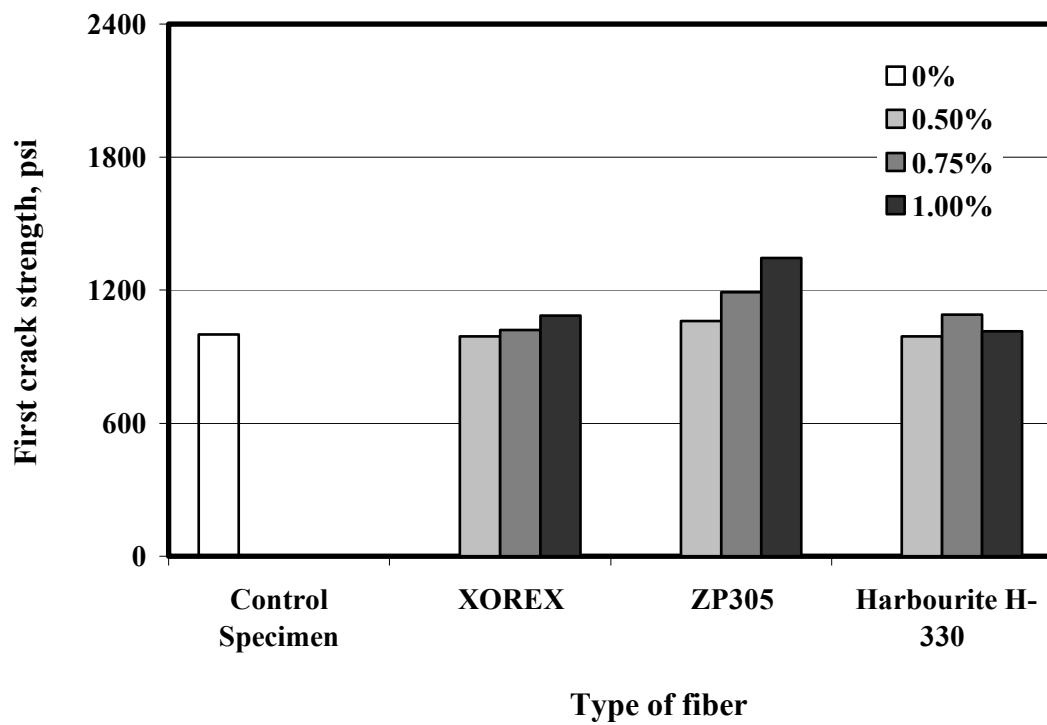


**Figure 4.19: Influence of fiber type and volume fractions on first crack strengths**

- (a) the region before the first crack point, and
- (b) the region after the first crack point.

The performance of the fiber up to the first crack may be measured by the first crack strength (ASTM C-1018 1997). The percentile change in first crack strength of FRC specimens compared to control specimens is presented in Table 4.3. In case of the XOREX, ZP305 and Harbourite H-330 fibers, a maximum of 8.5%, 34.5% and 9.0% increase in the first crack strength of FRC were obtained, respectively. Figure 4.19 shows bar chart representation of the first crack strengths of the specimens. It may be observed that greater volumes of fibers result in increasing first crack strengths, except for Harbourite H-330 polypropylene fiber. ZP305 steel FRC specimens achieved the greatest first crack strength for all three fiber volumes.

The performance of the fiber after the occurrence of the first crack is characterized by the toughness indices and the residual strength factors, calculated herein using ASTM C-1018 (1997) definition. The definitions of toughness, toughness indices and residual strength factors were presented in Chapter 2.

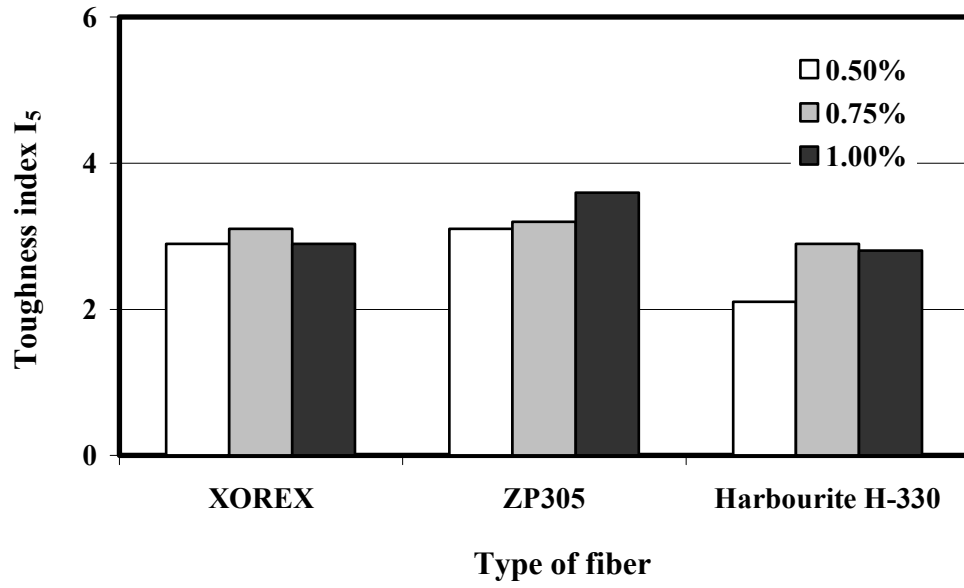
Table 4.4 presents the toughness indices and residual strength factors for XOREX, ZP305 and Harbourite H-330 fibers. The maximum values of toughness index  $I_5$  for XOREX, ZP305 and Harbourite H-330 fibers were 3.1, 3.6 and 2.9, respectively, and toughness index  $I_{10}$  for these three fibers were 5.5, 5.3 and 4.8, respectively. Figure 4.20 presents the calculated toughness indices for the three types of fibers and the three different fiber volume fractions. For XOREX steel fiber, toughness index  $I_5$  remained almost the same for the three fiber volumes, whereas toughness index  $I_{10}$  increased consistently for increases in fiber content. For ZP305 steel fiber, the toughness indices  $I_5$

**Table 4.3: First crack strengths of FRC and control specimens**

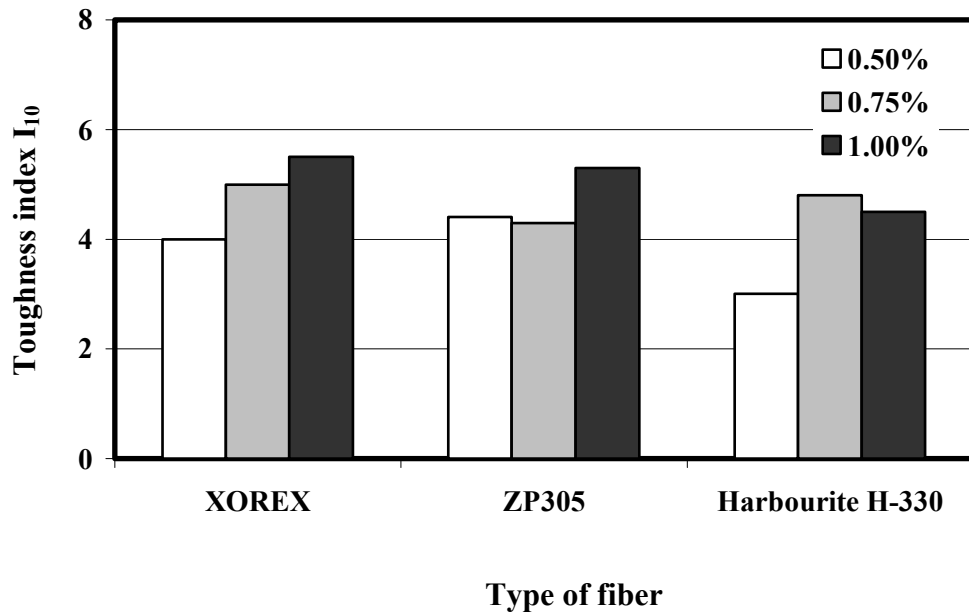
Type of fiber	Fiber volume (%)	Flexural toughness results	
		First crack strength, psi (MPa)	Difference with control (%)
<b>Control specimen with no fiber</b>	0.00	1000 (6.9)	----
<b>XOREX</b>	0.50	990 (6.8)	-1.0
	0.75	1020 (7.0)	+2.0
	1.00	1085 (7.5)	+8.5
<b>ZP305</b>	0.50	1160 (7.3)	+6.0
	0.75	1190 (8.2)	+19.0
	1.00	1345 (9.3)	+34.5
<b>Harbourite H-330</b>	0.50	990 (6.8)	-1.0
	0.75	1090 (7.5)	+9.0
	1.00	1015 (7.0)	+1.5

**Table 4.4: Comparisons of residual strength factors of various FRC**

Type of fiber	Fiber volume (%)	Toughness indices		Residual strength factor
		$I_5$	$I_{10}$	
<b>XOREX</b>	0.50	2.9	4	21
	0.75	3.1	5	37
	1.00	2.9	5.5	52
<b>ZP305</b>	0.50	3.1	4.4	26
	0.75	3.2	4.3	22
	1.00	3.6	5.3	34
<b>Harbourite H-330</b>	0.50	2.1	3	18
	0.75	2.9	4.8	38
	1.00	2.8	4.5	33



(a) Toughness index  $I_5$



(b) Toughness index  $I_{10}$

**Figure 4.20: Influence of fiber types and volume fractions on toughness indices**

and  $I_{10}$  for 0.50% and 0.75% volume remained almost constant, but an increase in these values is observed for 1.0% volume of ZP305 fiber. For Harbourite H-330 synthetic fiber, an increase in toughness indices for 0.50% and 0.75% volumes of fibers is observed, but these values remained almost constant for 0.75% and 1.00% volumes of fibers.

From Table 4.4, it is observed that for XOREX, ZP305 and Harbourite H-330 fibers, the maximum values of calculated residual strength factors were 52, 34 and 38, respectively. Figure 4.21 shows the bar charts for the calculated residual strength factors for the three types and three different volume fractions of fibers. It is observed that greater volumes of fibers result in greater residual strength factors.

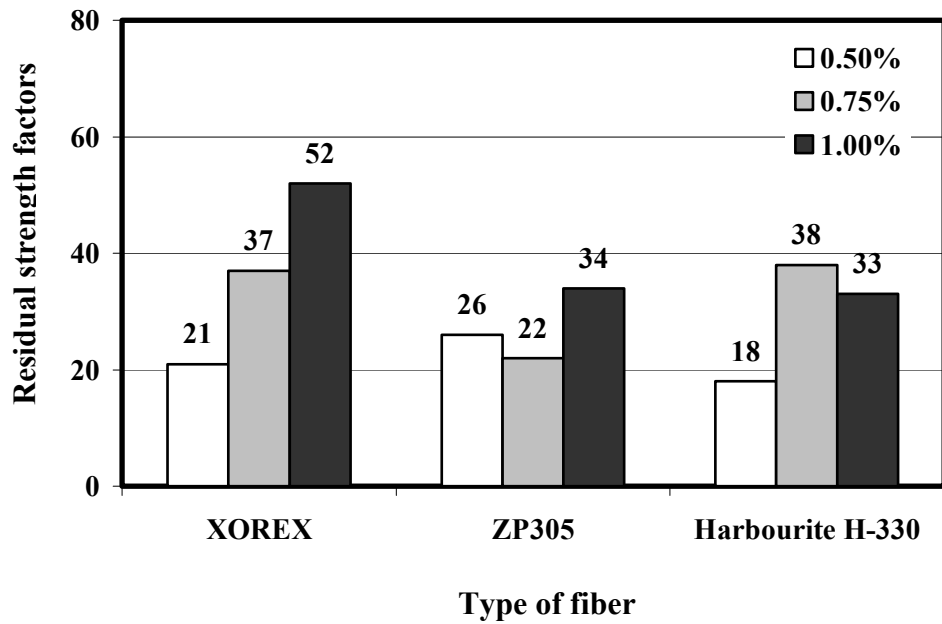


**Figure 4.21: Influence of fiber types and volume fractions on residual strength factors**

## **CHAPTER 5**

# **AASHTO SPECIAL ANCHORAGE DEVICE ACCEPTANCE TEST**

### **5.1. Introduction**

This chapter describes the experimental program for the AASHTO Special Anchorage Device Acceptance Test (AASHTO 1998). The details of the test specimen and the test procedure are presented here. Fiber types and amounts were selected for the tests based on the previous laboratory testing described in Chapters 3 and 4.

### **5.2 AASHTO Special Anchorage Device Acceptance Test**

AASHTO (1998) Article 10.3.2.3 describes the Special Anchorage Device Acceptance Test. This section outlines the dimensions and reinforcement of the test block, local zone reinforcement, loading procedure and evaluation criteria in detail. Three tests procedures are specified by AASHTO (1998) for the evaluation of local anchorage zone reinforcement. They are:

1. Cyclic Loading Test: In this test, the load is first increased to  $0.8F_{pu}$  ( $F_{pu}$  is the ultimate tensile strength of the largest tendon that the anchorage device is designed to accommodate). Then the load is cycled from  $0.1F_{pu}$  to  $0.8F_{pu}$  (for a minimum of 10 cycles) until the crack widths stabilize. After completion of the cyclic loading, the specimen is loaded to failure.
2. Sustained Loading Test: In this test, the load is first increased to  $0.8F_{pu}$  and held constant until the crack widths stabilize, for a minimum of 48 hours. After sustained loading is completed, the specimen is loaded to failure.
3. Monotonic Loading Test: In this test, the load is first increased to  $0.9F_{pu}$  and held constant for an hour. Then the specimen is loaded to failure.

The ultimate failure load of a test block is not greatly affected by the test procedure (Breen *et al* 1994). Therefore, if ultimate load criteria were the only measure of performance, the simple monotonic testing procedure would be adequate. But according to AASHTO (1998), the acceptance of a test block is controlled by the failure load and the crack width of the block. The number of widths and cracks are greatly influenced by the test method (Breen *et al* 1994). The cyclic and sustained load tests result in the greatest amount of distress, while the monotonically loaded specimens show the least. On the other hand, the sustained load transfer test is tedious and expensive. It is not always possible to tie up an expensive piece of testing equipment for the minimum required 48 hours for this test. The cyclic loading test solves this problem. The levels of specimen distress at the end of the sustained load and the cyclic load are very similar (Breen *et al* 1994). Therefore, the cyclic loading test was preferred in this study.

### **5.2.1. Selection of Anchorage Type**

A VSL EC 5-7 type anchorage was selected for this study. Figure 5.1 shows the details of the selected anchorage (VSL Corporation 2002). VSL type EC anchorage is frequently used in prestressed bridge girders. However, larger anchorage sizes such as EC 5-12 and EC 5-19 are more common. According to the cyclic loading test procedure, a load at least equal to the ultimate load of the largest tendon is to be applied on the test block. For anchorage type EC 5-12, a load of at least 496 kips (2200 kN) is to be applied on the specimen (Appendix A). A test machine of this high capacity was not available to this study. So, a smaller size anchorage was used herein.

### **5.2.2. Configuration of The Test Block**

#### **Components of the anchorage**

As per AASHTO (1998): *“The test block for the acceptance test is a rectangular prism. It shall contain those anchorage components that will also be embedded in structure’s concrete. Their arrangement shall comply with the practical application and the suppliers’ specifications. The test block shall contain an empty duct of size appropriate for the maximum tendon size that can be accommodated by the anchorage device”.*

The appropriate diameter of the duct for the chosen VSL EC 5-7 type anchorage is 2.5 in (64 mm). All the ducts for the acceptance test were supplied by VSL Corporation.

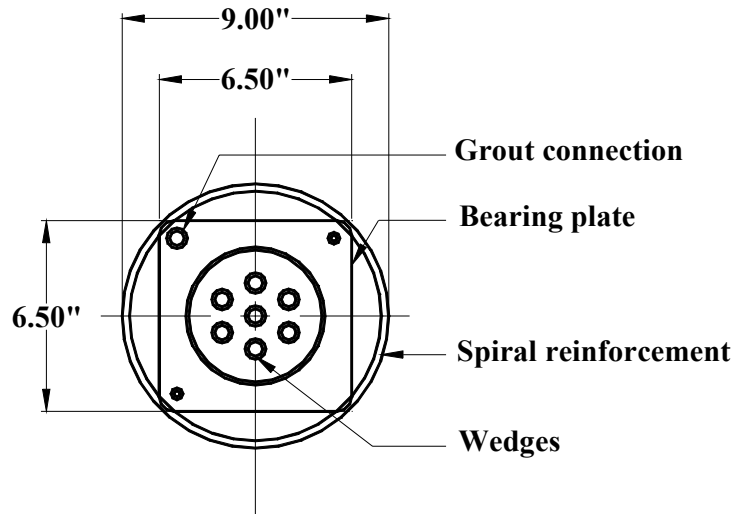
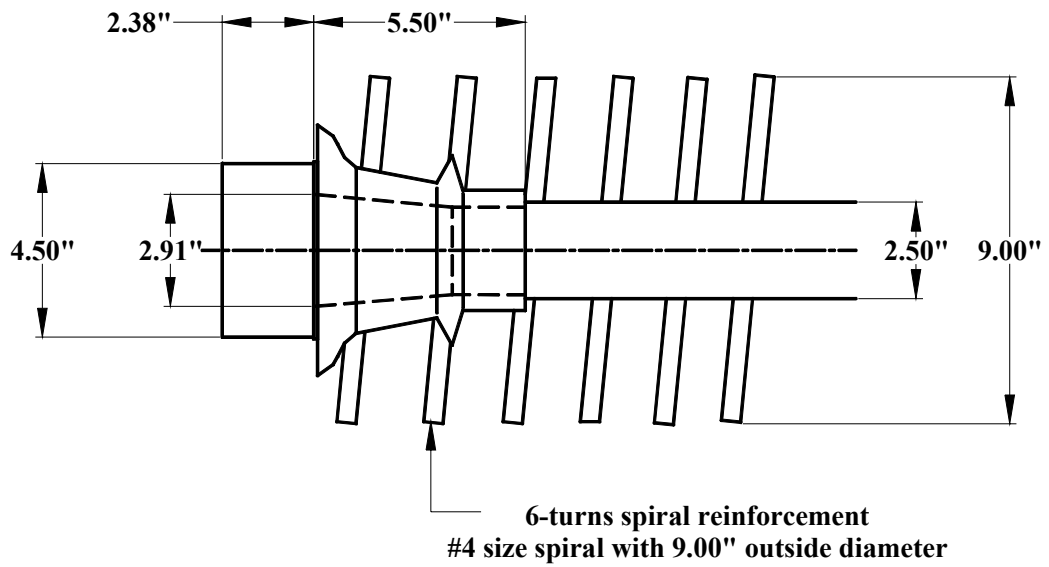


**Figure 5.1: VSL EC 5-7 type anchorage (VSL 2002)**

## **Size and Shape of the test block**

According to AASHTO (1998): *“The dimension of the test block perpendicular to the tendon in each direction shall be the smaller of the minimum edge distance or the minimum spacing specified by the anchorage device supplier, with the stipulation that the cover over any confining reinforcing steel or supplementary skin reinforcement be appropriate for the particular application and environment. The length of the block along the axis of the tendon shall be at least two times the larger of the cross-section dimensions”*.

The test block dimensions typically are controlled by one of the following:

- *Cover over spiral:* As per VSL Corporation (2002), Type EC 5-7 anchorage requires a spiral reinforcement of 9 in (228.6 mm) diameter and the minimum cover over the spiral is 1 in (25.4 mm). Based on this criteria, the dimension of the test block is 11 by 11 in (279.4 by 279.4 mm).
- *Cover over skin reinforcement:* The dimension of the skin reinforcement is controlled by the diameter of the spiral. It requires a dimension of 10 by 10 in (254 by 254 mm) to avoid interference with the 9 in (228.6 mm) diameter spiral. A skin reinforcement of 10 by 10 in (254 by 254 mm) dimension with 1 in (25.4 mm) clear cover results in a test block size of 12 by 12 in (305 by 305 mm).
- *Strength of concrete in lower (lightly reinforced) portion of test block:* Equation 2.1 mentioned in Chapter 2 also controls the dimension of the test block (Wollmann and Roberts-Wollmann 2000). As shown in the Appendix A, for Type EC 5-7 anchorage, the ultimate strength of tendon is 289 kips (1286 kN). The minimum strength of concrete at the time of testing, as per VSL Corporation, is

3500 psi (24 MPa). This results in a test block dimension of 9.75 by 9.75 in (248 by 248 mm).

So, for the VSL system including spiral and ties, a 12 by 12 in (305 by 305 mm) test block should be used for anchorage type EC 5-7. As the block contains both the spiral and the skin reinforcement, a test block of 12.5 by 12.5 in (317.5 by 317.5 mm) dimension was used to place the reinforcement with ease. For a test block of dimensions 12.5 by 12.5 in (317.5 by 317.5 mm), the required length is twice the width, *i.e.* 25 in (635 mm).

### **Spiral Reinforcement**

As per AASHTO (1998): *“The confining reinforcing steel in the local zone shall be the same as that specified by the anchorage device supplier for the particular system”*.

As mentioned earlier, VSL Type EC 5-7 anchorage requires #4 spiral reinforcement with an outside diameter of 9 in (228.6 mm). The spiral shall have 6 number of turns with 2 in (50.8 mm) pitch.

### **Skin Reinforcement**

According to AASHTO (1998): *“In addition to the anchorage device and its specified confining reinforcement steel, supplementary skin reinforcement may be provided throughout the specimen. This supplementary skin reinforcement shall be specified by the anchorage device supplier but shall not exceed a volumetric ratio of 0.01”*.

In this study, skin reinforcement with a volumetric ratio of 0.01 was used. Five #4 rebars (Appendix A) were used as the skin reinforcement. Skin reinforcement was placed with equal spacing and 1 in (25.4 mm) cover from the side face of the block.

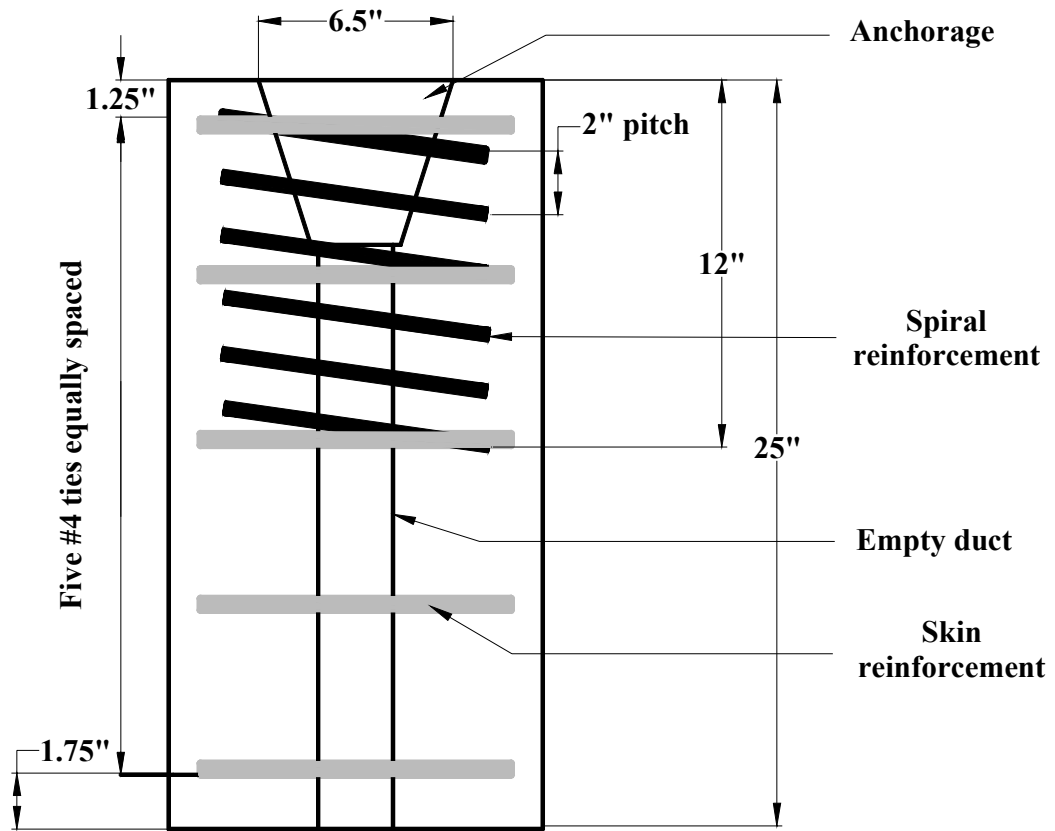
### **Summary of the test block**

Figure 5.2 shows the configuration of the control test specimen with no fiber. The details are as follows:

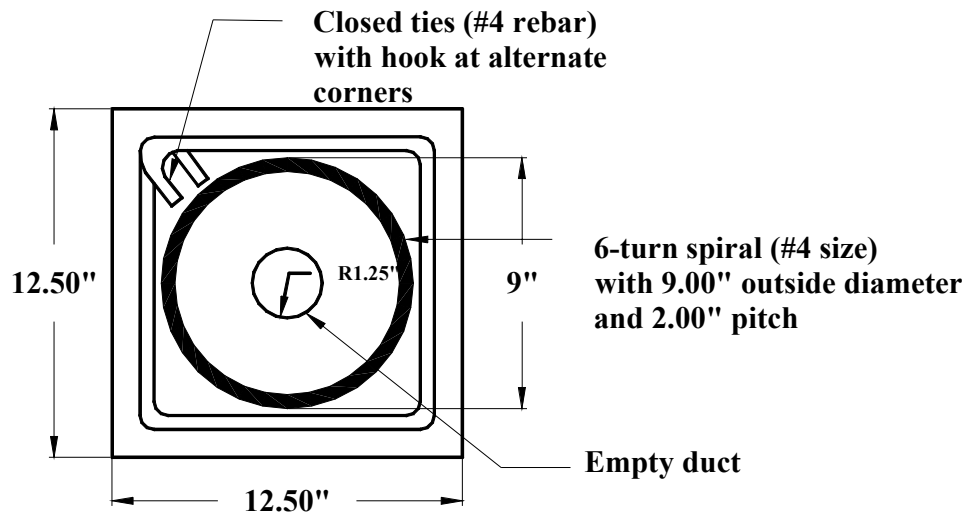
- Cross section: 12.5 by 12.5 in (317.5 by 317.5 mm)
- Length: 25 in (635 mm)
- Anchorage type: EC 5-7 with plastic duct
- Confining reinforcement: #4 spiral with 6-turns
- Supplementary skin reinforcement: 5 #4 equally spaced stirrups with 1 in (25.4 mm) clear cover
- An empty duct of 2.5 in (64 mm) diameter

### **Test Procedure**

The cyclic loading test procedure requires that the specimen be placed in a calibrated test machine. The compressive load must be applied corresponding to normal applications either by loading the tendon or applying the force directly to the anchor. The load on the test block is increased up to  $0.8F_{pu}$ . After reaching the  $0.8F_{pu}$  load, at least ten load cycles are to be applied with the upper and lower limits of  $0.8F_{pu}$  and  $0.1F_{pu}$ , respectively. The necessary number of cycles depends on the stabilization of crack widths, but shall be no less than 10. Following the completion of the cycles, the specimen is to be loaded to failure. Figure 5.3 shows the schematic diagram of the experimental set up and loading of the test. Crack widths are considered to be stabilized when they do not

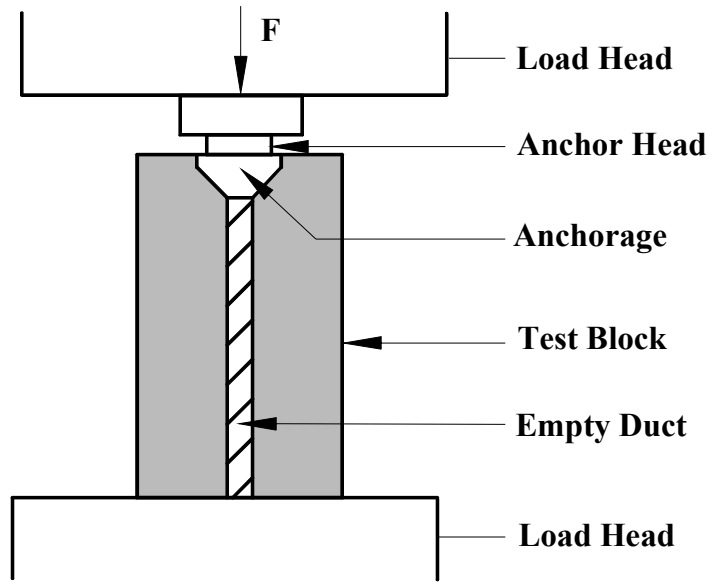


(a) Elevation

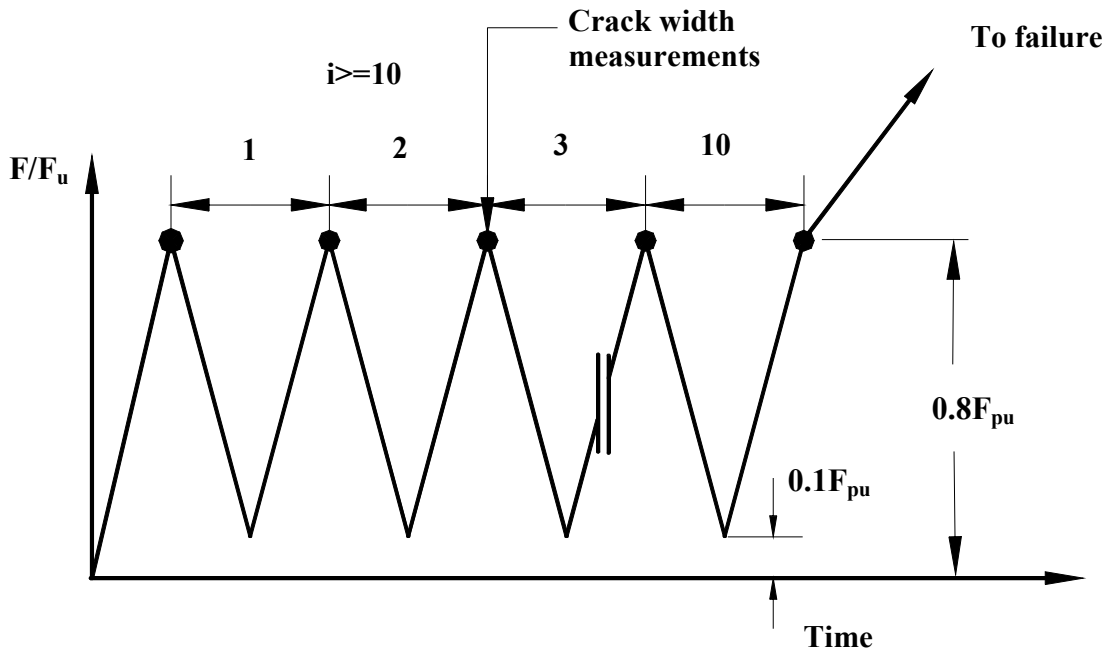


(b) Plan

Figure 5.2: Configuration of AASHTO test block



(a) Experimental set up



(b) Cyclic load details

Figure 5.3: Schematic diagram of the experimental set up and cyclic loading

change by more than 0.001 in (0.0254 mm) over the last three cycles. The following measurements and observations are made in a cyclic loading test:

- Crack widths and crack patterns recorded at the initial load of  $0.8F_{pu}$ .
- Crack widths and crack patterns recorded at the last three consecutive peak loadings before termination of the cyclic loading.
- Crack widths and crack patterns recorded at the load of  $0.9F_{pu}$ .
- The maximum failure load recorded.

### **Acceptance Criteria**

AASHTO (1998) Specifications have two criteria for the acceptance of the cyclic loading test. They are:

- Failure Load: The strength of the anchorage zone must exceed  $1.1 F_{pu}$ .
- Crack Width: There are two conditions for crack widths:
  - No cracks shall be greater than 0.01 in (0.254 mm) at  $0.8F_{pu}$  after completion of the cyclic loading.
  - No cracks shall be greater than 0.016 in (0.406 mm) at  $0.9F_{pu}$ .

## **5.3. Test Plan**

### **5.3.1. Selection of Fiber Configuration**

Chapter 4 described the mechanical performance of FRC with three types of fibers. The fibers investigated were XOREX steel fiber, ZP305 steel fiber and Harbourite H-330 synthetic fiber. It was observed that FRC with steel fibers performed better than the synthetic fiber in general. FRC with synthetic fiber demonstrated erratic results. It

was also observed that the compressive and tensile strengths of FRC increased with the increase in the volume percentage of fibers. FRC with ZP305 steel fiber produced the best overall mechanical properties. To reduce the number of variables in the test matrix, the following three types of fiber configurations were used in the AASHTO acceptance test:

- 1% XOREX steel fiber
- 0.75% ZP305 steel fiber
- 1% ZP305 steel fiber

### **5.3.2. Selection of Specimen Reinforcement**

As mentioned earlier, the main objective of this study was to reduce or replace the secondary reinforcement, i.e. spiral and skin reinforcement, by fibers. Various configurations of spiral and skin reinforcements were used for the AASHTO cyclic loading test, along with variations in fiber type and volume. The standard specimen configuration for the anchorage Type EC 5-7 was considered herein to be 6-turn spiral and 5 number of skin reinforcement, as shown in Fig. 5.2. In the experimental program, spiral and skin reinforcement were gradually reduced to determine the best possible combination of reinforcement and fiber. Three variations of the spiral and skin reinforcement were considered:

- Spiral Reinforcement: (1) 6-turn spiral (2) 3-turn spiral (3) No spiral
- Skin Reinforcement: (1) 5 skin (2) 3 skin (3) No skin

Figure 5.4 shows the test matrix for each fiber type and dosage configuration. Table 5.1 presents the combinations of spiral and skin reinforcement used in the test

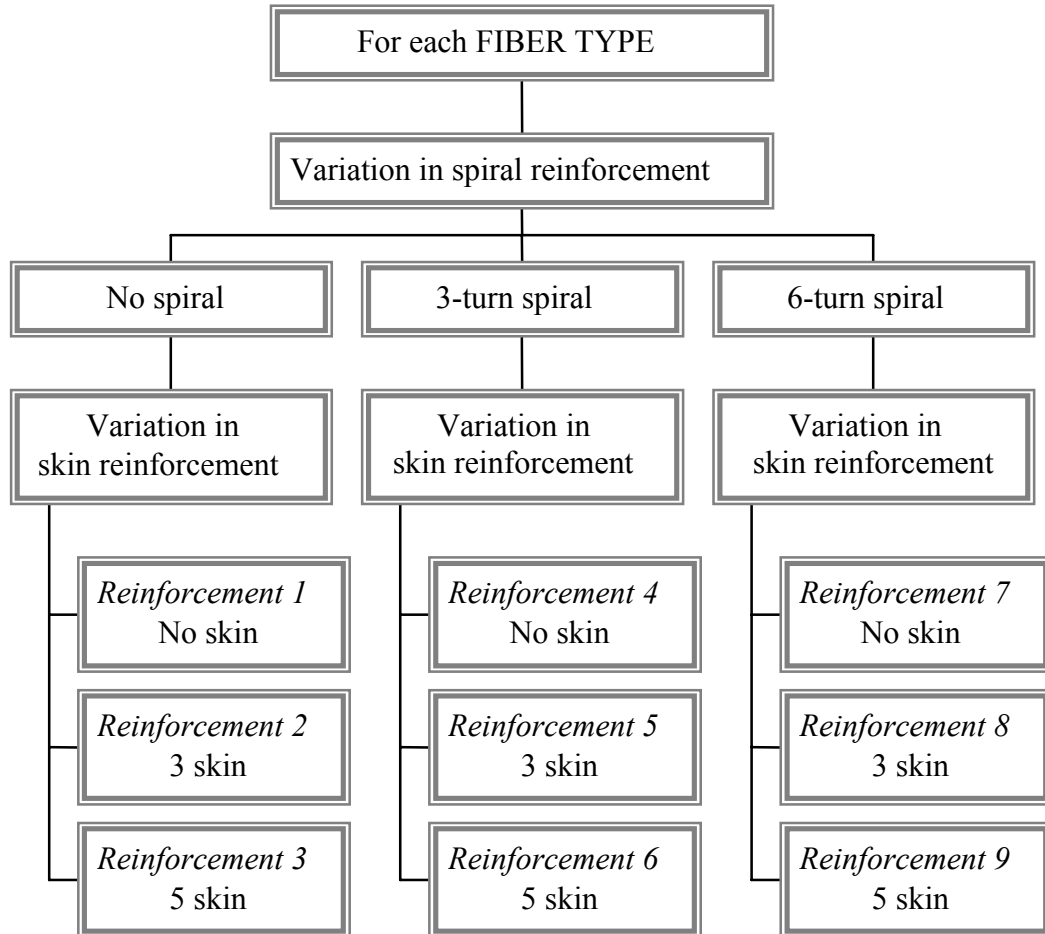


**Figure 5.4: Test matrix for each fiber configuration**

**Table 5.1: Spiral and skin combinations**

<b>ID</b>	<b>Spiral reinforcement</b>	<b>Skin reinforcement</b>
<i>Reinforcement 1</i>	None	None
<i>Reinforcement 2</i>	None	3
<i>Reinforcement 3</i>	None	5
<i>Reinforcement 4</i>	3-turn	None
<i>Reinforcement 5</i>	3-turn	3
<i>Reinforcement 6</i>	3-turn	5
<i>Reinforcement 7</i>	6-turn	None
<i>Reinforcement 8</i>	6-turn	3
<i>Reinforcement 9</i>	6-turn	5

matrix, with designated combination IDs, such as Reinforcement 1, Reinforcement 2, ..., Reinforcement 8 for convenience.

### **5.3.3 Compressive Strength Validation**

According to VSL Corporation (2002), the compressive strength of concrete at the time of the AASHTO acceptance test should not be less than 3500 psi (24 MPa) for a design 28-day strength of 4000 psi (27.5 MPa). Table 4.1 shows that the 28-day compressive strength of the FRC with XOREX and ZP305 steel fibers varied between 6600 to 7510 psi (45.5 to 51.7 MPa). So, the FRC compressive strengths were acceptable according to the VSL guidelines. As per AASHTO (1998): *“The concrete strength at the time of stressing should be greater than the concrete strength of test specimen at time of testing”*. In this study, AASHTO acceptance tests were performed with two ranges of compressive strengths, one with a lower range from 3500 to 5000 psi (24 to 34.5 MPa) and the other with a higher range from 5500 to 7500 psi (37.9 to 51.7 MPa). The lower strength range specimens were tested initially. The higher strength range specimens were tested later on, because they are more representative of the concrete strengths in typical prestressed girders.

## **5.4. Construction Details**

All specimens were cast vertically. Figure 5.5 shows the schematic diagram for the typical formwork. Wood formwork was used to cast the specimens. All spirals were obtained from VSL Corporation. Spirals were subjected to compressive load to obtain the

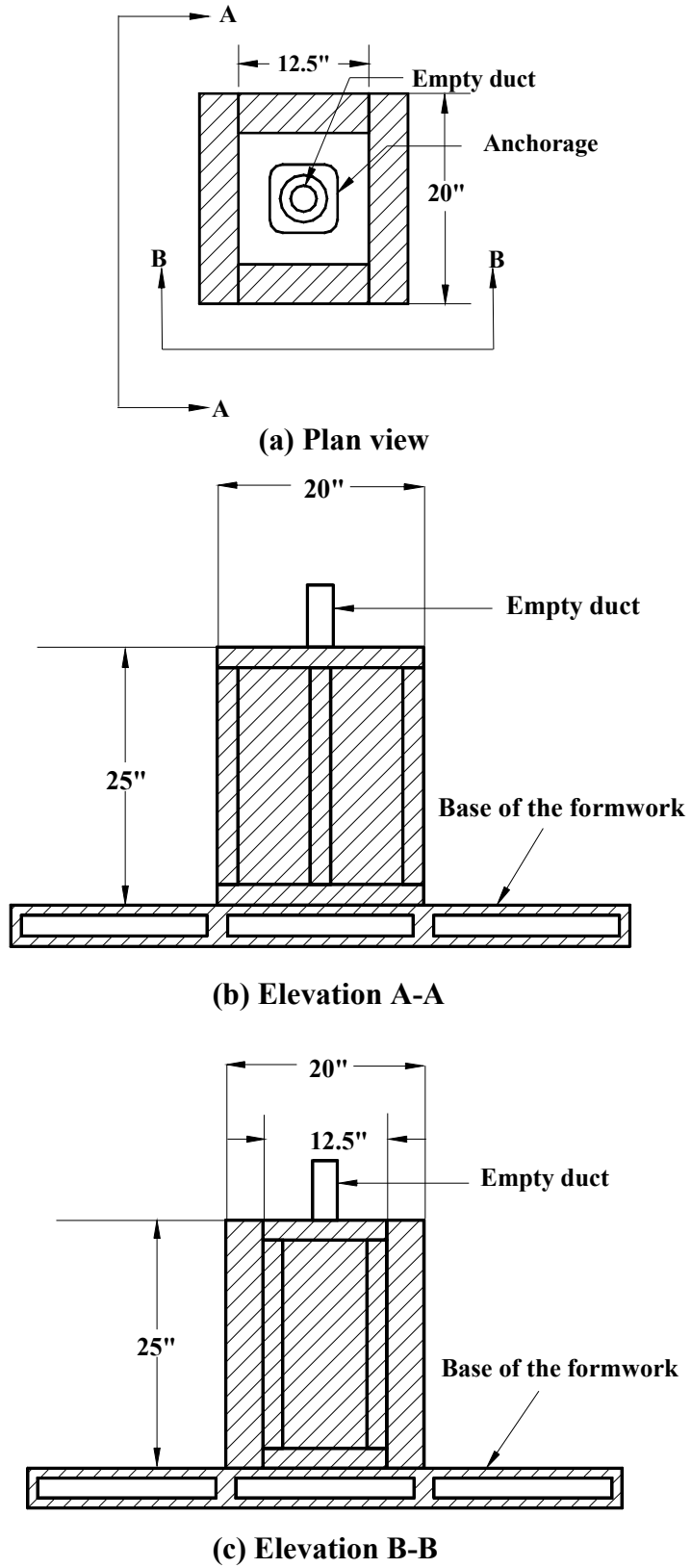


**Figure 5.5: Formwork for the AASHTO test block**

required 2 in (50.8 mm) pitch. Stirrups were obtained from J.H. Dowling in Tallahassee. All reinforcement cages and formwork were fabricated at the FAMU-FSU College of Engineering. The design concrete mix described in Chapter 3 was used herein.

All specimens were cast and cured at the FAMU-FSU College of Engineering. The mixing procedure and curing of specimens were described in Chapter 3. Instead of the external vibrator, an internal vibrator was used for compaction. Four cylinder specimens were prepared along with the AASHTO test block to measure the compressive strength of concrete. Each of these cylinders was tested sequentially at regular intervals to keep track of the compressive strength of concrete. When concrete gained sufficient strength as per Section 5.3.3, the AASHTO block was then tested.

## **5.5. Testing Details**

All specimens were tested at the FDOT Structural Research Center in Tallahassee. A 550 kip (2450 kN) deflection controlled Material Testing System (MTS) was used to perform the test. In this vertical testing machine, each specimen was placed on a rubber pad and carefully centered to ensure the concentric loading of the anchor. The load was applied to the specimen through a spherical loading head into the anchor head. This anchor head was seated against the embedded anchor as in normal post-tensioning application.

Crack comparator cards were used initially to measure crack widths. To obtain a more reliable result, a crack detection microscope was subsequently used instead of crack comparator cards. Figure 5.6 shows a photograph of the crack detection microscope.



**Figure 5.6: Crack detection microscope**

Four inch (100 mm) long crack gages were used on a few samples to measure the strain in concrete. Five gages were attached on each face for specimens with the lower 3500 to 5000 psi (24 to 34.5 MPa) range of compressive strength (Fig. 5.7). For the higher 5500 to 7500 psi (37.9 to 51.7 MPa) range specimens, three gages were used on each face (Fig. 5.8). Crack gages and the load cell were connected to a computer data acquisition system. Figure 5.9 shows the photograph of an actual test set up.

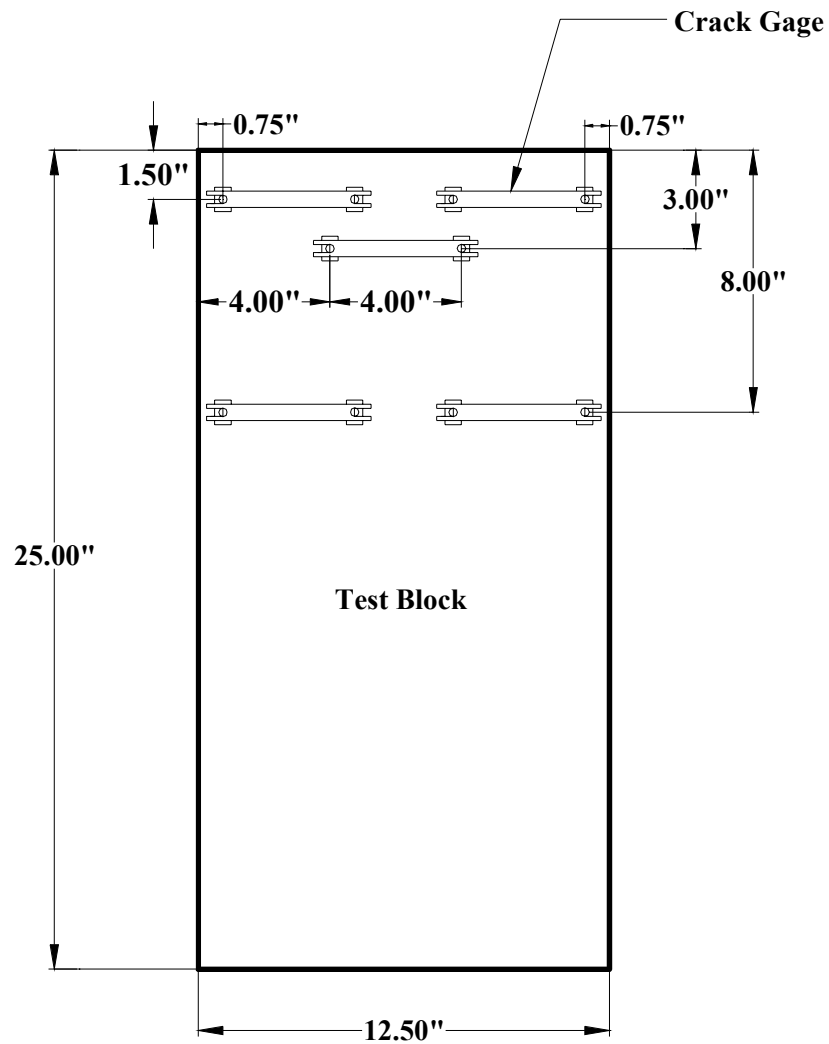


**Figure 5.7: Location of crack gages on AASHTO test blocks with lower concrete strengths**

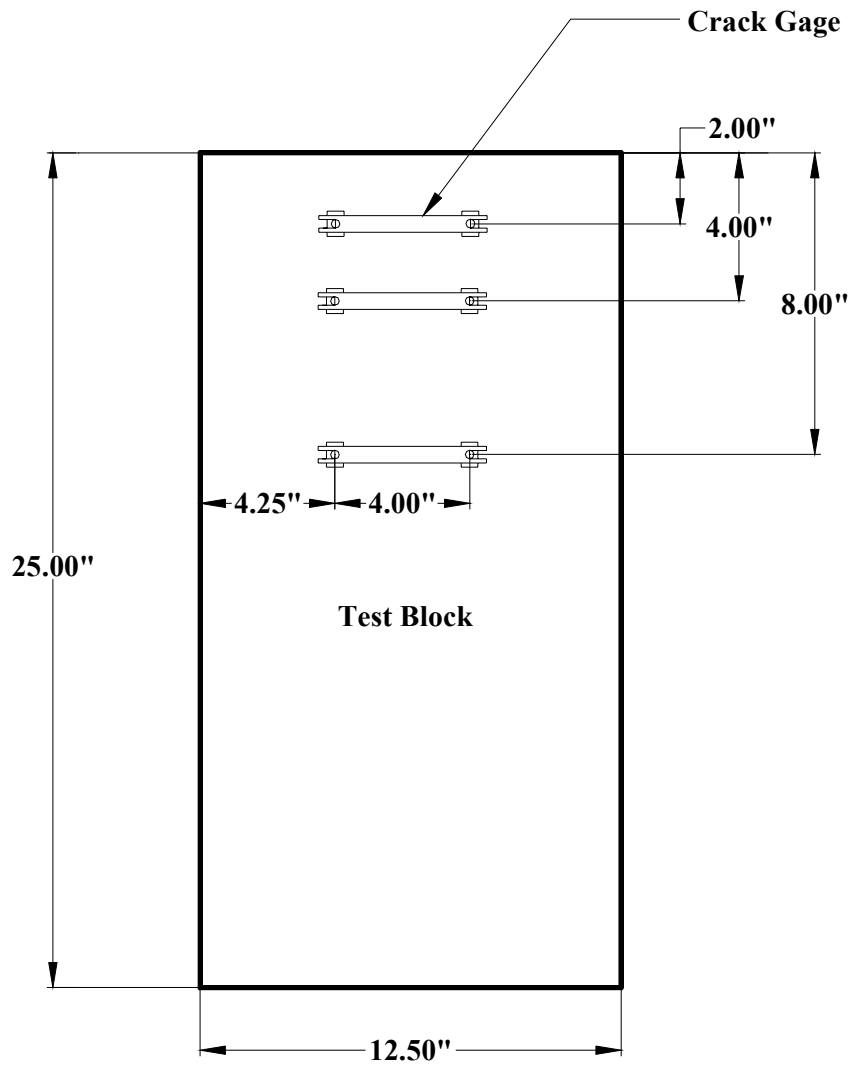


**Figure 5.8: Location of crack gages on AASHTO test blocks with higher concrete strengths**



**Figure 5.9: AASHTO cyclic loading test set up**

# **CHAPTER 6**

## **AASHTO AACCEPTANCE TEST RESULTS**

### **6.1. Introduction**

Results obtained from the AASHTO cyclic loading test described in Chapter 5 are presented and discussed in this chapter. A discussion of the reason behind performing each test series is included. Test results for each series are presented separately. Finally, comparisons for each series are presented.

### **6.2. Test Hierarchy**

As mentioned earlier (Section 5.3.1), three configurations of fibers were used in the AASHTO test programs. Figures 6.1 and 6.2 show the flow chart of the test plan and the reinforcement in specimens, respectively. Tests were initiated with specimens containing either full spiral requirement or full skin reinforcement requirement i.e. either 6-turns spiral (*Reinforcement 7*) or 5 skin (*Reinforcement 3*) reinforcement in all fiber

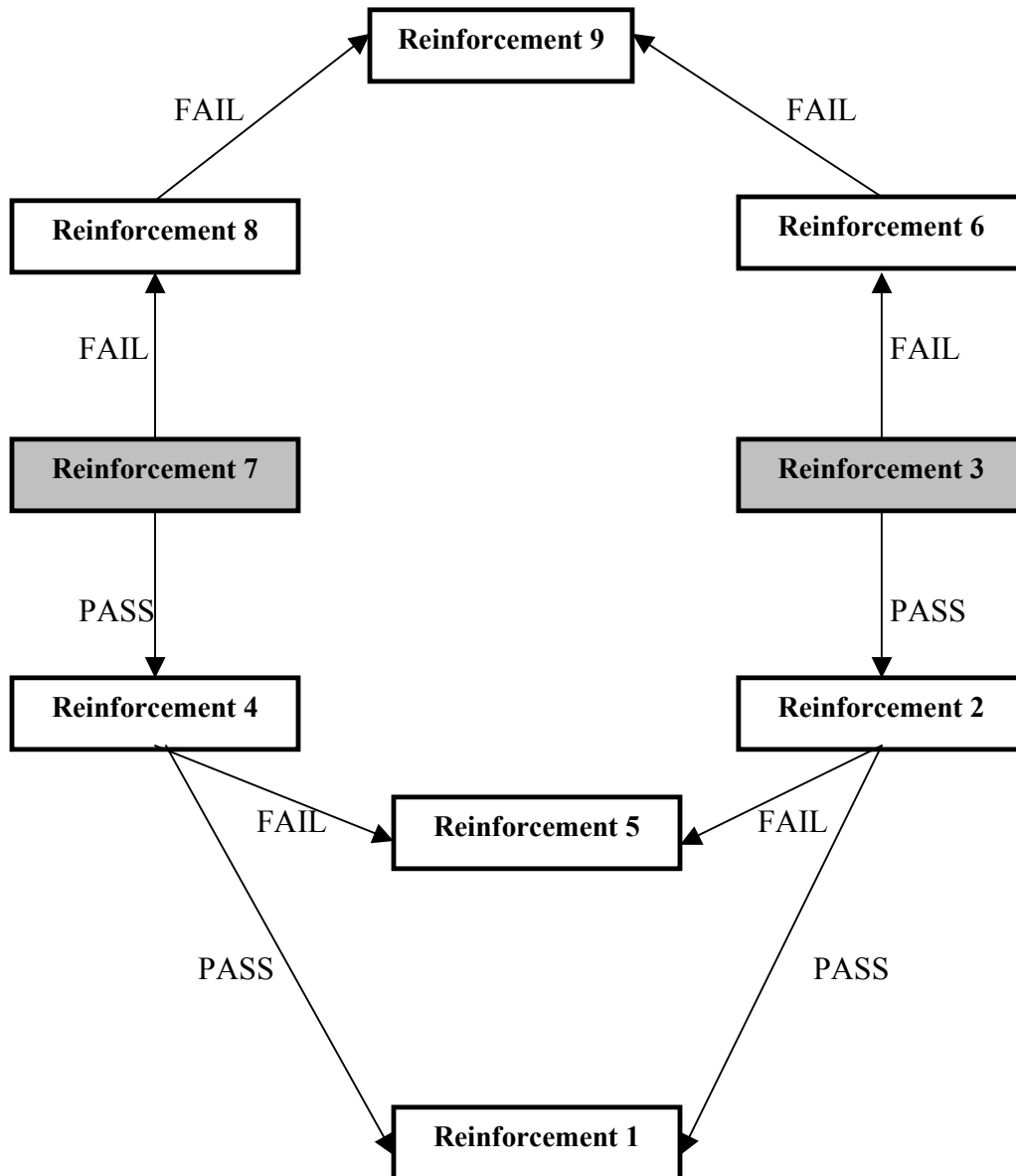
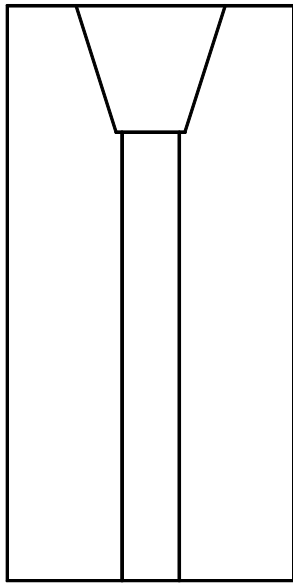
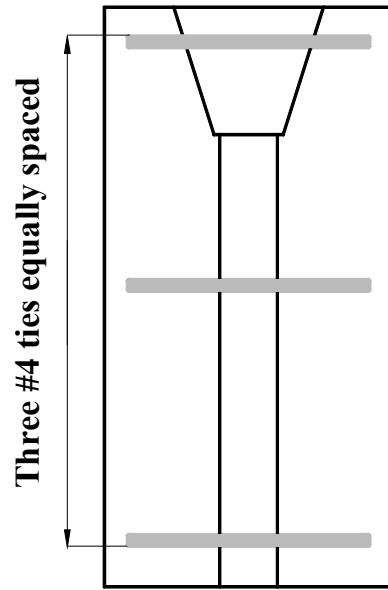


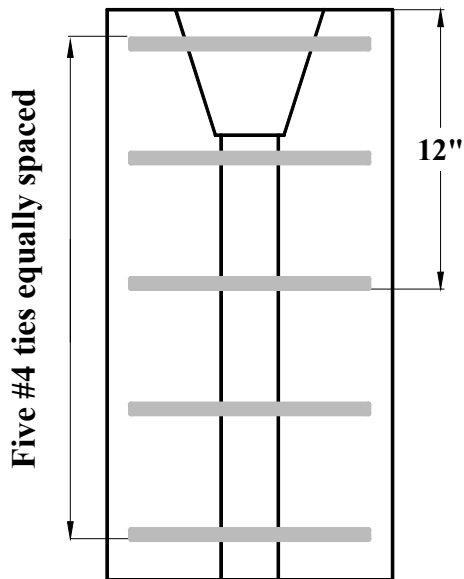
**Figure 6.1: Flow chart of the test hierarchy**



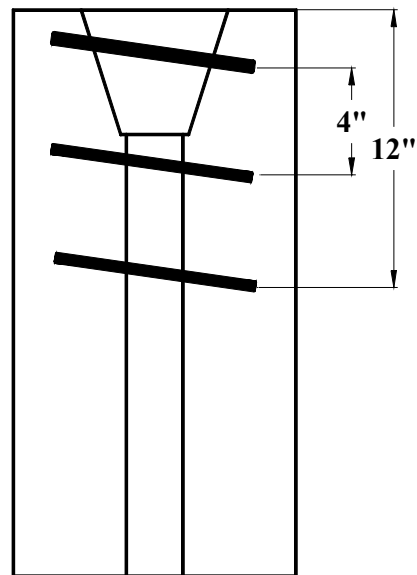
(a) No spiral and no skin  
(Reinforcement 1)



(b) No spiral and 3 skin  
(Reinforcement 2)

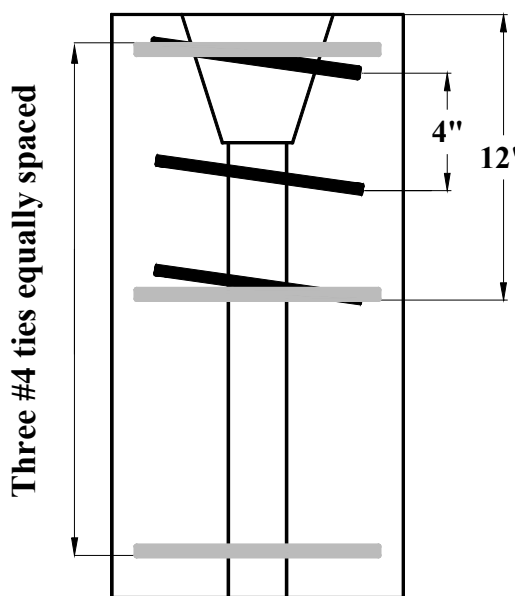


(c) No spiral and 5 skin  
(Reinforcement 3)

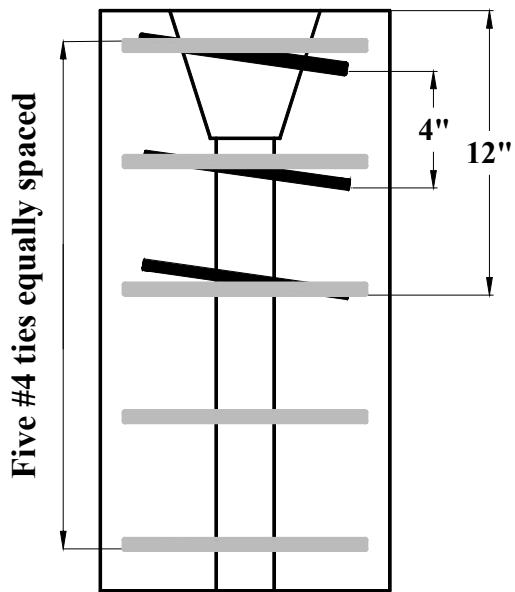


(d) 3-turn spiral and no skin  
(Reinforcement 4)

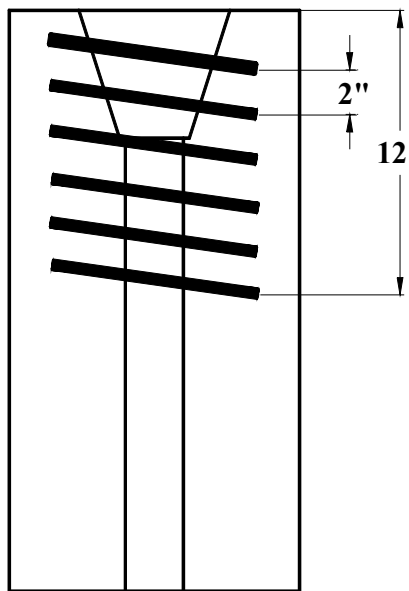
**Figure 6.2: Spiral and skin reinforcement in specimens**



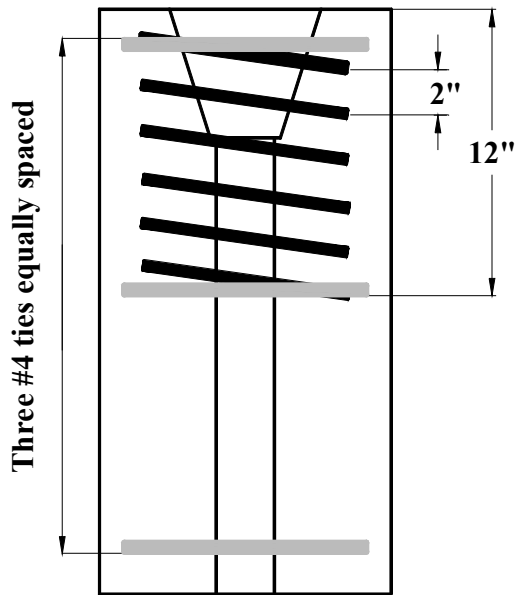
(e) 3-turn spiral and 3 skin  
(Reinforcement 5)



(f) 3-turn spiral and 5 skin  
(Reinforcement 6)



(e) 6-turn spiral and no skin  
(Reinforcement 7)



(e) 6-turn spiral and 3 skin  
(Reinforcement 8)

**Figure 6.2: Spiral and skin reinforcement in specimens (contd.)**

configurations. The next specimen was chosen based on the previous result. If a specimen passed the test, the next test specimen would contain the next lower order reinforcement. On the other hand, if the initial specimen failed, the subsequent specimen would contain the next higher order reinforcement. It was mentioned in Chapter 5 that tests were performed using two ranges of compressive strength at the time of tests:

- Lower compressive strength range from 3500 to 5000 psi (24 to 34.5 MPa) – designated Type 1 herein.
- Higher compressive strength range from 5500 to 7500 psi (37.9 to 51.7 MPa) – designated Type 2 herein.

## **6.3 Results from Type 1 Specimens**

### **6.3.1. Results for Type 1 Specimens with 1% ZP305 Steel Fiber**

Test results for specimens with 1% ZP305 steel fiber are presented in Table 6.1.

#### *TEST 1: Reinforcement 7*

Three specimens containing this reinforcement were tested. The compressive strengths at the time of testing ranged from 4200 to 4500 psi (28.9 to 31 MPa). Crack widths in these specimens at  $0.8F_{pu}$  were 0.0, 0.002 and 0.002 in (0.0, 0.051 and 0.051 mm), respectively. These crack widths were less than 0.01 in (0.254 mm), the maximum permissible crack width at  $0.8 F_{pu}$ . Similarly, all the crack widths at  $0.9F_{pu}$  were less than 0.016 in (0.406 mm). So, the specimen passed the crack width criteria of the acceptance test. The minimum failure load for EC 5-7 anchorage is 318 kips (1415 kN), as shown in Appendix A. The failure loads for these three specimens were 359, 380 and

**Table 6.1: Test results for Type 1 specimens with 1% ZP305 steel fiber**

Test	Reinforcement type	Specimen age, days	Reinforcement		Compressive strength, (psi)	First crack (cycle number)	Maximum crack width (in)		Failure load (kips)	Comment
			Spiral	Skin			At 0.8F <sub>pu</sub>	At 0.9F <sub>pu</sub>		
1	7	6	6-turn	None	4500	5th	0.002	0.002	465	Pass
		4	6-turn	None	4350	2nd	0.002	0.002	380	Pass
		3	6-turn	None	4200	10th	No crack	0.0043	359	Pass
2	4	5	3-turn	None	4710	9th	0.002	0.002	417	Pass
		7	None	5	4580	No crack	No crack	No crack	457	Pass
3	3	4	None	5	4000	3rd	0.0047	0.0047	342	Pass
		4	None	3	3550	1st	0.011	0.011	281	Fail
4	2	5	None	3	3790	1st	0.0108	0.0108	310	Fail
		7	None	3	4250	1st	0.0071	0.0094	321	Pass
5	1	10	None	None	5000	1st	0.012	0.015	320	Fail

*AASHTO acceptance criteria:*

- Failure load: 318 kips (minimum)
- Crack widths: 0.01 in (maximum) at 0.8F<sub>pu</sub>  
0.016 in (maximum) at 0.9F<sub>pu</sub>

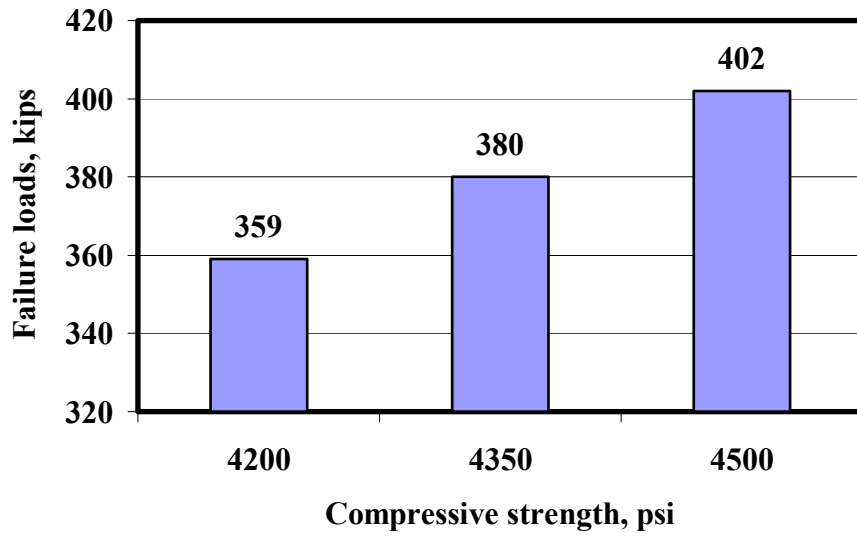
465 kips (1598, 1691 and 2069 kN), respectively, which are greater than the required failure load criteria. So, all three specimens passed the acceptance test. Figure 6.3 shows failure loads and maximum crack widths for the three specimens with differing compressive strengths. It is clear that, as the compressive strength increased, the failure load increased, and the crack widths decreased or remained the same, as expected. So the next specimen tested was *Reinforcement 4* with 3-turn spiral and no skin (Fig. 6.2.d).

#### *TEST 2: Reinforcement 4*

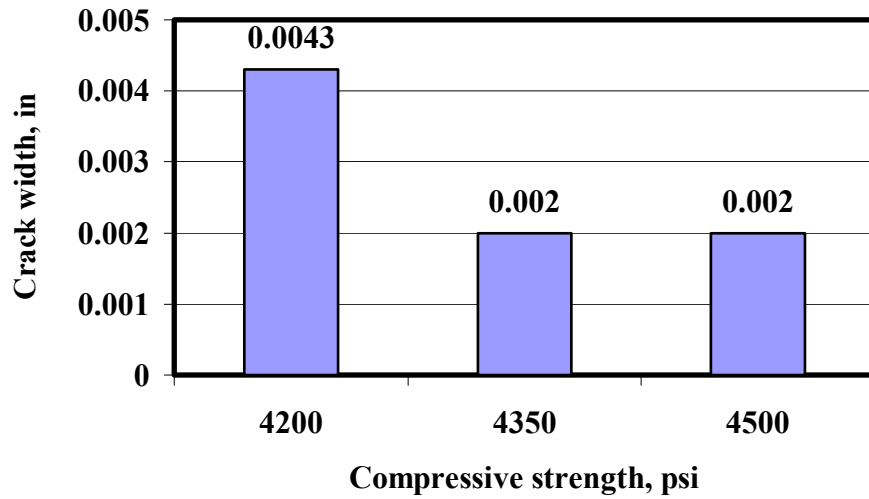
This specimen was reinforced with 3-turn spiral and no skin reinforcement. The length of the spiral was kept at 12 inch (305 mm) with a pitch of 4 inch (102 mm). One specimen of this type was tested. The compressive strength of the specimens at the time of testing was 4710 psi (32.5 MPa). This specimen also passed the AASHTO acceptance criteria. The next test specimen should have been reinforced with *Reinforcement 1* (no spiral and no skin). However, the performance of the test specimen with skin reinforcement only was not tested yet, which was evaluated next.

#### *TEST 3: Reinforcement 3*

This specimen was reinforced with 5 skin and no spiral reinforcement (Fig. 6.2.c). Two specimens of this type were tested. The compressive strengths of the two specimens at the time of testing were 4000 psi (27.5 MPa) and 4580 psi (31.6 MPa). Both specimens passed the acceptance test. So the next specimen tested was with *Reinforcement 2*, 3 skin and no spiral (Fig. 6.2.b).



(a) Failure loads



(b) Crack widths

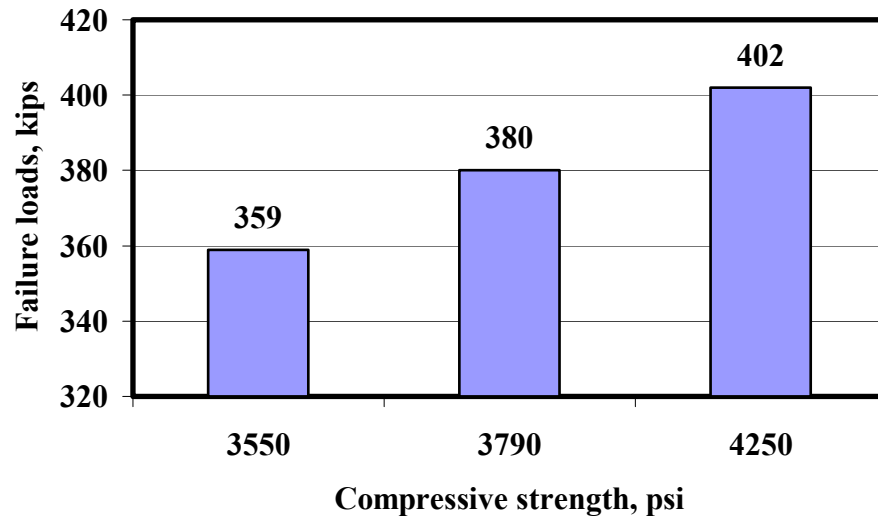
**Figure 6.3: Failure loads and crack widths for Reinforcement 7, 6-turn spiral, no skin, 1% ZP305 steel fiber, Type 1 concrete**

#### *TEST 4: Reinforcement 2*

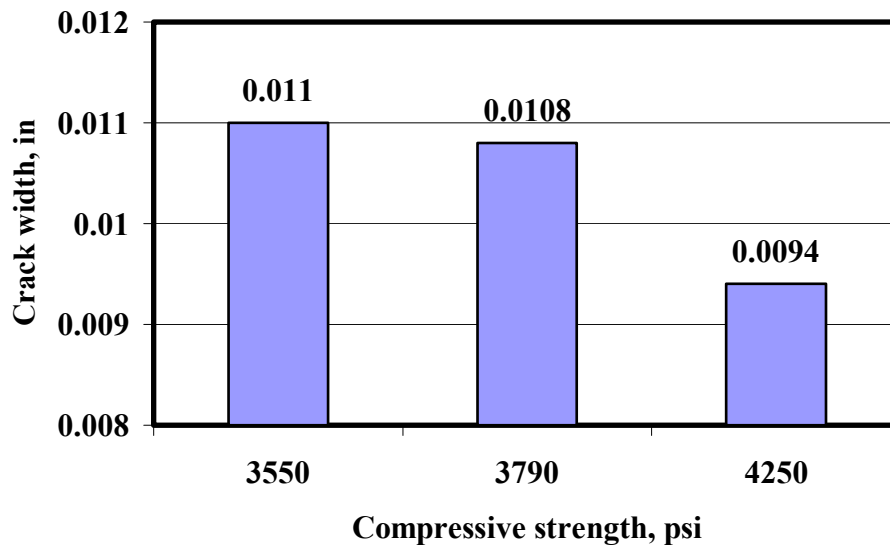
This specimen was reinforced with 3 skin and no spiral reinforcement. The skin reinforcement was uniformly distributed. Three specimens containing this reinforcement were tested. The compressive strengths of specimens at the time of testing ranged from 3550 to 4250 psi (24.5 to 29.3 MPa). The first specimen was tested at a compressive strength of 3550 psi (24.5 MPa). The crack width at  $0.8F_{pu}$  and  $0.9F_{pu}$  were 0.011 in (0.279 mm) and 0.011 in (0.279 mm), respectively. The crack width at  $0.9F_{pu}$  passed the acceptance criteria, but the crack width at  $0.8F_{pu}$  failed as it was greater than 0.01 in (0.254 mm). So, the specimen failed to meet the crack width criteria of AASHTO acceptance test. The specimen also failed in the failure load criteria, as the failure load (281 kips or 1250 kN) was less than 318 kips (1415 kN). Similar results were obtained for the second specimen with a compressive strength of 3790 psi (26.1 MPa). The third specimen with a compressive strength of 4250 psi (29.3 MPa) passed the AASHTO acceptance criteria.

Figure 6.4 compares the failure loads and maximum crack widths of specimens for the change in compressive strengths for this test. From this figure, it is observed that greater compressive strengths result in greater failure loads and smaller crack widths, which is identical to results obtained for specimens reinforced with 6-turn spiral and no skin (*Reinforcement 7*).

From *TEST 2*, it was observed that a specimen reinforced with 3-turn spiral only passed the acceptance test for a compressive strength of 4710 psi (32.5 MPa). Similarly, it was observed in *TEST 4* that a specimen reinforced with 3 skin only passed the acceptance test for a compressive strength of 4250 psi (29.3 MPa). So the next step



(a) Failure loads



(b) Crack widths

**Figure 6.4: Failure loads and crack widths for Reinforcement 2, 3 skin, no spiral, 1% ZP305 steel fiber, Type 1 concrete**

was to try a specimen with no reinforcement (*Reinforcement 1*) and a compressive strength of 4710 psi (32.5 MPa) or higher.

*TEST 5: Reinforcement 1*

This specimen was reinforced with no spiral and no skin reinforcement (Fig. 6.2.a). Only reinforcement in the specimen was 1% ZP305 steel fiber. One specimen with this reinforcement was tested. The compressive strength of specimen at the time of testing was 5000 psi (34.5 MPa). Though the specimen passed by the failure load criteria (318 kips or 1415 kN), it failed by the crack width criteria. The maximum crack width on the surface of the specimen at  $0.8F_{pu}$  was 0.012 in (0.305 mm).

**6.3.2. Results for Type 1 Specimens with 0.75% ZP305 Steel Fiber**

Test results for Type 1 specimens with 0.75% ZP305 steel fiber are presented in Table 6.2.

*TEST 1: Reinforcement 7*

This specimen was reinforced with 6-turn spiral and no skin reinforcement (Fig. 6.2.g). One specimen containing this reinforcement was tested. The compressive strength of specimen at the time of testing was 3760 psi (25.9 MPa). The failure load of the specimen was 337 kips (1500 kN), which is more than 318 kips (1415 kN) and the crack width was recorded 0.011 in (0.279 mm) at  $0.8F_{pu}$  which is more than the limit (0.01 in or 0.254 mm). However, the specimen passed by the crack width criteria at  $0.9F_{pu}$ .

As this specimen failed to satisfy AASHTO criteria, the next specimen to be tested was *Reinforcement 8* with 6-turn spiral and 3 skin.

**Table 6.2: Test results for Type 1 specimens with 0.75% ZP305 steel fiber**

Test	Reinforcement type	Specimen age, days	Reinforcement		Compressive strength, (psi)	First crack (cycle number)	Maximum crack width (in)		Failure load (kips)	Comment
			Spiral	Skin			At $0.8F_{pu}$	At $0.9F_{pu}$		
1	7	4	6-turn	None	3760	3rd	0.011	0.015	337	Fail
2	8	7	6-turn	3	4800	No crack	No crack	No crack	461	Pass
3	3	4	None	5	3970	7th	0.0071	0.012	373	Pass
		3	None	5	3810	1st	0.0031	0.0039	390	Pass
4	2	4	None	5	3650	1st	0.0125	0.013	287	Fail
		4	None	3	3800	1st	0.0126	0.016	297	Fail

*AASHTO acceptance criteria:*

- Failure load: 318 kips (minimum)
- Crack widths: 0.01 in (maximum) at  $0.8F_{pu}$   
0.016 in (maximum) at  $0.9F_{pu}$

#### *TEST 2: Reinforcement 8*

This specimen was reinforced with 6-turn spiral and 3 skin reinforcement (Fig. 6.2.h). One specimen containing this reinforcement was tested. The compressive strength of specimen at the time of testing was 4800 psi (33.1 MPa). This specimen passed the AASHTO cyclic loading test without showing any crack during the load cycles and with a failure load well above the limit.

#### *TEST 3: Reinforcement 3*

This specimen was reinforced with 5 skin and no spiral reinforcement (Fig. 6.2.c). Two specimens of this type were tested. The compressive strengths of the specimens at the time of testing ranged from 3810 to 3970 psi (26.3 to 27.4 MPa). Both specimens passed the AASHTO acceptance criteria.

#### *TEST 4: Reinforcement 2*

This specimen was reinforced with 3 skin and no spiral reinforcement (Fig. 6.2.b). The skins were uniformly distributed. One specimen containing this reinforcement was tested. The compressive strength of the specimen at the time of testing was 3650 psi (25.1 MPa). This specimen failed in both the failure load and the crack width criteria.

#### *TEST 5: Reinforcement 5*

This specimen was reinforced with 3-turn spiral and 3 skin reinforcement (Fig. 6.2.e). The length of the spiral was kept at 12 in (305 mm) with a pitch of 4 in (102 mm). One specimen with this reinforcement was tested. The compressive strength of the specimen at the time of testing was 3800 psi (26.2 MPa). This specimen also failed in both the failure load and the crack width criteria.

### **6.3.3. Results for Type 1 Specimens with 1% XOREX Steel Fiber**

Test results for Type 1 specimens with 1% XOREX steel fiber are presented in Table 6.3.

#### *TEST 1: Reinforcement 7*

This specimen was reinforced with 6-turn spiral and no skin reinforcement (Fig. 6.2.g). One specimen containing this reinforcement was tested. The compressive strength of specimen at the time of testing was 4510 psi (31.1 MPa). Though the specimen passed in the failure load criteria, it failed in the crack width criteria. As this specimen failed, the next specimen to be tested was with *Reinforcement 8*.

#### *TEST 2: Reinforcement 8*

This specimen was reinforced with 6-turn spiral and 3 skin reinforcement (Fig. 6.2.h). Three skins were placed uniformly in the test specimen. One specimen containing this reinforcement was tested. The compressive strength of specimen at the time of testing was 5120 psi (35.3 MPa). This specimen passed both the AASHTO criteria.

#### *TEST 3: Reinforcement 3*

This specimen was reinforced with 5 skin reinforcement and no spiral reinforcement (Fig. 6.2.c). Three specimens of this type were tested. The compressive strengths of the specimens at the time of testing ranged from 3510 to 4500 psi (24.2 to 31 MPa). The first specimen tested had a compressive strength of 3510 psi (24.2 MPa), which failed in both the crack width and failure load criteria. The second specimen had a higher compressive strength (4000 psi or 27.6 MPa). The specimen also failed in both AASHTO criteria. The third specimen had a compressive strength of 4500 psi (31 MPa) and passed the AASHTO acceptance criteria. These three specimens displayed similar

**Table 6.3: Test results for Type 1 specimens with 1% XOREX steel fiber**

Test	Reinforcement type	Specimen age, days	Reinforcement		Compressive strength, (psi)	First crack (cycle number)	Maximum crack width (in)		Failure load (kips)	Comment
			Spiral	Skin			At 0.8F <sub>pu</sub>	At 0.9F <sub>pu</sub>		
<b>1</b>	7	5	6-turn	None	4510	1st	0.0126	0.0126	345	Fail
<b>2</b>	8	7	6-turn	3	5000	No crack	No crack	No crack	460	Pass
<b>3</b>	3	3	None	5	3510	1st	0.016	0.02	275	Fail
		5	None	5	4000	1st	0.012	0.0197	289	Fail
		7	None	5	4500	1st	0.0071	0.0085	352	Pass
<b>4</b>	2	3	None	3	3600	1st	0.016	0.02	269	Fail
<b>5</b>	5	3	3-turn	3	3500	1st	0.015	0.018	270	Fail

*AASHTO acceptance criteria:*

- Failure load: 318 kips (minimum)
- Crack widths: 0.01 in (maximum) at 0.8F<sub>pu</sub>  
0.016 in (maximum) at 0.9F<sub>pu</sub>

results as specimens with 1% ZP305 steel fiber. *Test 3* showed that increase in the compressive strength of concrete increased the failure load and decreased the maximum crack widths.

*TEST 4: Reinforcement 2*

This specimen was reinforced with 3 skin and no spiral reinforcement (Fig. 6.2.b). The skin reinforcement was uniformly distributed. One specimen containing this reinforcement was tested. The compressive strength of the specimen at the time of testing was 3600 psi (24.8 MPa). This specimen failed in both criteria of the AASHTO cyclic loading test.

*TEST 5: Reinforcement 5*

This specimen was reinforced with 3-turn spiral and 3 skin reinforcement (Fig. 6.2.e). The length of the spiral was kept at 12 in (305 mm) with a pitch of 4 in (102 mm). One specimen with this reinforcement was tested. The compressive strength of specimen at the time of testing was 3500 psi (24 MPa). This specimen failed in both the failure load and the crack width criteria of the AASHTO cyclic loading test.

#### **6.3.4. Results for Type 1 control Specimens without Fiber**

Test results for Type 1 control specimens without any fiber are presented in Table 6.4.

*TEST 1: Reinforcement 9*

This specimen was reinforced with 5 skin and 6-turn spiral reinforcement. The skin reinforcement was uniformly distributed. One specimen containing this reinforcement was tested. The compressive strength of the specimen at the time of testing

**Table 6.4: Test results for Type 1 specimens without any fiber**

Test	Reinforcement type	Specimen age, days	Reinforcement		Compressive strength, (psi)	First crack (cycle number)	Maximum crack width (in)		Failure load (kips)	Comment
			Spiral	Skin			At 0.8F <sub>pu</sub>	At 0.9F <sub>pu</sub>		
1	9	18	6-turn	5	4050	1st	0.0063	0.007	370	Pass
2	7	10	6-turn	None	3600	1st	---	---	230	Fail
		19	6-turn	None	5000	1st	---	---	230	Fail
3	3	10	None	5	3650	1st	---	---	230	Fail

**Table 6.5: Test results for Type 2 specimens with 1% ZP305 steel fiber**

Test	Reinforcement type	Specimen age, days	Reinforcement		Compressive strength, (psi)	First crack (cycle number)	Maximum crack width (in)		Failure load (kips)	Comment
			Spiral	Skin			At 0.8F <sub>pu</sub>	At 0.9F <sub>pu</sub>		
1	1	14	None	None	6000	No crack	No crack	No crack	368	Pass
		14	None	None	5900	1st	0.0079	0.0011	321	Pass

*AASHTO acceptance criteria:*

- Failure load: 318 kips (minimum)
- Crack widths: 0.01 in (maximum) at 0.8F<sub>pu</sub>  
0.016 in (maximum) at 0.9F<sub>pu</sub>

was 4050 psi (27.9 MPa). This specimen passed both criteria of the AASHTO acceptance test.

#### *TEST 2: Reinforcement 7*

This specimen was reinforced with 6-turn spiral and no skin reinforcement (Fig. 6.2.g). Two specimens containing this reinforcement were tested. The compressive strengths of the specimen at the time of testing were 3650 psi (25.1 MPa) and 5000 psi (34.5 MPa). The specimen with 3650 psi (25.1 MPa) strength failed at the end of 1st cycle of loading, and the specimen with 5000 psi (34.5 MPa) strength failed at the end of 2nd cycle of loading.

#### *TEST 3: Reinforcement 3*

This specimen was reinforced with 5 skins only (Fig. 6.2.c). The skin reinforcement was uniformly distributed in the specimen. One specimen containing this reinforcement and with 3600 psi (24.8 MPa) was tested. This specimen also failed at the end of first cycle of loading.

## **6.4. Results from Type 2 Specimens**

In this phase, specimens with higher compressive strengths, 5500 to 7500 psi (37.9 to 51.7 MPa), were tested. Reinforcement of specimens for various configurations of fibers was selected based on the results obtained from the previous tests.

#### 6.4.1. Results for Type 2 Specimens with 1% ZP305 Steel Fiber

It is observed from Table 6.1 that the following Type 1 lower strength specimens with minimum amount of secondary reinforcement passed the AASHTO acceptance test:

- *Reinforcement 2* (no spiral and 3 skin reinforcement) with 4250 psi (29.3 MPa) strength
- *Reinforcement 4* (3-turn spiral and no skin reinforcement) with 4710 psi (32.5 MPa) strength

In this phase, Type 2 specimens would be used, which had greater concrete strengths than Type 1 specimens. It was also found that increased compressive strength resulted in better failure load and crack performance. It was, therefore, expected that Type 2 specimens with *Reinforcement 2* or *Reinforcement 4* would pass the AASHTO acceptance test. So, tests in this phase were performed with scaled down reinforcement from the two best performing Type 1 configurations. Test results are presented in Table 6.5.

##### *TEST 1: Reinforcement 1*

The specimen did not have any spiral or skin reinforcement (Fig. 6.2.a). The only reinforcement in the specimen was 1% ZP305 steel fiber. Two specimens of this type were tested. The compressive strengths of the specimen at the time of testing were 6000 psi (41.3 MPa) and 5900 psi (40.7 MPa). The specimen with 6000 psi (41.3 MPa) concrete did not show any crack on the surface during the load cycles, but cracks developed on the surface of the other specimen at the very 1st cycle. The crack widths were below the acceptance limit. Both specimens passed the AASHTO acceptance criteria. So, no other tests for this fiber volume was necessary.

#### 6.4.2. Results for Type 2 Specimens with 0.75% ZP305 Steel Fiber

For this fiber configuration, the following Type 1 lower strength specimens with minimum amount of secondary reinforcement passed the AASHTO acceptance test (Table 6.2):

- *Reinforcement 3* (no spiral and 5 skin reinforcement) with 3810 psi (26.3 MPa)
- *Reinforcement 8* (6-turn spiral and 3 skin reinforcement) with 4800 psi (33 MPa)

As Type 2 specimens were expected to perform better than Type 1 specimens because of increased compressive strengths, tests in this phase were initiated with *Reinforcement 2* (no spiral and 3 skin reinforcement) and *Reinforcement 7* (6-turn spiral and no skin reinforcement) specimens. Test results are presented in Table 6.6.

##### *TEST 1: Reinforcement 7*

The test was performed on specimens with *Reinforcement 7*, i.e. reinforced with 6-turn spiral and no skin reinforcement (Fig. 6.2.g). One specimen containing this reinforcement was tested. The compressive strength of the specimen at the time of testing was 5500 psi (37.9 MPa). The maximum crack width of the specimen was recorded 0.0055 in (0.14 mm) and the failure load was 435 psi (1936 kN). So, the specimen passed the AASHTO acceptance criteria.

##### *TEST 2: Reinforcement 4*

This specimen was reinforced with 3-turn spiral and no skin reinforcement (Fig. 6.2.d). The length of the spiral was kept at 12 in (305 mm) with a pitch of 4 in (102 mm). Two specimens of this type were tested. The compressive strength of the specimens at the time of testing ranged from 6260 to 6500 psi (43.1 to 44.8 MPa). Both specimens

**Table 6.6: Test results for Type 2 specimens with 0.75% ZP305 steel fiber**

Test	Reinforcement type	Specimen age, days	Reinforcement		Compressive strength, (psi)	First crack (cycle number)	Maximum crack width (in)		Failure load (kips)	Comment
			Spiral	Skin			At $0.8F_{pu}$	At $0.9F_{pu}$		
1	7	8	6-turn	None	5500	1st	0.0055	0.0071	435	Pass
2	4	14	3-turn	None	6500	No crack	No crack	No crack	493	Pass
		14	3-turn	None	6260	No crack	No crack	No crack	462	Pass
3	2	15	None	3	6170	1st	0.0024	0.0024	393	Pass
4	1	21	None	None	7050	No crack	No crack	No crack	437	Pass
		23	None	None	7200	3rd	0.0055	0.0055	390	Pass

*AASHTO acceptance criteria:*

- Failure load: 318 kips (minimum)
- Crack widths: 0.01 in (maximum) at  $0.8F_{pu}$   
0.016 in (maximum) at  $0.9F_{pu}$

passed the AASHTO acceptance criteria without showing any crack on the surface and with failure loads of 462 kips (2056 kN) and 493 kips (2194 kN), respectively.

*TEST 3: Reinforcement 2*

This specimen was reinforced with 3 skin and no spiral reinforcement (Fig. 6.2.b). The skin reinforcement were uniformly distributed. One specimen containing this reinforcement was tested. The compressive strength of the specimen at the time of testing was 6170 psi (42.5 MPa). This specimen passed both criteria of the AASHTO cyclic loading test. As this specimen passed, the next specimen tested was without any reinforcement (*Reinforcement 1*).

*TEST 4: Reinforcement 1*

The specimen did not have any spiral or skin reinforcement (Fig. 6.2.a). The only reinforcement in the specimen was 0.75% ZP305 steel fiber. Two specimens of this type were tested. The compressive strengths of the specimen at the time of testing were 7050 psi (48.6 MPa) and 7200 psi (49.6 MPa). The specimen with 7050 psi (48.6 MPa) concrete did not show any crack on the surface during the load cycles, but cracks developed on the surface of the other specimen at the 3rd cycle. The crack width at  $0.8F_{pu}$  was 0.0055 in (0.14 mm), which is below the acceptance limit. Both specimens passed the AASHTO failure load criteria.

### **6.4.3. Results for Type 2 Specimens with 1% XOREX Steel Fiber**

The following Type 1 lower strength specimens with minimum amount of secondary reinforcement passed the AASHTO acceptance test for this fiber configuration (Table 6.3):

- *Reinforcement 3* (no spiral and 5 skin reinforcement) with 4500 psi (31 MPa)
- *Reinforcement 8* (6-turn spiral and 3 skin reinforcement) with 5000 psi (34.5 MPa)

This result is identical to the results for specimens with 0.75% ZP305 steel fiber (Table 6.2). To reduce the number of tests in this study, tests were initiated with *Reinforcement 1* (no spiral and no skin reinforcement). No more test was required, If the specimen with *Reinforcement 1* would pass the acceptance test. Test results are presented in Table 6.7.

#### *TEST 1: Reinforcement 1*

The specimen did not have any spiral or skin reinforcement (Fig. 6.2.a). The only reinforcement in the specimen was 1% XOREX steel fiber. Two specimens of this type were tested. The compressive strengths of the specimen at the time of testing were 6980 psi (48.1 MPa) and 7320 psi (50.4 MPa). Cracks developed in both the specimens. However, they were well below the acceptance criteria. Both specimens passed the AASHTO criteria.

### **6.5. Observations from AASHTO Cyclic Load Test**

As the load was applied on the specimen through the anchor head, large stresses developed at the upper portion of the specimens. So all cracks developed during the load cycles were located at the upper-half of the specimen (Fig. 6.5). In all tests, vertical cracks first developed in the mid-zone of the specimen. After the application of a few more load cycles, horizontal cracks became visible at each corner at a distance of 2 to 3 in (51 to 76.2 mm) from the top of the specimen. At failure, cracks also developed at the

**Table 6.7: Test results for Type 2 specimens with 1% XOREX steel fiber**

Test	Reinforcement type	Specimen age, days	Reinforcement		Compressive strength, (psi)	First crack (cycle number)	Maximum crack width (in)		Failure load (kips)	Comment
			Spiral	Skin			At $0.8F_{pu}$	At $0.9F_{pu}$		
<b>1</b>	<i>I</i>	20	None	None	6980	5th	0.0047	0.0055	343	Pass
		25	None	None	7320	7th	0.002	0.0047	363	Pass

*AASHTO acceptance criteria:*

- *Failure load: 318 kips (minimum)*
- *Crack widths: 0.01 in (maximum) at  $0.8F_{pu}$   
0.016 in (maximum) at  $0.9F_{pu}$*

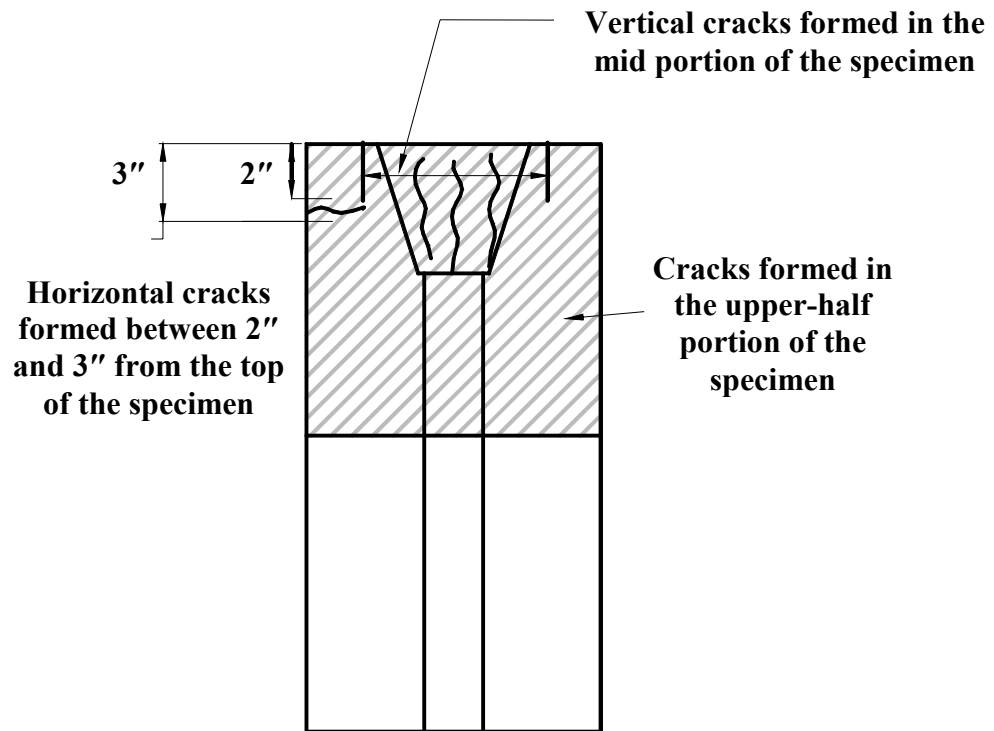


**Figure 6.5: Typical location of crack formation in AASHTO specimens**



**Figure 6.6: Horizontal cracks at the upper corner of AASHTO specimen**

top surface of the specimen. Figures 6.6 and 6.7 show horizontal cracks at the corner of the specimen and the vertical cracks in the upper mid portion of a specimen, respectively. Figure 6.8 shows developed cracks at the top surface of a specimen. These cracks propagated with the application of increasing load cycles. Crack widths also increased with addition of load cycles. If cracks developed during the first cycle of loading, they stabilized within 5 or 6 cycles.

Failure of control specimens without fibers occurred suddenly with bursting and spalling of concrete. The failure was often brittle and explosive in nature. Figure 6.9 shows the spalling from a control specimen. In case of FRC specimens, no spalling or brittle failure of concrete was observed. Only large cracks were visible at failure (Figs. 6.6, 6.7, 6.8 and 6.10). This is because fibers helped in bridging across the cracks. Fibers prevent the cracks from widening, and maintaining the integrity of the specimen. Figure 6.11 shows bridging of fibers across a crack. In most cases, the anchorage was suppressed or separated from the specimen at failure. Figure 6.12 shows the separation or suppression of the anchorage.

The maximum crack width and the failure load depended on the reinforcement in the specimen, amount of fibers and the concrete strength at the time of the test. For specimens with identical type and amount of fiber, and spiral and skin reinforcement, the failure load of the specimen increased and the crack width decreased with increasing compressive strength.

All specimens passing AASHTO cyclic load criteria are summarized in Tables 6.8, 6.9 and 6.10, respectively, for 1% ZP305, 0.75% ZP305 and 1% XOREX steel fibers.



**Figure 6.7: Horizontal and vertical cracks in AASHTO specimen**



**(a) Photograph 1**



**(b) Photograph 2**

**Figure 6.8: Cracks at the upper face of AASHTO specimen**



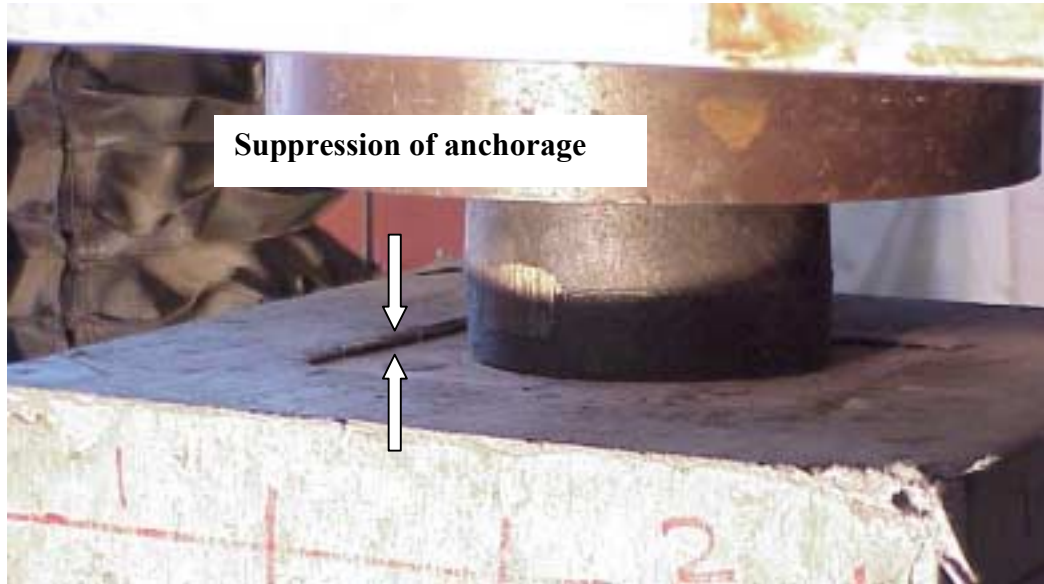
**Figure 6.9: Spalling of concrete in control AASHTO specimen without fibers**



**Figure 6.10: Failure of a FRC AASHTO specimen**



**Figure 6.11: Bridging of fibers across cracks**



**(a) Suppression of anchorage**



**(b) Separation of anchorage**

**Figure 6.12: Suppression or separation of anchorage at failure**

**Table 6.8: Acceptable anchorage zone reinforcement with 1% ZP305 steel fiber**

<b>Type 1 compressive strength (3500 to 5000 psi or 24 to 34.5 MPa)</b>						
<b>Reinforcement type</b>	<b>Reinforcement</b>		<b>Minimum compressive strength, psi (MPa)</b>	<b>Reduction in reinforcement from standard (Reinforcement 9)</b>		
	<b>Spiral turns</b>	<b>Skin reinforcement</b>		<b>Spiral</b>	<b>Skin</b>	<b>Over all</b>
7	6	0	4200 (28.9)	0	100	42
4	3	0	4710 (32.5)	50	100	79
3	0	5	4000 (27.6)	100	0	58
2	0	3	4250 (29.3)	100	40	65
<b>Type 2 compressive strength (5500 to 7500 psi or 37.9 to 44.8 MPa)</b>						
1	0	0	5900 (40.7)	100	100	100

**Table 6.9: Acceptable anchorage zone reinforcement with 0.75% ZP305 steel fiber**

<b>Type 1 compressive strength (3500 to 5000 psi or 24 to 34.5 MPa)</b>						
<b>Reinforcement type</b>	<b>Reinforcement</b>		<b>Minimum compressive strength, psi (MPa)</b>	<b>Reduction in reinforcement from standard (Reinforcement 9)</b>		
	<b>Spiral turns</b>	<b>Skin reinforcement</b>		<b>Spiral</b>	<b>Skin</b>	<b>Over all</b>
8	6	3	4800 (33.1)	0	40	23
3	0	5	3810 (26.3)	100	0	58
<b>Type 2 compressive strength (5500 to 7500 psi or 37.9 to 44.8 MPa)</b>						
1	0	0	7050 (48.6)	100	100	100

**Table 6.10: Acceptable anchorage zone reinforcement with 1% XOREX steel fiber**

<b>Type 1 compressive strength (3500 to 5000 psi or 24 to 34.5 MPa)</b>						
<b>Reinforcement type</b>	<b>Reinforcement</b>		<b>Minimum compressive strength, psi (MPa)</b>	<b>Reduction in reinforcement from standard (Reinforcement 9)</b>		
	<b>Spiral turns</b>	<b>Skin reinforcement</b>		<b>Spiral</b>	<b>Skin</b>	<b>Over all</b>
8	6	3	5000 (34.5)	0	40	23
3	0	5	4500 (31)	100	0	58
<b>Type 2 compressive strength (5500 to 7500 psi or 37.9 to 44.8 MPa)</b>						
1	0	0	6980 (48.1)	100	100	100

These tables also present the minimum compressive strengths of concrete at the time of testing and percent reduction in the spiral and skin reinforcement through the use of SFRC.

For Type 1 concrete strengths of 3500 to 5000 psi (24 to 34.5 MPa) and 1% ZP305 fibers, the best performances were obtained from (Table 6.8):

- *Reinforcement 4* specimens with 3-turn spiral and no skin reinforcement (Fig. 6.2.d), resulting in 79% reduction of the total secondary reinforcement.
- *Reinforcement 2* specimens with no spiral and 3 skin reinforcement (Fig. 6.2.b), which reduced the total secondary reinforcement by 65%.

For Type 2 concrete strengths ranging from 5500 to 7500 psi (37.9 to 44.8 MPa) and 1% ZP305 fibers, the best performing reinforcement configuration was (Table 6.8):

- *Reinforcement 1* specimens with no spiral and no skin reinforcement (Fig. 6.2.a). This configuration resulted in 100% total elimination of the secondary reinforcement.

With 0.75% ZP305 (Table 6.9) and 1% XOREX (Table 6.10) steel fibers, and Type 1 compressive strengths ranging from 3500 to 5000 psi (24 to 34.5 MPa), similar results were obtained and the best performing specimens were:

- *Reinforcement 3* specimens with no spiral and 5 skin reinforcement (Fig. 6.2.c), which reduced the total secondary reinforcement by 58%.
- *Reinforcement 8* specimens with 6-turn spiral and 3 skin reinforcement (Fig. 6.2.h), resulting in 23% reduction of the total secondary reinforcement.

For Type 2 concrete strengths ranging from 5500 to 7500 psi (37.9 to 44.8 MPa), and 0.75% ZP305 and 1% XOREX fibers, the best performing reinforcement configuration was (Tables 6.9 and 6.10):

- *Reinforcement 1* specimens with no spiral and no skin reinforcement (Fig. 6.2.a), resulting in 100% total elimination of the secondary reinforcement.

# **CHAPTER 7**

## **FINITE ELEMENT MODELING**

### **7.1. Introduction to Finite Element Methods**

The finite element method (FEM) is one of the best methods for calculating the detailed state of stresses in structures of arbitrary shape. Modern computer programs allow the user to model arbitrary structures and to define sophisticated material laws for the model. The FEM consists in dividing the continuum in elements interconnected at nodes. The values of the variable are then determined at each node, and interpolation functions are used to approximate the values in the remaining regions (Huebner and Thornton 1982). The FEM is usually employed when an analytical solution cannot be obtained due to complicated geometries, loadings and material properties (Logan 1993). The finite element models were used herein to better understand the time, origin and location of cracks in AASHTO specimens, as well as strain evolution during different loadings.

ANSYS 6.1 finite element analysis software was used to model the AASHTO specimens described in Chapter 5. ANSYS has the capability of performing structural, mechanical, thermal, electromagnetic, fluid, and couple-field analysis. Structural analysis is the most commonly used type, and has the ability to determine deformations, stresses, strains, and reaction forces (ANSYS 2001). ANSYS was chosen because of the availability of wide range of elements, including a concrete element, which can be used with or without reinforcement.

The FEM analysis was used herein only for the purpose of validating the experimental results from the AASHTO cyclic load test.

## **7.2. Types of Elements**

The first stage in developing the FEM was to determine the necessary properties and geometry of the AASHTO specimen. The geometry of the specimen is described in Chapter 5. The specimen consisted of three materials: a) steel anchorage, b) concrete, and c) plastic duct.

### **7.2.1. Structural Solid Element for the Anchorage and the Duct**

The steel anchorage and the plastic duct in the AASHTO specimen were modeled using the SOLID45-3D element from ANSYS. This element is used for three-dimensional modeling of solids. The element is defined by eight nodes having three degrees of freedom at each node: translations in the nodal x, y, and z directions. The element has plasticity, creep, swelling, stress stiffening, large deflection and large strain

capabilities. The required material properties for the element include density, modulus of elasticity and Poisson's ratio.

### **7.2.2. Concrete Element**

The concrete portion of the AASHTO specimen was modeled using SOLID65-3D reinforced concrete element from ANSYS. This element is used for three-dimensional concrete modeling with or without reinforcement. The element is capable of simulating concrete cracking and crushing, plastic deformation, and creep. The required material properties for the element include density, modulus of elasticity and Poisson's ratio. The concrete properties of the SOLID65 elements were used as input for the preprocessor to represent the behavior of concrete with reinforcement.

Simplifying hypothesis is necessary for the analysis of the very complex behavior of anchorage zones. The simplest model is to assume the material to be linearly elastic as the stresses in the concrete and the reinforcing steel are generally small up to the cracking of concrete (Breen *et al* 1994).

### **7.2.3. Spar Element for the Skin Reinforcement**

LINK8 – 3-D Spar from ANSYS was selected for the modeling of the skin reinforcement. The three-dimensional spar element is a uniaxial tension-compression element with three degrees of freedom at each node: translations in the nodal x, y, and z directions. The required properties of the element include area and initial strain, while the material properties include modulus of elasticity and Poisson's ratio.

## 7.3. Development of FEM

### 7.3.1. Material Properties

The first step in the development of the model was the determination of the properties of three materials. Typical values for normal weight concrete, steel and plastic properties were used in the FEM analysis. A summary of the input properties for the FEM is provided in Table 7.1. Equation 7.1 was used to calculate Young's modulus of elasticity of concrete (ACI 318 2002):

$$E_c = 57000\sqrt{f'_c} \text{ (psi)} \quad (7.1)$$

where,  $E_c$  = Young's modulus of elasticity of concrete (psi)

$f'_c$  = Compressive strength of concrete at the time of the AASHTO cyclic loading test

The tensile strength of concrete was assumed to be 10% of the compressive strength, which was reasonable based on results, obtained from Chapter 4. It was assumed that there would be no residual strength in concrete at the formation of a crack, which might be the worst possible case.

### 7.3.2. The Anchorage

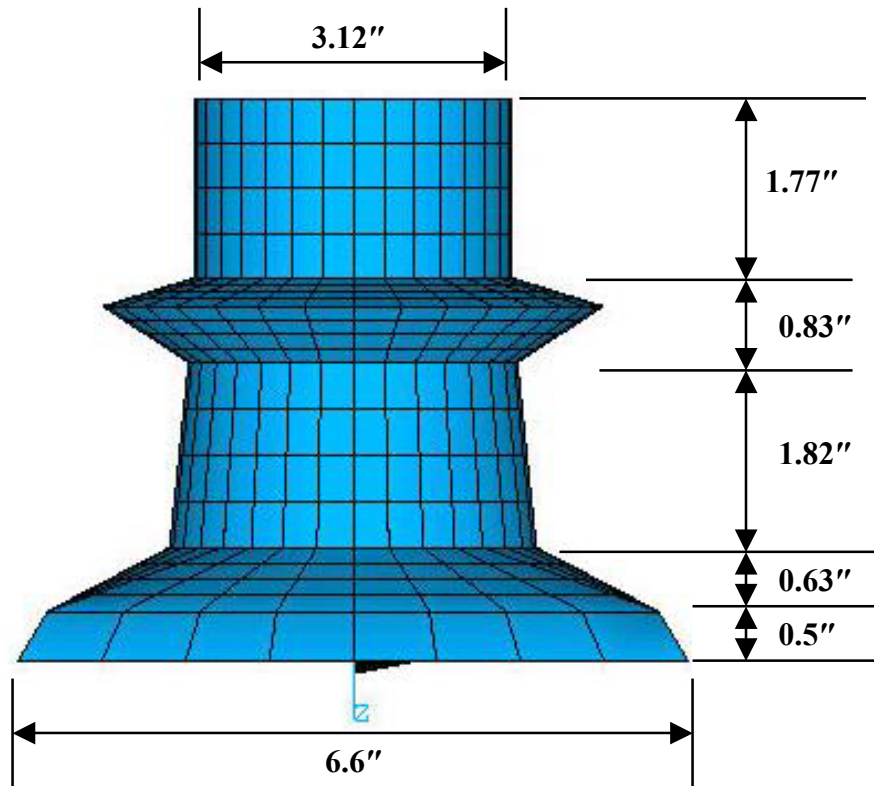
The steel anchorage was modeled using ANSYS SOLID45 structural element. Figure 7.1 (a) shows the photograph of an EC5-7 VSL type anchorage. It is clear from the figure that the anchorage does not have a regular geometry. All the control dimensions of the anchorage were measured with the help of a slide calipers. The dimensions of the anchorage were then input as key points during the development of the model. The key

**Table 7.1: Material Properties for ANSYS FEM**

<b>Concrete properties</b>	
Density	4.66 slug/ft <sup>3</sup> (2,400 kg/m <sup>3</sup> )
Poisson's ratio	0.2
<b>Steel properties</b>	
Density	15.2 slug/ft <sup>3</sup> (7,850 kg/m <sup>3</sup> )
Modulus of elasticity	29,000,000 psi (20,000 MPa)
Poisson's ratio	0.35
<b>Plastic properties</b>	
Density	2.52 slug/ft <sup>3</sup> (1300 kg/m <sup>3</sup> )
Modulus of elasticity	35,000 psi (240 MPa)
Poisson's ratio	0.35



(a) Photograph



(b) FEM mesh

Figure 7.1: VSL type EC 5-7 anchorage

points were subsequently joined to form an area. The created areas were then used to form volumes. After creating the volume, the model was then meshed to create 2688 elements. Figure 7.1 (b) shows the ANSYS model of the anchorage.

### **7.3.3. The Plastic Duct**

The plastic duct was also modeled using SOLID45 structural element. Figure 7.2 (a) shows the photograph of the plastic duct. The thickness of the duct was measured by a slide caliper. The length and the cross-section of the duct were divided into 40 and 32 divisions, respectively, which results in 1280 elements along the duct length, as shown in Fig. 7.2 (b).

### **7.3.4. Concrete**

Concrete surrounding the anchorage and the empty duct was modeled using SOLID65 reinforced concrete element. The model was created following the same method as the anchorage modeling. The model was meshed to form 12928 elements. Figure 7.3 shows the combined model of the AASHTO specimen.

### **7.3.5. Fiber**

Fibers were assumed to be uniformly distributed in the concrete. They were modeled by using the ANSYS smearing technique in the global coordinate system. Fibers provided reinforcement uniformly in x, y and z directions. They were input as the volume percentage of concrete.

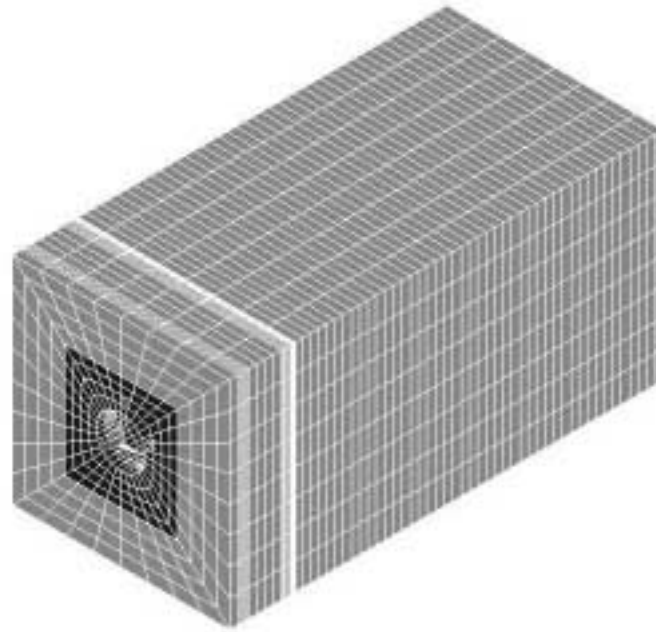


**(a) Photograph**

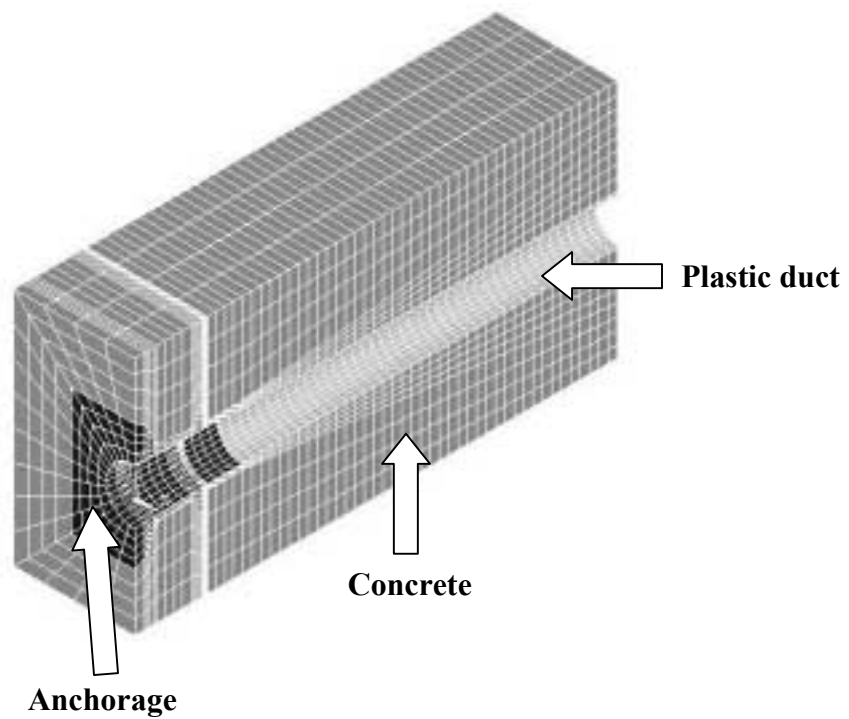


**(b) FEM mesh**

**Figure 7.2: Plastic post-tensioning duct**



(a) Isometric view



(b) Isometric section showing the anchorage, concrete and the empty duct

**Figure 7.3: ANSYS model of the AASHTO specimen**

### **7.3.6. Skin Reinforcement**

The #4 skin reinforcement in the AASHTO specimen was placed as shown in Fig. 6.2. They were equally spaced as mentioned in Chapter 5. Grade 60 steel was used.

## **7.4. Loading**

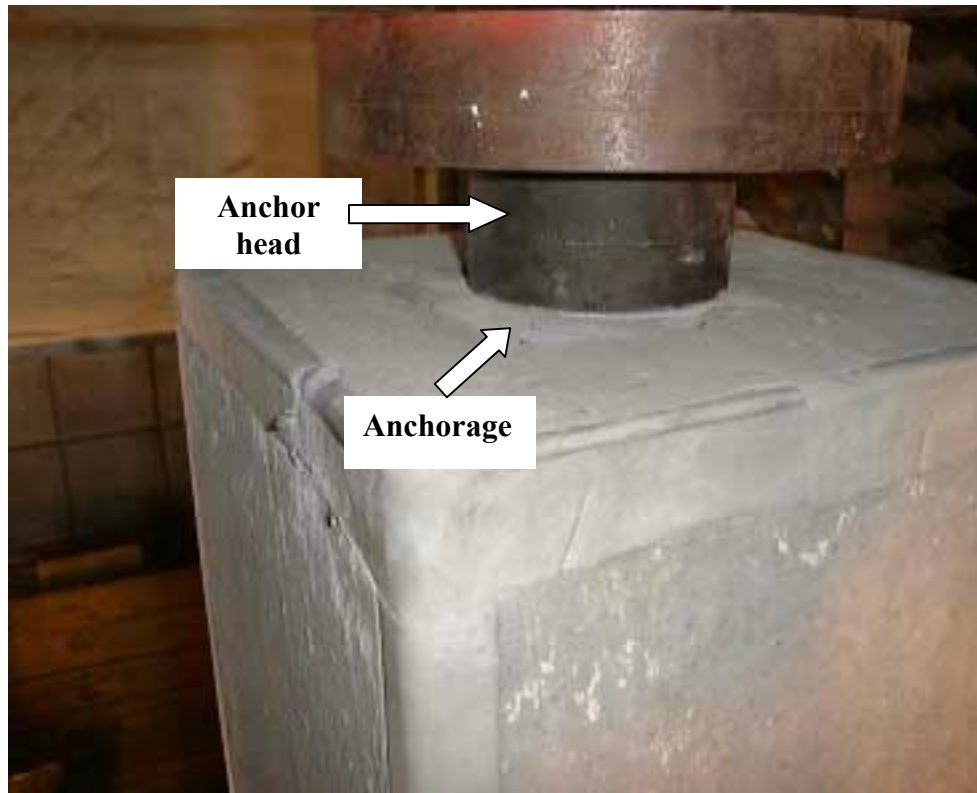
The load on the AASHTO specimen was applied through an anchor head. Figure 7.4 (a) shows the photograph of an anchor head, and Fig. 7.4 (b) shows the application of the load on the AASHTO specimen through the anchor head. The anchor head was in contact with the steel anchorage when the load is applied. To represent this application of load, the total applied load was distributed in 64 nodes near the hole of the anchorage. Figure 7.5 shows the 64 nodes on which the load was applied. The load used in the FEM and shown in Table 7.2 is the maximum load usable in the ANSYS model with which convergence was achieved.

## **7.5. Specimens Modeled for FEM Analysis**

Three specimens were modeled for the FEM analysis. Table 7.2 lists these specimens, their parameters and loading used in the analysis. The first specimen was *Reinforcement 1* type (no spiral or skin reinforcement), reinforced with 1% steel fiber only. The concrete strength was considered to be 6000 psi (41.3 MPa). This specimen is comparable to the Type 2 concrete specimen, reinforced with 1% ZP305 steel fiber, listed in Table 6.5. The second Type 2 concrete specimen, *Reinforcement 2* type (no spiral and



**(a) Photograph**



**(b) Application of load through the anchor head**

**Figure 7.4: Anchor head in the AASHTO cyclic loading test**

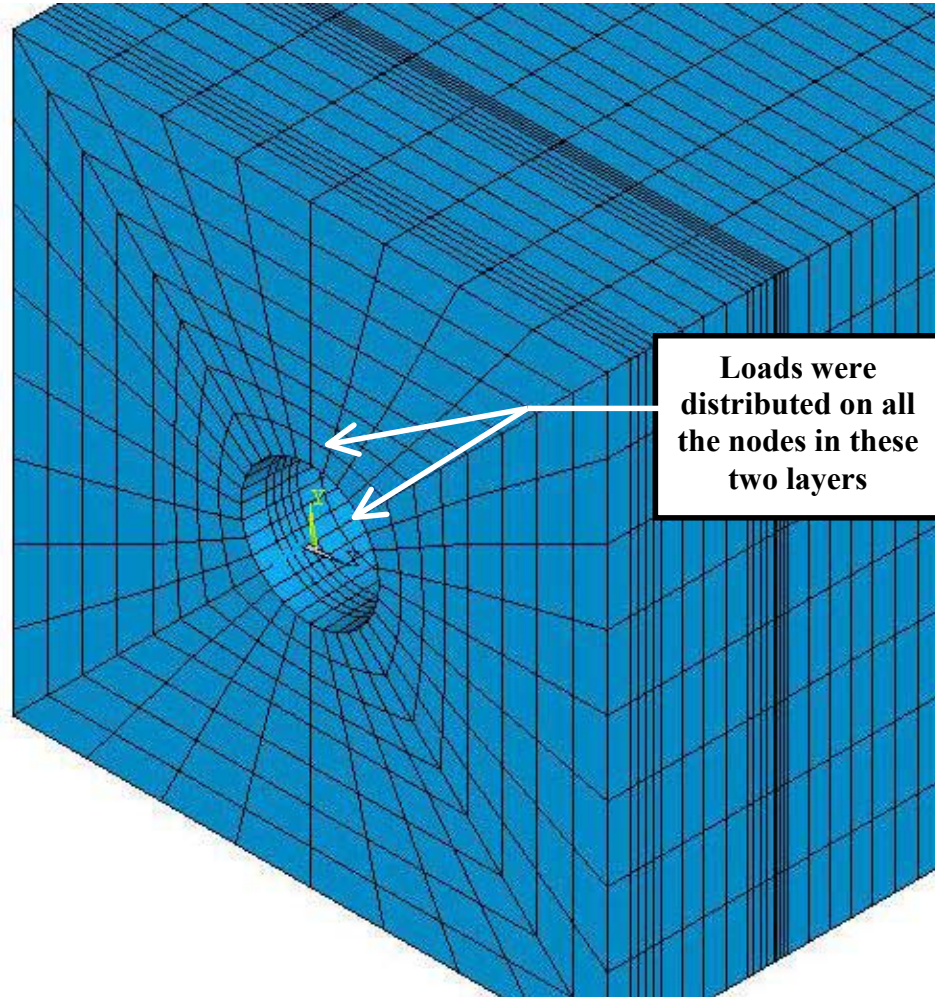


**Figure 7.5: Loaded nodes on the AASHTO specimen FEM**

**Table 7.2: Specimens modeled using ANSYS**

<b>FE Model No.</b>	<b>Fiber type</b>	<b>Fiber volume (%)</b>	<b>Reinforcement type</b>	<b>Compressive strength, psi (MPa)</b>	<b>Applied load, kip (kN)</b>
<b>1</b>	ZP305	1	<i>1</i>	6000 (41.3)	144 (640)
<b>2</b>	ZP305	0.75	<i>2</i>	6170 (42.5)	96 (427)
<b>3</b>	XOREX	1	<i>2</i>	3600 (24.8)	80 (356)

3 skin) and reinforced with 0.75% steel fiber, may be compared with *TEST 3* from Table 6.6. The compressive strength of this specimen was 6170 psi (42.5 MPa). The third specimen, also *Reinforcement 2* type (no spiral and 3 skin) and with 1% steel fiber, was a Type 1 concrete specimen with 3600 psi (24.8 MPa) strength, and may be compared with *TEST 4* from Table 6.3.

The three specimens selected for the FEM, included both Type 1 and Type 2 concrete strengths and all three configurations of fibers. These specimens were reinforced with either 3 skin or no skin reinforcement, and no spiral steel. It is difficult to model the spiral in ANSYS because of its shape. The spiral could be modeled using the smearing technique of ANSYS. However, it was difficult to identify the volume of the specimen strengthened by spiral reinforcement.

## **7.6. Limitations of FEM Analysis**

Nonlinear analyses of the FEM were performed in this study. According to AASHTO (1998), a cyclic load was supposed to be applied on the AASHTO specimen from 28.9 kips (128.6 kN) to 231.2 kips (1028.4 kN). The FEM analysis did not converge at the upper limit of the cyclic load. The possible reason was the local failure of concrete. Nodal stresses of concrete close to the steel anchorage exceeded the strength of concrete, which resulted in the non-convergence of the ANSYS analysis. So, a static load was applied in the FEM to compare the strains obtained from the FEM analysis and the laboratory experiments at a load at which the FEM analysis converged.

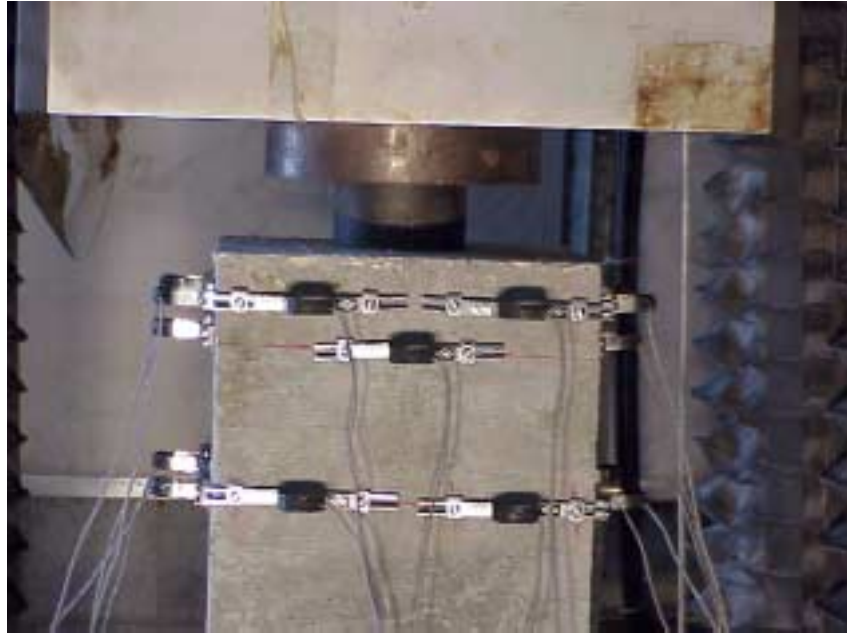
## **CHAPTER 8**

### **THEORETICAL VS. EXPERIMENTAL COMPARISON**

#### **8.1. Comparison of Strains**

Figure 8.1 shows the location of the crack gages used in the laboratory experiments to obtain the strains at the surface of the AASHTO specimens. Using a data acquisition system, the loads and strains were obtained at 1-second interval. It should be noted that strain values reported herein were measured at the maximum load used in the FEM (Table 7.2). The strain values obtained from the crack gages were not constant. Crack gages provided a range of values of strains. Figure 8.2 shows the time versus load/strain graph obtained for specimen. Figure 8.3 shows the first load cycle and corresponding strains for the same sample. Trend lines were drawn in the graph to obtain the average value of the strain at any load.

Figure 8.4 shows the FEM strain contour for an AASHTO specimen reinforced with 0.75% ZP305 steel fiber and 3 skin only (Model 2, Table 7.2). Table 8.1 lists the strain values obtained from the FEM trend line analysis and the strain gages for the three



**(a) Type 1 specimens**



**(b) Type 2 specimens**

**Figure 8.1: Crack gages locations on AASHTO specimens**

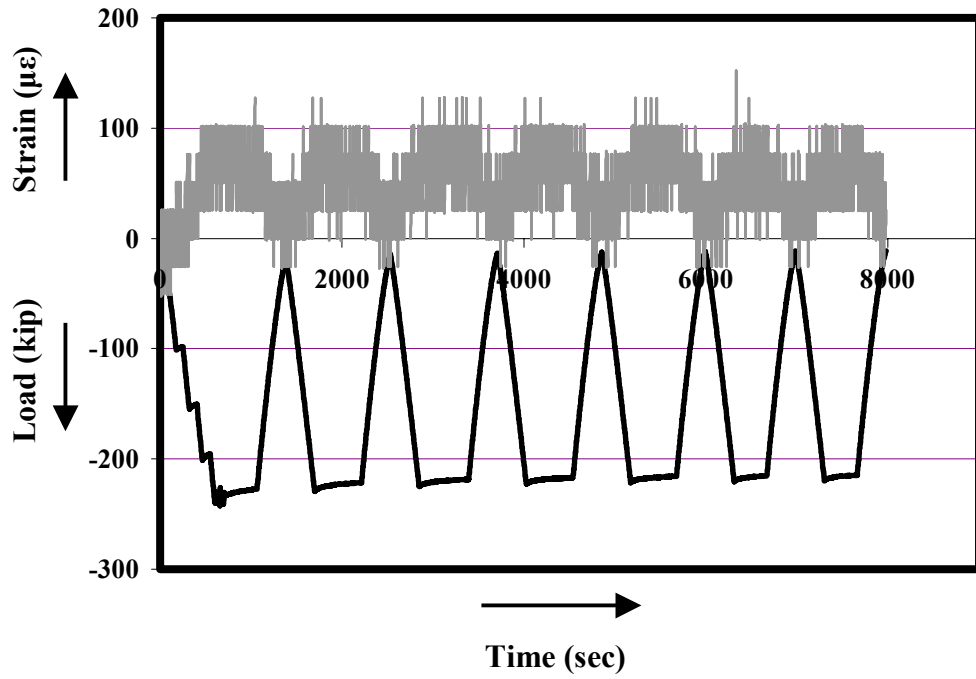


**Figure 8.2: Cyclic loads and strains**

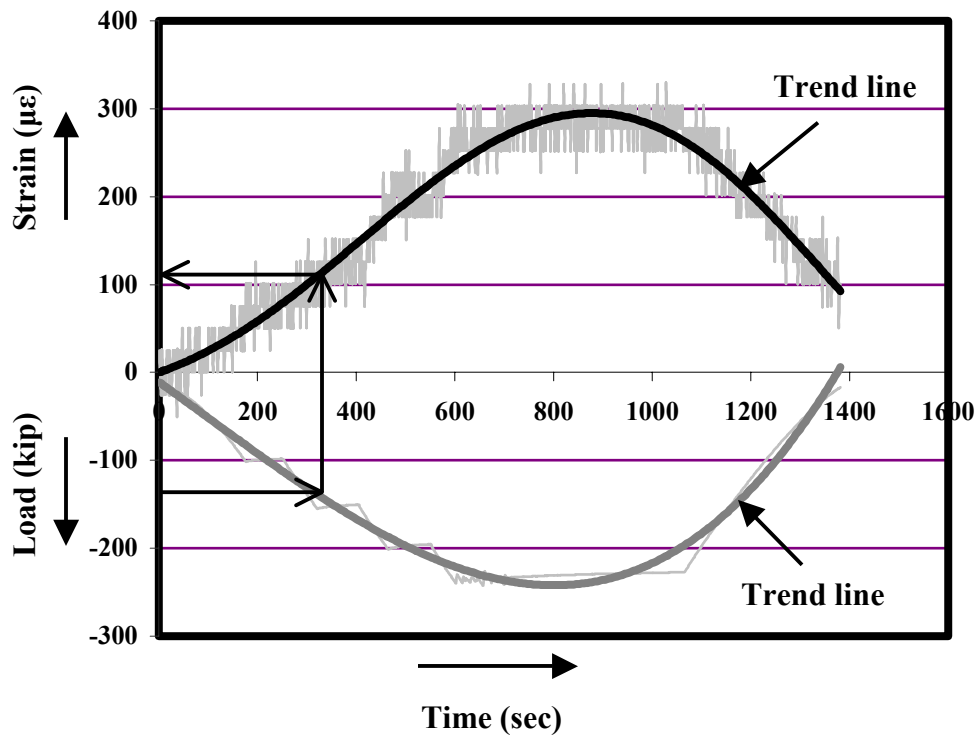


**Figure 8.3: Trend lines for loading and strains in Model 1, Reinforcement 1, Type 2 concrete**

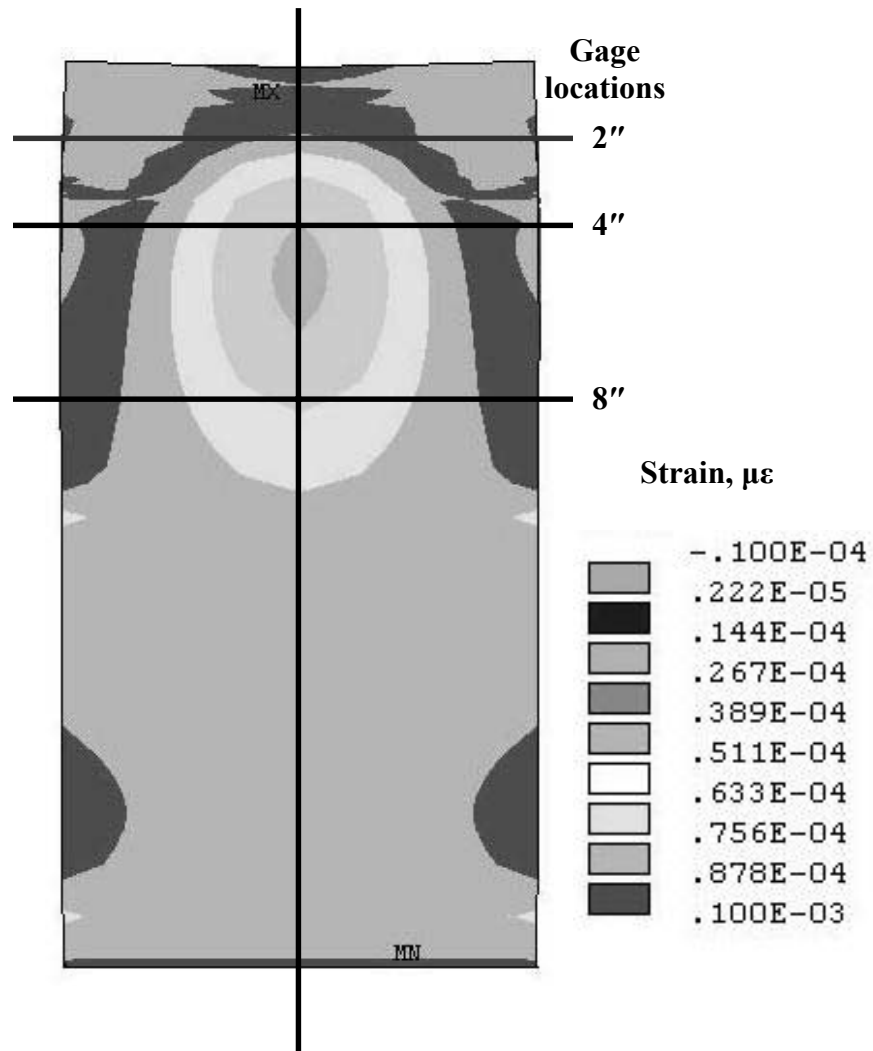


**Figure 8.4: FEM nodal strain contour for Model 2, Reinforcement 2, Type 2 concrete**

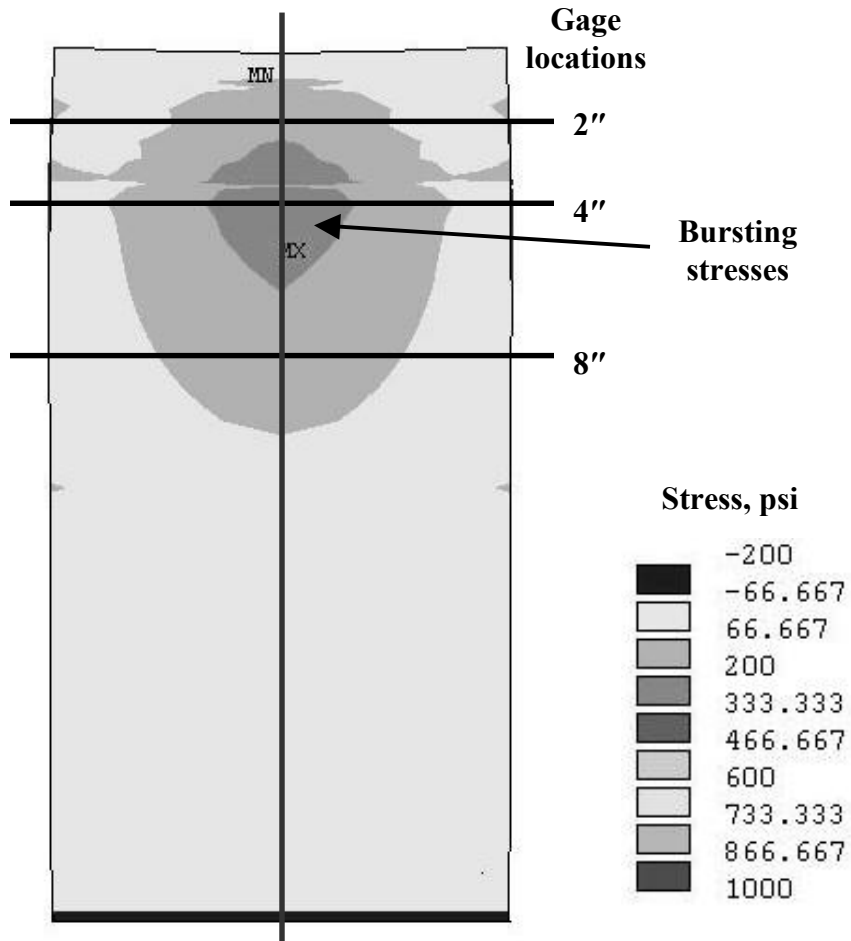
**Table 8.1: Strain comparisons from the cyclic loading test and FEM**

Specimen	Applied load, kip (kN)	Gage location from the top of the specimen	Strains ( $\mu\epsilon$ )	
			From experiment	From FEM
1.0% ZP305 steel fiber with no spiral and no skin reinforcement	144 (640)	2" (50 mm)	55	52.6
		4" (100 mm)	105	97.9
		8" (200 mm)	95	87.9
0.75% ZP305 steel fiber with no spiral and 3-skin reinforcement	96 (427)	2" (50 mm)	50	35
		4" (100 mm)	77	64
		8" (200 mm)	60	59.5
1.0% XOREX steel fiber with no spiral and 3-skin reinforcement	80 (356)	1.5" (37.5 mm)	16	14
		3" (75 mm)	60	70.3
		8" (200 mm)	35	30

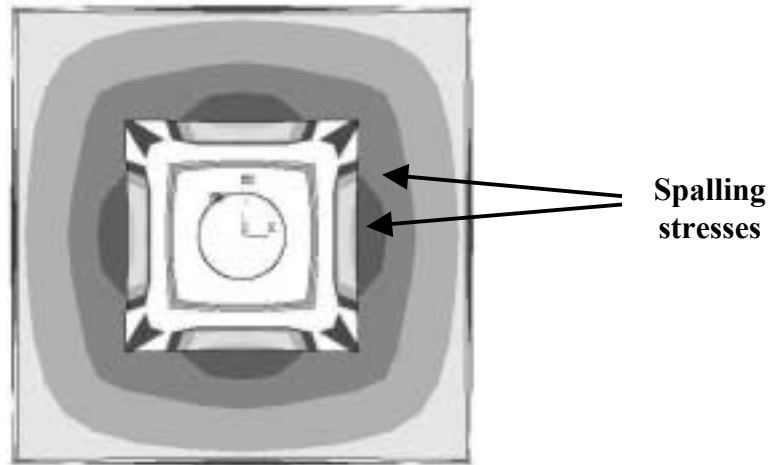
AASHTO specimens from Table 7.2. From this table, it is observed that the FEM analysis provided strain values well comparable to those obtained from the crack gages. Strain values at a distance 4 in (100 mm) from the top of the specimen were greater than that at 2 in (50 mm) and 8 in (200 mm). This trend in strain values was observed from both crack gages and FEM (Table 7.2).

## **8.2. Nature of Stress Contour**

Figure 8.5 shows the FEM bursting and spalling stress contours at the surface of Model 2 specimen (Table 7.2). Breen *et al* (1994) provided identical stress contours for bursting and spalling stresses (Figure 1.2) in the anchorage zone. It is observed from Fig. 8.5 that higher stresses developed at the upper middle portion of the specimen. When these maximum stresses exceed the tensile strength of FRC, cracks develop in this zone. Similar crack patterns were observed in the AASHTO experiments where cracks developed at the upper middle portion of the specimen (Fig. 6.5). It may also be noted that much lower stresses developed in the lower portion of the specimen. This indicates less chance of crack formation at that zone. In the AASHTO testing, no cracks formed in the lower portion of the specimen during the cyclic loading.



(a) At the side face



(b) At the top face

**Figure 8.5: FEM nodal stress contours in Model 2 specimen, Type 2 concrete, Reinforcement 2**

# **CHAPTER 9**

## **COST COMPARISON**

### **9.1. Introduction**

This chapter compares the cost for the usage of SFRC and non-fibrous concrete in the end zones of precast prestressed bridge girders. This will help the engineers in making decision on actual applications of SFRC. The cost comparison of SFRC and non-fibrous concrete involves material and labor costs. It is easy to determine the materials affecting the cost of the girder. But it is difficult to incorporate the labor cost in this study. So, this chapter does not include a quantitative comparison of the cost of SFRC and conventionally constructed bridge girders.

### **9.2. Factors Affecting Girder Cost**

Two types of factors affect the cost of SFRC precast prestressed bridge girders, as compared to non-fibrous concrete girders. These are:

- Detrimental cost factors
- Beneficial cost factors

### **9.2.1. Detrimental Cost Factors**

The cost of steel fibers will increase the girder cost. Other detrimental factor is the labor and equipment involved in the mixing, placing and finishing of SFRC.

#### **Steel fiber cost**

The objective of this study was to reduce or replace the spiral and skin reinforcement in the local end anchorage zone by using FRC. But, it will not be cost effective to cast the entire girder of fibrous concrete in order to obtain ductility at the ends of the girder. However, it has been shown that fibers help in reducing shear reinforcement at other locations in a prestressed girder (Júnior and Hanai 1999). Therefore, casting the whole girder with FRC may be feasible. The other option is to cast the girder with both fibrous and non-fibrous concrete, since some girders take more than a single batch of concrete to cast. It is also possible to use SFRC in the end or pier segments for segmental bridge girders. Producing the initial batch of fibrous concrete and placing it at the girder ends may be a suitable procedure for this study.

The nominal cost of steel fiber for estimating purposes is 38 to 40 cents per pound. This is a realistic cost for the Florida concrete market as quoted by a manufacturer. Using steel fibers only at the ends of girders will increase the cost of girder only by a small amount. For example, by adding steel fibers at 1% volumetric ratio, the cost of 1 yd<sup>3</sup> concrete will increase by \$53.0, from the basic \$ cost for 1 yd<sup>3</sup> non-fibrous concrete.

### **Labor and equipment involved in the steel fiber application**

The labor costs associated with steel fiber use in concrete are minimal. They involve the charging of the fibers into the mixer. In large projects, a fiber dispenser that meters the fibers in bulk to the mixer is used. The fibers are shipped in a 3000-pound bulk bag that is elevated above the dispenser from which the fibers are mechanically charged into the mixer. On small projects, the 55-pound bags of fibers are emptied on an inclined conveyor that carries fibers from ground level up to the mixer.

ACI 544.3R (1993) describes the procedures involved in the mixing, placing and finishing of SFRC. Conventional concrete equipment is adequate for the mixing, placing and finishing of SFRC. There are some important differences in mixing SFRC in a transit mixer or revolving drum mixer compared to conventional concrete (ACI 544.3R 1993). But these differences basically include the sequence of addition of concrete ingredients, which do not increase the production cost of SFRC. ACI 544.3R (1993) also provides a number of suggestions to facilitate the placing and finishing of SFRC. So, it may be inferred that SFRC can be placed and finished with conventional equipment with minor refinements in techniques and workmanship, at a negligible additional cost.

#### **9.2.2. Beneficial Cost Factors**

It was observed in this study that SFRC could reduce or replace the secondary spiral and skin reinforcement from the local anchorage zone, depending on the compressive strength of concrete. The cost saving in spiral and skin reinforcement reduction involve:

- Material saving
- Labor saving

Table 9.1 presents the approximate costs associated with the spiral reinforcement for various post-tensioning anchors (VSL Corporation). Reduction of total cost involves the size and number of anchorages used in the girder. The cost of skin reinforcement was not included herein, because it varies from project to project.

**Table 9.1: Costs associated with spiral reinforcement**

<b>Anchorage size</b>	<b>Spiral reinforcement</b>		<b>Cost</b>		<b>Total cost (\$)</b>
	<b>Size</b>	<b>Number of turns</b>	<b>Material (\$)</b>	<b>Labor (\$)</b>	
EC 5-7	#4	6	4.50	4.50	9.0
EC 5-12	#4	8	11.0	6.0	17.0
EC 5-19	#5	8	16.0	9.00	25.0
EC 5-27	#6	8	20.0	13.0	33.0
EC 5-31	#6	9	23.50	16.0	39.50

- *The material cost include freight charges*

# **CHAPTER 10**

## **CONCLUSIONS AND RECOMMENDATIONS**

### **10.1. Conclusions**

The objective of the present study was to determine the feasibility of reducing or eliminating the secondary reinforcement with steel or synthetic fibers for post-tensioned zones of precast prestressed girders. The control concrete mix used herein was a FDOT Class IV mix design with a target compressive strength of 5500 psi (37.9 MPa). In order to select fiber type and volume, various mechanical properties of FRC with two steel fibers (XOREX and ZP305) and one synthetic fiber (Harbourite H-330) were determined. Three fiber volumes were tested for each fiber type: 0.5%, 0.75% and 1.0%. The following conclusions can be made based on the results of the property testing phase of this study:

#### **Fresh concrete**

1. Fresh FRC is stiffer and less workable than non-fibrous concrete.

2. No special technique or equipment is required for mixing, placing and finishing of FRC. However, fresh FRC should be vibrated for a longer time than plain concrete.
3. Slump values for fresh FRC are typically lower than corresponding non-fibrous concrete. Slump values ranged from 1 to 3 in (25 to 75 mm) in this study, falling within the target range suggested by ACI 544.

### **Compressive strength**

1. The addition of steel fibers in concrete results in an increase in the compressive strength. The strength gain is greater for increased volumes of steel fibers. The ZP305 steel fiber had a more pronounced effect than the XOREX steel fiber in increasing the concrete compressive strength, even at a low 0.5% volume. The compressive strength increases from 4% to 16% and from 15% to 18% through the utilization of XOREX and ZP305 steel fibers, respectively, as compared to non-fibrous concrete.
2. The addition of Harbourite H-330 synthetic fiber results in decreased compressive strength of concrete, ranging from about 20% to as much as 40%. The reason for this negative effect may be the lack of bonding between the fiber and concrete.

### **Tensile strength**

1. The effect of fibers on concrete split tensile strength is similar to that on the compressive strength. Steel fibers increase concrete tensile strengths, increased volumes resulting in increasing tensile strengths. Increases in tensile strength vary from 5% to 10% and 6% to 37% when XOREX and ZP305 steel fibers are used,

respectively. The ZP305 steel fiber had a more pronounced effect on the concrete tensile strength.

2. Concrete split tensile strength decreases due to the addition of Harbourite H-330 synthetic fiber. The strength decrease ranges from about 7% to 37%, depending on the fiber volume.

### **Flexural toughness**

1. The pre-peak response of both the plain concrete and FRC is similar. Influence of fibers is only apparent after the occurrence of peak flexural loads.
2. The concrete post-crack energy absorption capacity increases due to fibers.
3. The flexural first crack strength of concrete is enhanced with the addition of fibers. The increase in first crack strength is greater for increased volumes of steel fibers, up to 8.5% and 34.5% strength increase for XOREX and ZP305, respectively. The addition of Harbourite H-330 synthetic fiber produced inconsistent first crack strength results.
4. Flexural toughness indices  $I_5$  and  $I_{10}$  for SFRC range from 2.9 to 3.6, and 4 to 5.5, respectively. The  $I_5$  and  $I_{10}$  indices for PFRC range from 2.1 to 2.9, and 3.0 to 4.5, respectively. Steel fibers better enhanced the toughness indices than synthetic fibers. The maximum toughness indices were obtained for XOREX steel fiber reinforced concrete.
5. Greater volumes of fibers result in increasing concrete flexural residual strength factors. The factors ranged from 21 to 52, 22 to 34 and 18 to 38 for concrete with XOREX steel fiber, ZP305 steel fiber and Harbourite H-330 synthetic fiber, respectively, based on fiber volume.

## **Failure Mode**

1. As compared to the brittle and explosive failure mode in non-fibrous concrete, fibrous concrete failure modes in compression, tension and flexure are more ductile. Fibers in concrete help in arresting and bridging tensile cracks, thereby slowing their growth rate.

Based on the mechanical properties, 1% ZP305, 0.75% ZP305 and 1% XOREX steel fibers were selected for the second phase AASHTO local zone acceptance testing and finite element modelling. The following conclusions can be made based on the second phase results:

### **For Type 1 (3500 to 5000 psi, or 24 to 34.5 MPa) concrete**

1. Control specimen without any fibers passed the AASHTO acceptance test when reinforced with 6-turn spiral and 5 skin steel. When the secondary reinforcement was reduced to either 6-turn spiral or 5 skins, specimens failed after the first cycle of loading.
2. 1% ZP305 steel fiber reinforced specimens performed better than the two other fiber configurations. With 3-turn spiral and no skin reinforcement in this fiber configuration, AASHTO acceptance with a maximum 79% reduction in the secondary reinforcement with a compressive strength of 4710 psi (32.5 MPa) may be achieved. No spiral and 3 skin specimens with a minimum 4250 psi (29.3 MPa) strength are also acceptable according to AASHTO criteria, with 65% reduction in secondary reinforcement.
3. Specimens with 0.75% ZP305 fibers, no spirals and 5 skin reinforcement passed AASHTO criteria with a maximum of 58% reduction in the secondary

reinforcement (minimum 3810 psi strength). In this fiber configuration, AASHTO acceptance and a 23% reduction of secondary reinforcement are also obtained by specimens with 6-turn spiral and 3 skins (minimum 4800 psi strength).

4. Specimens with 1% XOREX steel fibers, no spiral and 5 skin reinforcement achieved a maximum of 58% reduction in the secondary reinforcement and AASHTO acceptance (with minimum 4500 psi strength). In the same fiber configuration, AASHTO acceptance and 23% secondary steel reduction were achieved with 6-turn spiral and 3 skin specimens with a minimum compressive strength of 5000 psi (34.5 MPa).

**For Type 2 (5500 to 7500 psi, or 37.9 to 44.8 MPa) concrete**

1. For 1% ZP305 fiber specimens, the best performing configuration satisfying AASHTO criteria was no spiral and no skin reinforcement with a minimum compressive strength of 5900 psi (40.7 MPa). This configuration resulted in 100% total elimination of the secondary reinforcement. Similar eliminations were achieved for specimens with 0.75% ZP305 and 1% XOREX fibers, with minimum compressive strengths of 7050 psi (48.6 MPa) and 6980 psi (48 MPa), respectively.

**Test Observations**

1. All developed cracks during load cycles were located at the upper-half of the specimens. Vertical cracks first developed in the mid-zone of the specimens. After the application of a few more load cycles, horizontal cracks became visible at each corner at a distance of 2 to 3 in (50 to 75 mm) from the top of the specimens. At failure, cracks also developed at the top surface of the specimens.

2. Failure of control AASHTO specimens without fibers occurred in a brittle manner. In case of FRC samples, a more ductile failure was observed.
3. Suppression or separation of the anchorage occurred at failure.
4. For specimens with identical type and amount of fiber, and spiral and skin reinforcement, the failure load of the specimen increased and the crack width decreased with increasing compressive strengths.
5. VSL type EC 5-7 anchorage was utilized in this study due to limitations in the test machine capacity. However, the results are expected to be valid for other more popular and larger anchorages, such as EC 5-12 and EC 5-19.

### **Finite Element Modeling**

1. FEM models did not converge for load levels at failure because of the local failure of concrete close to the steel anchorage. Convergence may be achieved at lower load levels.
2. FEM analysis provided strain values well comparable to those obtained from the laboratory crack gages.
3. Development of cracks in the upper middle portion of the specimens corresponds to the presence of maximum stresses at this location, as evidenced from the FEM. Much lower stress developed at the lower half portion of the specimen, which indicates less chance of crack formation in that zone.

### **Cost comparison**

1. If fibers are used only at the end zones of girders, the cost of girders will not be affected significantly. The cost of girders will remain almost the same.

## 10.2. Recommendations

The following recommendations may be made based on the findings of this study:

1. Steel fiber reinforced concrete is recommended for use in the end zones of post-tensioned girders, based on the minimum properties of SFRC provided in Table 10.1.
2. Other steel fibers available in the market may also be used for this purpose, provided they are similar to the fibers investigated in this study, have properties presented in Table 10.1, and used in the volume ratios proposed.
3. Table 10.2 presents the recommended SFRC types together with acceptable fiber volume, secondary reinforcement configuration and minimum concrete compressive strength at the time of post-tensioning application. It is to be noted that recommendations made in Table 10.2 are based on test results from only one specimen per configuration. A total of 37 AASHTO blocks, with various spiral and skin reinforcement, fiber configurations and concrete strengths, were tested in this study. For Type 2 concrete, Table 10.2 shows three specimens producing identical reduction of secondary steel. For Type 1 concrete, at least two repetitions in most configurations were performed. This justifies the reliability of the recommendations in Table 10.2.
4. The proposed SFRC configurations together with reduction or elimination of end zone secondary reinforcement are recommended for all sizes and types of anchorage from any manufacturing company.

5. From the reinforcement congestion perspective, elimination of the spiral steel is more beneficial than the elimination or reduction of skin reinforcement. This is because the skin reinforcement is located near the girder perimeter, while the spiral steel is centrally located. Therefore, it may be more desirable to adopt or consider Specimen IDs 1, 3 or 4 from Table 10.2.
6. It is recommended that FDOT investigate the feasibility of utilizing steel fibers at other girder locations away from the end zones of prestressed girders. This may result in additional benefits such as shear steel reduction, impact resistance and crack control, together with ease of girder casting.
7. It is also recommended that FDOT look at the potential of utilizing steel fibers in other elements of transportation structures. Examples are prestressed piles (for impact resistance), bridge piers (for ship impact resistance and reducing secondary steel), flanges of box segments (for impact resistance) and bridge decks (for crack control).

**Table 10.1: Minimum properties of acceptable SFRC**

SFRC ID	Fiber type	Volume fraction, (%)	First crack strength, psi (MPa)	Toughness indices		Residual strength factor
				$I_5$	$I_{10}$	
1	ZP305	1	1345 (9.3)	3.6	5.3	34
2	ZP305	0.75	1190 (8.2)	3.2	4.3	22
3	XOREX	1	1085 (7.5)	2.9	5.5	52

**Table 10.2: Recommended SFRC configurations**

Specimen ID	Reduction or elimination of secondary reinforcement (%)		Fiber configuration		Minimum compressive strength at post-tensioning, psi (MPa)
	Spiral	Skin	Type	Volume fraction (%)	
1	100	100	ZP305	1	5900 (40.7)
			ZP305	0.75	7050 (48.6)
			XOREX	1	6980 (48)
2	50	100	ZP305	1	4710 (32.5)
3	100	40	ZP305	1	4250 (29.3)
4	100	0	ZP305	0.75	3810 (26.3)
			XOREX	1	4500 (31)
5	0	40	ZP305	0.75	4800 (33)
			XOREX	1	5000 (34.5)

## REFERENCES

American Association of State Highway Transportation Officials (AASHTO), “Standard Specifications for Highway Bridges”, Sixteenth Edition, 1996.

American Association of State Highway Transportation Officials (AASHTO), “AASHTO LRFD Bridge Construction Specifications”, 1st Edition, 1998.

American Concrete Institute, “ACI Manual of Concrete Practice”, Part 5, Detroit, MI, 1997.

ACI Committee 318, “Building Code Requirements for Structural Concrete and Commentary”, American Concrete Institute, Detroit, MI, 2002, 391 pp.

ACI Committee 544, “State-of-the-Art Report on Fiber Reinforced Concrete”, ACI 544.1R, American Concrete Institute, Detroit, MI, 1986, 22 pp.

ACI Committee 544, “Fiber Reinforced Concrete”, ACI 544.1R, American Concrete Institute, Detroit, MI, 1996, 66 pp.

ACI Committee 544, “Guide for Specifying, Proportioning, Mixing, Placing, and Finishing Steel Fiber Reinforced Concrete”, ACI 544.3R, American Concrete Institute, Detroit, MI, 1993, 10 pp.

ACI Committee 544, “Measurement of Properties of Fiber Reinforced Concrete”, ACI 544.2R, American Concrete Institute, Detroit, MI, 1989, 11 pp.

American Society for Standard Testing and Materials (ASTM), “Test Method for Compressive Strength of Cylindrical Concrete Specimens”, ASTM C-39, West Conshohocken, PA, 1996.

American Society for Standard Testing and Materials (ASTM), “Standard Test Method for Slump of Hydraulic Cement Concrete”, ASTM C-143, West Conshohocken, PA, 1990.

American Society for Standard Testing and Materials (ASTM), “Practice for Making and Curing Concrete Test Specimens in the Laboratory”, ASTM C-192, West Conshohocken, PA, 1995.

American Society for Standard Testing and Materials (ASTM), “Standard Test Method for Splitting Tensile Strength of Cylindrical Concrete Specimens”, ASTM C-496, West Conshohocken, PA, 1996.

American Society for Standard Testing and Materials (ASTM), “Standard Test Method for Time of Flow of Fiber-Reinforced Concrete Through Inverted Slump Cone”, ASTM C-995, West Conshohocken, PA, 2001.

American Society for Standard Testing and Materials (ASTM), “Standard Test Method for Flexural Toughness and First-Crack Strength of Fiber Reinforced Concrete (Using Beam With Third-Point Loading)”, ASTM C-1018, West Conshohocken, PA, 1997.

American Society for Standard Testing and Materials (ASTM), “Test Method for Obtaining Average Residual-Strength of Fiber-Reinforced Concrete”, ASTM C-1399, West Conshohocken, PA, 1998.

American Society for Standard Testing and Materials (ASTM), “Standard Test Method for Flexural Toughness of Fiber Reinforced Concrete (Using Centrally Loaded Round Panel)”, ASTM C-1550, West Conshohocken, PA, 2002.

ANSYS, Inc., “ANSYS 6.0 Online Documentation”, SAS IP, 2001.

Balaguru, P., and Ramakrishnan, V., “Comparison of Slump Cone and V-B Tests as Measures of Workability of Fiber Reinforced and Plain Concrete”, ASTM Journal, Cement, Concrete and Aggregates, Vol. 9, Summer 1987, pp. 3-11.

Banthia, N., Mindess, S., and Bentur, A., “Impact Behavior of Concrete, Materials and Structures”, RILEM 20 (119), Paris, 1987, pp. 293-302.

Barr, B., “The Fracture Characteristics of FRC Materials in Shear”, Fiber Reinforced Concrete - Properties and Applications, SP-105, American Concrete Institute, Detroit, MI, 1987, pp. 27-53.

Batson, G., Ball, C, Bailey, L, Landers, E., and Hooks, J., “Flexural Fatigue Strength of Steel Fiber Reinforced Concrete Beams”, ACI Journal Proceedings, Vol. 69, No. 11, Nov. 1972, pp. 673-677.

Beaudoin, J.J., “Handbook of Fiber-Reinforced Concrete. Principles, Properties, Developments and Applications”, Noyes Publications, Park Ridge, NJ, 1990, pp. 332.

Biryukovich, K.L., and Yu, D.L., "Glass Fiber Reinforced Cement", translated by G.L. Cairns, CERA Translation, No. 12, Civil Engineering Res. Association, London, 1965, 41 pp.

Brandshaug, T., Ramakrishnan, V., Coyle, W.V., and Schrader, E.K., "A Comparative Evaluation of Concrete Reinforced with Straight Steel Fibers and Collated Fibers with Deformed Ends", Report No. SDSM&T-CBS 7801, South Dakota School of Mines and Technology, Rapid City, SD, May 1978, 52 pp.

Breen, J.E., Burdet, O., Roberts, C., Sanders, D., and Wollmann G., "Anchorage Zone Reinforcement for Post-Tensioned Concrete Girders", National Cooperative Highway Research Program Report 356, Washington D.C., 1994, pp. 204.

Breen, J.E., Fenves, G., Sanders, D.H., Burdet, O.L., "Anchorage Zone Reinforcement for Post-Tensioned Concrete Girders", National Cooperative Highway Research Program Interim Report 10-29, University of Texas at Austin, August 1987.

Burdet, O. L., "Analysis and Design of Anchorage Zones in Post-tensioned Concrete Bridges", Ph.D. Dissertation, The University of Texas at Austin, May 1990.

Casanova, P. and Rossi, P, "Analysis and Design of Steel Fiber Reinforced Concrete Beams", ACI Structural Journal, V. 94, No. 5, September – October 1997, pp. 595-602.

Dardare, J., "Contribution à l'Étude du Comportement Mécanique des Bétons Renforcés avec des Fibres de Polypropylène", RILEM Symposium on Fiber-Reinforced Cement and Concrete, London, ed. A.M. Neville, 1975, pp. 227-235.

Dave, N.J., and Ellis, D.G., "Polypropylene Fiber Reinforced Cement", Cement Composites, Vol. 1, No. 1, 1979, pp. 19-28.

Dixon, J., and Mayfield, B., "Concrete Reinforced with Fibrous Wire", Journal of the Concrete Society, Vol. 5, No. 3, March 1971, pp 73-76.

Florida Department of Transportation (FDOT), "Standard Specification for Road and Bridge Construction", Section 346, FDOT Specifications Office, 2000.

Goldfein, S., "Fibrous Reinforcement for Portland Cement", Modern Plastics, Vol. 42, No. 8, 1965, pp 156-160.

Gopalaratnam, V.S., and Shah, S., "Failure Mechanisms and Fracture of Fiber Reinforced Concrete", Fiber Reinforced Concrete - Properties and Applications, SP-105, American Concrete Institute, Detroit, MI, 1987a, pp. 1-25.

Grzybowski, M., “Determination of Crack Arresting Properties of Fiber Reinforced Cementitious Composites”, Royal Institute of Technology, Stockholm, Sweden, Chapter 12, June 1989.

Grzybowski, M., and Shah, S.P., “Shrinkage Cracking in Fiber Reinforced Concrete”, ACI Materials Journal, Vol. 87, No. 2, Mar. - Apr. 1990, pp. 138-148.

Hannant, D. J., “Fiber Cements and Fiber Concrete”, John Wiley & Sons, Ltd., Chichester, UK, 1978, 53 pp.

Hoff, G., “Durability of Fiber Reinforced Concrete in a severe Marine Environment”, Fiber Reinforced Concrete Properties and Applications, SP-105, American Concrete Institute, Detroit, MI, 1987, pp. 997-1041.

Huebner, K.H., and Thornton, E.A., “The Finite Element Method for Engineers”, John Wiley and Sons, New York, 1982.

Hughes, B.P., and Fattuhi, N.I., “Stress-Strain Curves, for Fiber Reinforced Concrete in Compression, Cementitious Concrete Resources, Vol. 7, No. 2, 1977, pp. 173-184.

Jindal, R.L., “Shear and Moment Capacities of Steel Fiber Reinforced Concrete Beams”, Fiber Reinforced Concrete-International Symposium, SP-81, American Concrete Institute, Detroit, MI, 1984, pp. 1-16.

Johnston, C. D., “Steel Fiber Reinforced Mortar and Concrete – A Review of Mechanical Properties”, Fiber Reinforced Concrete, SP-44, American Concrete Institute, Detroit, MI, 1974, pp. 127-142.

Johnston, C. D., “Properties of Steel Fiber Reinforced Mortar and Concrete – A Review of Mechanical Properties”, Proceedings, International Symposium on Fibrous Concrete (CI-80), Construction Press, Lancaster, 1980, pp. 29-47.

Johnston, C. D., “Effects on Flexural Performance of Sawing Plain Concrete and of Sawing and other Methods of Altering Fiber Alignment in Fiber Reinforced Concrete”, Cement, Concrete and Aggregate, ASTM, CCAGDP, Vol. 11, No. 1, Summer 1989, pp. 23-29.

Júnior, S.F., and Hanai, J.B., “Prestressed Fiber Reinforced Concrete Beams with Reduced Ratios of Shear Reinforcement”, Cement & Concrete Composites, Elsevier Applied Science Publishers, Ltd., Vol. 21, No. 3, 1999, pp. 213-221.

Kormeling, H. A., Reinhardt, H. W., and Shah, S. P., “Static and Fatigue Properties of Concrete Beams Reinforced with Continuous Bars and with Fibers”, ACI Journal Proceedings, Vol. 77, No. 1, Jan. – Feb. 1980, pp. 36-43.

Libby, J., "Segmental Box Girder Bridge Superstructure Design", ACI Journal, Vol. 73, No. 5, May 1976, pp 279-290.

Logan, D.L., "A First Course in the Finite Element Method", PWS Publishing Company, Boston, MA, 1993.

Materschläger, A., and Bergmeister, K., "Fiber Added Concrete", 2nd International PhD Symposium in Civil Engineering, Budapest, 1998.

McKee, D.C., "Properties of an Expansive Cement Mortar Reinforced with Random Wire Fibers", Ph.D. Thesis, University of Illinois, Urbana, 1969.

Morse, D. C., and Williamson, G. R., "Corrosion Behavior of Steel Fibrous Concrete", Report No. CERL-TR-M-217, Construction Engineering Research Laboratory, Champaign, IL, May 1977, 37 pp.

Naaman, A.E., "Fiber Reinforcement for Concrete", Concrete International: Design and Construction, Vol. 7, No. 3, March 1985, pp 21-25.

Naaman, A.E., "New Fiber Technology". ACI Concrete International Magazine, July 1998, pp. 57-62.

Nagabhushanam, M., Ramakrishnan, V., and Vondran, G., "Fatigue Strength of Fibrillated Polypropylene Fiber Reinforced Concrete", Transportation Research Records 1226, National Research Council, Washington D.C., 1989, pp. 36-47.

Narayanan, R.; and Darwish, I. Y. S., "Use of Steel Fiber as Shear Reinforcement", ACI Structural Journal, May – June 1987, pp. 216-227.

Oh, B. H., Lim, D. H.; Hong, K. O.; Yoo, S. W., and Chae, S. T., "Structural Behavior of Steel Fiber Reinforced Concrete Beams in Shear", Structural Application of Fiber Reinforced Concrete, SP-182, American Concrete Institute, Detroit, MI, 1999, pp. 9-27.

Precast-Concrete, "Wire-Reinforced Precast Concrete Decking Panels", UK, December 1971, pp. 703-708.

Ramakrishnan, V., Gollapudi, S., and Zellers, R., "Performance Characteristics and Fatigue of Polypropylene Fiber Reinforced Concrete", SP-105, American Concrete Institute, Detroit, MI, 1987, pp. 159-177.

Ramakrishnan, V., and Josifek, C., "Performance Characteristics and Flexural Fatigue Strength of Concrete Steel Fiber Composites", Proceedings of the International Symposium on Fiber Reinforced Concrete, Dec. 1987, Madras, India, pp. 2.73-2.84.

Ramakrishnan, V., Oberling, G., and Tatnall, P., "Flexural Fatigue Strength of Steel Fiber Reinforced Concrete", Fiber Reinforced Concrete Properties and Applications, SP-105, American Concrete Institute, Detroit, 1987, pp. 225-245.

Ramakrishnan, V., Wu, G.Y., and Hosalli, G., "Flexural Fatigue Strength, Endurance Limit, and Impact Strength of Fiber Reinforced Concrete", Transportation Research Records 1226, National Research Council, Washington D.C., 1989, pp. 17-24.

Rapoport, J., Aldea, C., Shah, S.P., Ankenman, B., and Karr, A.F., "Permeability of Cracked Steel Fiber-Reinforced Concrete", Technical Report No. 115, National Institute of Statistical Sciences (NISS), Research Triangle Park, NC, January, 2001.

Rice, E., Vondran, G., and Kungbargi, H., "Bonding of Fibrillated Polypropylene Fibers to Cementitious Materials", Materials Research Society Proceedings, Pittsburgh, PA, Vol. 114, 1988, pp. 145-152.

Richard, P., Cheyrezy, M. and Dugat, J., "A Prestressed Beam without Conventional Reinforcing". FIP XIIth Congress, September 1998.

Roberts, C., "Behavior and Design of the Local Anchorage Zone in Post-Tensioned Concrete", M.S. Thesis, University of Texas at Austin, May 1990.

Romualdi, J.P., and Batson, G.B., "Mechanics of Crack Arrest in Concrete", Journal of Engineering Mechanics Division, ASCE, Vol. 89, No. EM3, June 1963, pp. 147-168.

Romualdi, J.P., and Mandel, J.A., "Tensile Strength of Concrete Affected by Uniformly Distributed and Closely Spaced Short Length of Wire Reinforcement", ACI Journal Proceedings, Vol. 61, No. 6, June 1964, pp 657-671.

Sanders, D.H., "Design and Behavior of Post-tensioned Concrete Anchorage Zones", Ph.D. Dissertation, The University of Texas at Austin, May 1990.

Schrader, E. K., "Studies in the Behavior of Fiber Reinforced Concrete", MS Thesis, Clarkson College of Technology, Potsdam, NY, 1971.

Schupack, M., "Durability of SFRC Exposed to Severe Environments", Steel Fiber Concrete, Elsevier Applied Science Publishers, Ltd., 1986, pp. 479-496.

Shah, S. P., "Do Fibers Increase the Tensile Strength of Cement Based Matrices?", ACI Materials Journal, Vol. 88, No. 6, Nov. 1991, pp. 595-602.

Shah, S. P., Stroeven, P., Dalhuisen, D., and Van Stekelenburg, P., "Complete Stress-strain Curves for Steel Fiber Reinforced Concrete in Uniaxial Tension and Compression", Testing and Test Methods of Fiber Cement Composites, RILEM Symposium, 1978, Construction Press, Lancaster, pp. 399-408.

Sharma, A.K., “Shear Strength of Steel Fiber Reinforced Concrete Beams”, ACI Journal Proceedings, Vol. 83, No. 4, July-August 1986, pp. 624-628.

SI Concrete Systems, Website of Synthetic Industry.

Snyder, M. L., and Lankard, D. R., “Factors Affecting the Strength of Steel Fibrous Concrete”, ACI Journal, Proceedings, Vol. 69, No. 2, Feb. 1972, pp. 96-100.

Stone, W.C., “Measurement of Internal Strain in Cast-Concrete Structures”, Experimental Mechanics, Vol. 23, No. 4, December 1983, pp 361-369.

Swamy, R. N., and Al-Ta’an, Sa’ad A., “Deformation and Ultimate Strength in Flexure of Reinforced Concrete Beams Made with Steel Fiber Concrete”, ACI Journal Proceedings, V. 78, No. 5, Sept.-Oct. 1981, pp. 395-405.

Vondran, G. L., “Application of Steel Fiber Reinforced Concrete”, Steel Fiber Reinforced Concrete, C-27, American Concrete Institute, Detroit, MI, pp. 14-19.

VSL Corporation, “VSL Post-Tensioning Systems”, Website of VSL Structural Group, 2002.

Waterhouse, B. L., and Luke, C. E., “Steel Fiber Optimization”, Conference Proceedings M-28, Fibrous Concrete – Construction Materials for the Seventies, December 1972, pp. 630-681.

Williamson, G.R., “The Effect of Steel Fibers on the Compressive Strength of Concrete”, Fiber Reinforced Concrete, SP-44, American Concrete Institute, Detroit, MI, 1974, pp. 195-207.

Williamson, G.R., “Steel Fibers as Web Reinforcement in Reinforced Concrete”, Proceedings, US Army Science Conference, West Point, Vol. 3, June 1978, pp. 363-377.

Wollmann, G.P., and Roberts-Wollmann, C.L., “Anchorage Zone Design”, Preprint of Chapter VIII, Post-Tensioning Manual, Sixth Edition, October 2000, pp. 46.

Zollo, R.F., “Collated Fibrillated Polypropylene Fibers in FRC”, International Symposium on Fiber Reinforced Concrete, American Concrete Institute, SP-81, 1984, pp. 397-409.

Zollo, R.F., Ilter, J.A., and Bouchacourt, G.B., “Plastic and Drying Shrinkage in Concrete Containing Collated Fibrillated Polypropylene Fiber”, Third International Symposium on Developments in Fiber Reinforced Cement and Concrete, RILEM Symposium FRC 86, Vol. 1, RILEM Technical Committee 49-TFR, 1986.

Zonsveld, J.J., "Properties and Testing of Concrete Containing Fibers Other Than Steel", RILEM Symposium on Fiber-Reinforced Cement Concrete, London, 1975, pp 217-226.

# APPENDIX A

## CALCULATIONS

### A.1. The Ultimate Tensile Capacity for a Tendon

#### A.1.1. General Equation

The ultimate tensile capacity of a tendon is calculated using the fundamental formula:

Force = Stress x Area

For this study, this formula may be expressed as:

$$F_{pu} = nA_s f_{pu}$$

where,  $F_{pu}$  = the ultimate tensile load of the largest tendon

$n$  = the largest number of strands

$A_s$  = nominal area of a tendon

$f_{pu}$  = the ultimate tensile strength of a tendon

### A.1.2. Ultimate Load for VSL EC Type Anchorage

According to the VSL Corporation (2002), the designation EC 5-Y refers to an EC type anchorage, which can accommodate Y number of strands with a nominal diameter of 0.5 in (12.7 mm). The nominal area and ultimate tensile strength of the strand are  $0.153 \text{ in}^2$  ( $98.7 \text{ mm}^2$ ) and 270,000 psi (1860 MPa), respectively.

The ultimate load for EC 5-7 anchorage is therefore:

$$F_{pu} = 7 \times 0.153 \times 270,000 = 289,000 \text{ lb} = 289 \text{ kips}$$

According to the AASHTO Special Anchorage Device Acceptance Test, a test block is required to be strong enough to sustain  $1.1F_{pu}$  (the ultimate tensile strength of the largest tendon of the anchorage) to pass the test. For EC 5-7 anchorage type, this load is:

$$1.1F_{pu} = 1.1 \times 289 = 318 \text{ kips}$$

For EC 5-12, calculations for  $F_{pu}$  and  $1.1F_{pu}$  are as follows:

$$F_{pu} = 12 \times 0.153 \times 270,000 = 496,000 \text{ lb} = 496 \text{ kips}$$

$$1.1F_{pu} = 1.1 \times 496 = 545 \text{ kips}$$

## A.2. Skin Reinforcement

$$\text{The volume of the test block} = 12.5 \times 12.5 \times 25 \text{ in}^3 = 3906.25 \text{ in}^3$$

$$\text{The volume of the skin reinforcement} = 0.01 \times 3906.25 = 39.06 \text{ in}^3 \approx 40 \text{ in}^3$$

$$\text{The length of each skin reinforcement} = 4 [12.5 - 2(1) - 2(0.25)] = 40.0 \text{ in}$$

$$\text{For a \#4 size rebar, the volume of each skin reinforcement} = 40 \times 0.2 = 8.0 \text{ in}^3$$

$$\text{The number of skin reinforcement} = 40 / 8 = 5$$